REFERENCE ONLY

UNIVERSITY OF LONDON THESIS

Degree PhD Year 2005 Name of Author ASHIQ W

This thesis comes within category D.

☑ This copy has been deposited in the Library of UCL

☐ This copy has been deposited in the Senate House Library, Senate House, Malet Street, London WC1E 7HU.

THE INVESTIGATION OF PATHOGENESIS IN MULTIPLE SCLEROSIS USING QUANTITATIVE MAGNETIC RESONANCE PARAMETERS

WAQAR RASHID, MRCP(UK) BSc

NMR Research Unit
Institute of Neurology
University College London, UK.

Thesis submitted for:
DOCTOR OF PHILOSOPHY (PhD)
NEUROLOGICAL STUDIES
UNIVERSITY OF LONDON

ProQuest LLC
789 East Eisenhower Parkway
P.O. Box 1346
Ann Arbor, MI 48106-1346

ABSTRACT

This thesis studies the use of several quantitative MR techniques to investigate further the pathophysiology of multiple sclerosis (MS) and to evaluate the sensitivity of quantitative MRI parameters in early disease both for prognostic purposes and as potential outcome measures in treatment monitoring trials. Presented are investigations using multiple MR techniques into clinically early relapsing-remitting MS and also a non-invasive MR technique (Continuous Arterial Spin Labelling [CASL]) to determine cerebral perfusion in patients with a wide spectrum of MS severity.

Presented are cross-sectional and longitudinal investigations of several MR parameters - enhancing lesions, diffusion tensor imaging and cord area – acquired from a cohort of relapsing-remitting MS patients recruited within three years of first symptom onset to assess the clinical and pathological evolution of the disease from its earliest clinical stages. Results from the presented studies include: (i) a high degree of gadolinium enhancement which relates to relapse frequency but not clinical impairment or disability in the medium term; (ii) evidence of progressive loss of cervical cord area and (iii) subtle diffusion changes in normal appearing brain tissue but no definitive longitudinal changes in comparison to healthy controls.

Also presented is the first application of non-invasive cerebral perfusion measurement using a MR technique which models for blood brain barrier permeability (CASL with two-compartment methodology). The most significant finding was a consistent decrease in perfusion in patients with progressive disease in comparison to controls particularly in the deep grey matter, probably reflecting neuronal loss or dysfunction; and increased perfusion in white matter in patients with relapse onset MS which may reflect underlying inflammation.

Overall, promising and novel results using several quantitative MR parameters investigating specific MS cohorts have been detailed in this thesis and provide useful insights for further work in MS.

DECLARATION

Patient recruitment and examinations for the studies detailed in Chapters 4 and 5 were carried out in the NMR Unit, Institute of Neurology, London, UK by Dr Declan Chard, Dr Colette Griffin, Dr Gerard Davies and myself. Cohort recruitment for the study in Chapter 3 was undertaken by Dr Laura Parkes, Dr Gordon Ingle, Dr Declan Chard and myself.

Baseline conventional structural MR images from all studies described in this thesis were reviewed by Dr. Katherine Miszkiel (Consultant Neuroradiologist, National Hospital for Neurology and Neurosurgery). Statistical analysis for all studies included in this thesis was provided by Dr Dan R. Altmann.

Brain tissue volume data on 20 MS patients and 10 controls included in studies detailed in Chapters 4.3, 5.3 and 5.5 was collected and analysed by Dr Michela Tiberio, whilst she was a Research Fellow in the NMR Unit, Institute of Neurology, London, UK.

ACKNOWLEDGEMENTS

Firstly, I would like to thank all those people, both patients and controls, who kindly volunteered and gave up their time to spend many hours in a MRI scanner and consented to have numerous clinical tests carried out. Without their help I would not have been able to carry out this work.

I would like to thank Dr Laura Parkes for all her help and advice during our implementation of the non-invasive MR perfusion measurement study detailed in Chapter 3. I am grateful for her patience and expert help both during the study and also for the subsequent paper and resultant presentations of the data at various meetings.

I am also indebted to my collaborators in the early relapsing-remitting multiple sclerosis studies (Chapters 4 and 5): Dr Gerard Davies, Dr Declan Chard, Dr Colette Griffin and Dr Michela Tiberio for their help in recruitment, patient examination and advice regarding analysis.

I am grateful to the radiographers David MacManus, Ros Gordon and Chris Benton for imaging all the subjects in the studies detailed in this thesis. They had to, at times, work extra hours to fit in all the scans and also put up with my 'unique' sense of humour. I really appreciate their efforts.

The support of the fellows' room and others in the Institute of Neurology was also extremely important to me, not least Gerard Davies, Gary Price, Juliet Solomon, Andreas Hadjiprocopis, Anand Trip, Klaus Schmierer, Ee Tuan Lim, Derek Soon, Olga Ciccarelli, Declan Chard, Simon Hickman, Gordon Ingle, Dan Tozer, Claire Middleditch, Lesley Hearsum, Krishanyi Fernando, Tina Holmes and many others.

I would also like to thank the Physicists who have been of great help to me in providing technical support for the studies described in this thesis, particularly Prof. Gareth Barker who also acted as my secondary supervisor, Dr Andreas Hadjiprocopis, Dr Claudia Wheeler-Kingshott, Dr Laura Parkes and Prof. Paul Tofts. A special mention should also be made for Dr Dan R Altmann who worked non-stop in

providing me statistical support to the ever increasing amount of data I generated whilst at NMR Unit.

I am deeply indebted to Profs David Miller and Alan Thompson for the setting up of the projects I worked on and providing the excellent structures within the unit that made this research possible. I am particularly grateful to my principal supervisor, Prof. Miller, for his help during my time at the NMR Unit, not least for all his experience, advice and expertise and also persistence in making me stick to my deadlines. It is in large part through his support and motivation that I was able to produce this work and publish data.

The NMR Research Unit is supported by the Multiple Sclerosis Society of Great Britain and Northern Ireland, and my research in the Unit was supported by a project grant from the society. I am thankful to them for making this thesis possible.

Finally, I would like to thank all my friends and family for putting up with me throughout the last few years and for always being there.

PUBLICATIONS ASSOCIATED WITH THIS THESIS

Rashid W, Davies GR, Chard DT, Griffin CM, Altmann DR, Gordon R, Thompson AJ, Miller DH. Increasing cord atrophy in early relapsing-remitting multiple sclerosis: a three year study. *J Neurol Neurosurg Psychiatry* 2005; in press.

Rashid W, Davies GR, Chard DT, Griffin CM, Altmann DR, Gordon R, Kapoor R, Thompson AJ, Miller DH. Upper cervical cord area in early relapsing-remitting multiple sclerosis: cross-sectional study of factors influencing cord size. *J Magn Reson Imaging* 2005; in press.

Rashid W, Parkes LM, Ingle GT, Chard DT, Toosy AT, Altmann DR, Symms MR, Tofts PS, Thompson AJ, Miller DH. Abnormalities of cerebral perfusion in multiple sclerosis. *J Neurol Neurosurg Psychiatry* 2004; **75:** 1288-1293.

Rashid W, Hadjiprocopis A, Griffin CM, Chard DT, Davies GR, Barker GJ, Tofts PS, Thompson AJ, Miller DH. Diffusion tensor imaging of early relapsing-remitting multiple sclerosis with histogram analysis using automated segmentation and brain volume correction. *Mult Scler* 2004; **10:** 9-15.

Rashid W, Miller DH. Perfusion MRI. In: Eds: M Filippi, G Comi. *The New Frontiers of MR-based Techniques in Multiple Sclerosis.* Pub: Springer-Verlag, Italia. 2003: 73-82.

Hadjiprocopis A, Rashid W, Tofts PS. Unbiased segmentation of diffusion-weighted magnetic resonance images of the brain using iterative clustering. *Magn Reson Imaging* 2005; in press.

Parkes LM, Rashid W, Chard DT, Tofts PS. Normal cerebral perfusion measurements using arterial spin labelling: reproducibility, stability and age and gender effects. *Magn Reson Med* 2004; **51:** 736-743.

TABLE OF CONTENTS

ABBREVIATIONS

α	Flip angle
ADC	Apparent diffusion coefficient
ADEM	Acute disseminated encephalomyelitis
AIR	Automated image registration
APP	Amyloid precursor protein
ASL	Arterial spin labelling
b	Scalar diffusion weighting factor
BBB	Blood brain barrier
BDNF	Brain derived neurotrophic factor
BIFN	Interferon-beta
BPF	Brain parenchymal fraction
BPV	Brain parenchymal volume
CASL	Continuous arterial spin labelling
CBF	Cerebral blood flow
CBV	Cerebral blood volume
CIS	Clinically isolated syndrome
CNS	Central nervous system
CSE	Conventional spin echo
CSF	Cerebrospinal fluid
DTI	Diffusion tensor imaging
DW	Diffusion weighting
EDSS	Expanded disability status scale
EPI	Echo planar imaging
EPISTAR	Echo planar imaging and signal targeting with alternating radiofrequency
ETL	Echo train length
FA	Fractional anisotropy
FAIR	Flow-sensitive alternating inversion recovery
FID	Free induction decay
FSE	Fast spin echo
FSPGR	Fast spoiled gradient echo recall
FOV	Field of view

GMF	Grey matter fraction
IR	Inversion recovery
MD	Mean diffusivity
MHC	Major histocompatibility complex
MRI	Magnetic resonance imaging
MS	Multiple sclerosis
MSFC	Multiple sclerosis functional composite score
MTR	Magnetisation transfer ratio
MTT	Mean transit time
NAA	N-acetyl-aspartate
NABT	Normal appearing brain tissue
NAWM	Normal appearing white matter
NEX	Number of excitations
PASAT	Three second paced auditory serial addition test
PASL	Pulsed arterial spin labelling
PD	Proton density
PEG	Nine-hole peg test
PET	Positron emission tomography
PS	Permeability surface area product
RF	Radiofrequency
ROI	Region of interest
SIENA	Structured imaging evaluation, using normalisation, of atrophy
SNR	Signal-to-noise ratio
SPECT	Single photon emission tomography
SPM	Statistical parametric mapping
TE	Echo delay time
TI	Inversion time
TICV	Total intracranial volume
TNF	Tumour necrosis factor
TR	Repetition time
TWT	25 foot timed walk test
UCCA	Upper cervical cord area
v_{bw}	Fractional blood water per unit volume of tissue
VEGF	Vascular endothelial growth factor

VEP	Visual evoked potentials
WBT	Whole brain tissue
WBV	Whole brain volume
WMF	White matter fraction

TABLES

FIGURES

CHAPTER 1

Multiple Sclerosis

1.1 Introduction

Multiple sclerosis (MS) is a chronic demyelinating disease of the central nervous system (CNS) with both inflammatory and neurodegenerative components (Lassman, 1998a; Trapp *et al.*, 1998) usually causing multiple lesions in the white matter of the brain. The cause remains unknown, although autoimmune factors with possible genetic and environmental components may be relevant. The mechanisms underlying these processes and how early in the disease course they evolve remain unclear.

The first study of demyelinating disease in humans was probably made in 19th century France at the Salpetriere, Paris (Charcot, 1865), with further possible cases of patients with *la sclerose en plaques disseminées* described with features likely to have been MS recorded (Vulpian, 1866). Pathological descriptions preceded these clinical reports by almost 30 years (Carswell, 1838; Cruveilhier c1841). With the publication of the monograph *Multiple Sclerosis* in 1955 (McAlpine *et al.*, 1955), the condition became universally known by its present name.

The incidence of MS has been noted to increase, although whether this is because detection rates are improving or the disease is genuinely becoming more common is unclear (Pryse-Phillips, 1986; Hammond *et al.*, 1988a; Wynn *et al.*, 1990; Granieri *et al.*, 1993; McLeod *et al.*, 1994). The presentation of MS is usually with an episode of neurological dysfunction which builds over a few days and then partially or fully resolves often after a few weeks or months. Such events are termed relapses provided

that they last for at least 24 hours, with no concurrent fever or infection and with a period of at least 30 days separating them from any previous event (McDonald *et al.*, 2001). Additionally, a significant minority of patients with MS (~15%) present with evolving, slowly progressive symptoms. In those with relapse-onset MS, the course of the disease is unpredictable, but over time progressive disability often occurs, with half of those affected requiring help with walking after 15 years (Weinshenker *et al.*, 1989a). The differences in presentation and natural history of the condition suggest that different pathological mechanisms occur in the disease and this has stimulated research studies to elucidate the evolving pathogenesis of the condition.

Magnetic Resonance Imaging (MRI) was introduced over two decades ago. Its first application in MS was described in 1981 (Young *et al.*, 1981) and it has become increasingly used in clinical and research practice. As MRI technology has advanced, it has been used in MS to aid describing: (i) the pathogenesis of the condition; (ii) the natural history and prognosis particularly with respect to clinical correlations and (iii) aid in the evaluation of potential therapeutic drug agents. Its main routine clinical use is in diagnosis.

Presented in this thesis is an overview of the features of MS, together with an explanation of diagnostic investigative criteria and current management strategies. Following a summary of the concepts of MRI methodology and quantitative parameters currently available for investigating MS, the body of the thesis concentrates on studies investigating the use of several quantitative MRI techniques to provide further insights into the pathogenesis and evolution of the condition.

1.2 Aetiology

MS is a worldwide condition with an estimated 2.5 million affected people. It is the most common chronic neurological disease of young adults in the United Kingdom, and is estimated to cost £1.2 billion per annum (Homes *et al.*, 1995). The UK prevalence is approximately 1 in 800, with 80000 people affected by the disease (Kapoor, 2003). Most present between the ages of 20 and 40 years with a mean age of onset of 30 years (Paty *et al.*, 1997; Vukusic and Confavreux, 2001). Cases can also present in childhood (Miller, 2001) and above the age of 60 (Ebers and Sadovnick, 1997). Females are more at risk with figures showing a female: male ratio of 2:1, particularly in patients who experience relapses, irrespective of ethnicity (Compston, 1998). There is a more equal gender distribution in patients with primary progressive MS (Ebers and Sadovnick, 1997).

The geographical pattern of the disease shows areas of differing risk (Kurtzke, 1975). MS is particularly common in North America, Australasia and northern Europe and rare in the Orient, Africa and Middle East with certain racial groups having consistently low rates of MS, for example black Africans (Dean, 1967) and East Asians (Kuroiwa *et al.*, 1983; Yu *et al.*, 1989). There is a trend for the prevalence to increase with latitude, even in countries that are relatively racially homogenous (Kurtzke *et al.*, 1979; Kuroiwa *et al.*, 1983; Skegg *et al.*, 1987; Hammond *et al.*, 1988b). Such regional and racial differences suggest that both genetic and environmental factors play a part in the development of MS.

1.2.1 Genetic factors

A striking finding in MS is that major differences in prevalence occur in populations of different ethnic backgrounds living in close proximity, for example prevalence in Malta (4.2 per 100,000) and the neighbouring island of Sicily (53.3 per 100,000) (Dean *et al.*, 1979; Vassallo *et al.*, 1979). These differences are difficult to explain purely in environmental terms because of the geographical similarities of the areas.

Additional genetic evidence comes from familial studies. Population–based twin studies show a concordance rate in monozygotic pairs of around 30% and dizygotic pairs 3-5% (Bobowick *et al.*, 1978; Heltberg and Holm, 1982; Kinnunen *et al.*, 1988; Sadovnick *et al.*, 1993; Mumford *et al.*, 1994), whilst the lifetime risk in first-degree relatives of patients with MS is also 3-5% (Sadovnick and Baird, 1988; Sadovnick *et al.*, 1988). Further, the concordance rate for MS is similar in half-siblings raised together and apart (1.2% and 1.5% respectively) (Sadovnick *et al.*, 1996), indicating that differing environmental factors have minimal influence on this group.

MS appears to be polygenic with each polymorphism exerting a contributory effect (Compston, 1999). However, few definite chromosomal regions have been identified. It is known that a factor in the HLA class II region on the short arm of chromosome six plays a role, particularly the HLA-Dw2 haplotype is associated with an increased risk of the disease (Hillert and Masterman, 2001). It is also possible that carriers of the apolipoprotein-ϵ4 allele may have an unfavourable course of MS (Enzinger *et al.*, 2004) however other studies have not noted this phenomenon (Weatherby *et al.*, 2000).

1.2.2 Environmental factors

Evidence against a purely genetic aetiology exists, particularly the relatively limited concordance in monozygotic twins – when one considers the concordance of other diseases such as type II diabetes mellitus - and the unpredictable pattern of inheritance from pedigree studies. Also the distributional data cannot be solely explained by genetic influences, especially in Australia where a 5-fold gradient of prevalence exists from south (higher) to north (lower) (Hammond *et al.*, 1998b). Moreover, it has also been shown that whilst MS is uncommon in the Caribbean, the risk increases substantially for first generation Afro-Caribbean descendants raised in the UK (Compston and Coles, 2002). In addition, people migrating to South Africa from Northern Europe as adults have been shown to retain their high European risk, whilst those migrating in childhood acquired the lower risk evident in the Southern African population, suggesting that MS susceptibility occurs during childhood (Dean, 1967). Hence, environmental factors – possibly acquired relatively early in life - are thought to play a significant role in the aetiology of MS.

The evidence for an environmental factor or factors has led to speculation of an infective agent, for instance Epstein Barr Virus (Martyn 1997; Sundstrom *et al.*, 2004). Other postulated triggers include; (i) surgery, anaesthesia and other forms of physical trauma (Goodin *et al.*, 1999); (ii) immunisation (Rutschmann *et al.*, 2002); (iii) ultraviolet light and subsequent vitamin D production (Hayes *et al.*, 1997) and (iv) diet (Lauer, 1997). No definite data exists and current evidence suggests that environmental factors may interact with a susceptible genetic make-up, possibly at an age of greatest potential risk, resulting in the triggering of the condition at a later date.

1.3 Clinical course and diagnosis

1.3.1 Symptoms and signs

MS can affect any part of the CNS, although certain areas are more susceptible giving rise to symptoms and signs which, although rarely pathognomonic, are often characteristic for the disease (Paty and Ebers, 1997). Most often the affected structures are the optic nerves, cervical spinal cord, brainstem and cerebellum (O'Connor, 2002). Although lesions in the cerebral white matter are common they are less likely to manifest clinically. Table 1.1 lists the most common symptoms experienced as seen in a community study (Paty and Ebers, 1997; O'Connor, 2002).

Patients also suffer from symptoms not related to a specific anatomic area, such fatigue (seen in up to 80% of patients) (Roelcke *et al.*, 1997) and cognitive changes - especially deficits of attention and executive function - as well as short term memory and verbal intellectual ability loss (seen in 30-70% of cases) (Piras *et al.*, 2003). Cognitive deficits are also partially correlated with the lesion load seen in the cerebral hemisphere white matter on MRI (Hohol *et al.*, 1997).

The onset for most patients (85%) is with relapses and remissions. The frequency of these events varies between 0.14 to 1.1 per patient per year (Weinshenker and Ebers, 1987) with increased risk in younger patients during the early stages of MS (O'Connor, 2002). Distinction is made from a 'pseudoattack' (a group of symptoms in which a precipitant cause can be attributed such as fever or infection) (McDonald *et al.*, 2001). Such events are thought to be due to a transient increase in the synthesis

of inflammatory mediators, such as nitric oxide, which may produce a reversible conduction block in previously demyelinated nerve pathways (Coles *et al.*, 1999). Further, paroxysmal symptoms which tend to be short-lived and stereotyped with similar distribution to a previous clinical relapse are common. These are likely to be due to hyperexcitability of previously demyelinated axons due to spontaneous trains of spurious impulses from a site of demyelination which can spread in either direction (Smith and McDonald, 1980).

Table 1.1 *The overall frequency of symptoms and signs seen in 50% or more of MS patients at any time (%) adapted from a community study (Paty and Ebers, 1997)*

Symptom and signs	**% Frequency**
Increased deep tendon reflexes	90
Sensory loss (most commonly in legs and implica the posterior columns of cord)	90
Leg weakness	90
Spasticity	90
Nystagmus	85
Bladder disturbance	80
Fatigue	80
Retinal fibre loss	80
Optic atrophy	77

Regarding the 15% of patients who present with progressive symptoms (primary progressive MS), in 80-90% the clinical presentation is of a cord syndrome, with a tendency to progress in the same system (Stevenson *et al.*, 1999). Other progressive syndromes include ataxia and (rarely) dementia or visual loss. Differences in symptomatology and signs of patients allows sub-grouping into differing clinical phenotypes to aid characterisation of the disease and allow improved prognostication.

Life expectancy in patients with MS is usually at least 25 years from disease onset with most patients dying from unrelated causes (Compston and Coles, 2002). Also, there is evidence that survival is improving (Brønnum-Hansen *et al.*, 2004).

1.3.2 Clinical phenotypes

Relative differences between patient groups allow sub-grouping into clinical phenotype categories which best describe the nature of an individual's disease. This was formally described in 1996 with four main types of MS recognised (Lublin and Reingold, 1996). These are: (i) *relapsing-remitting MS* in which there are clearly defined clinical relapses without significant progression in-between these events; (ii) *primary progressive MS* in which disease onset is associated with slowly evolving and progressive symptoms without relapses (Cottrell *et al.*, 1999); (iii) *secondary progressive MS* which occurs after an initial period of relapsing-remitting MS, where disease progression occurs with or without relapses and (iv) *relapsing progressive MS* where disease progression occurs from onset but there are also episodic relapses. The distinction between primary progressive and relapsing progressive phenotypes is debatable and often patients are classified only as primary progressive

(Kremenchutzky *et al.*, 1999). A further sub-division was created to describe patients (around 15% of all MS sufferers) who developed no significant disability over a sustained period of time (15 or more years), *benign MS* (Lublin and Reingold, 1996).

The majority of patients (85% approximately) initially present with the relapsing-remitting form with the remainder (15%) presenting with primary progressive MS (Runmarker and Andersen, 1993). In those who have experienced just one clinical relapse, i.e. a clinically isolated syndrome (CIS) suggestive of MS, further symptomatic and/or paraclinical investigative evidence is required for a formal diagnosis of MS (see later in this chapter). The time course of the relapsing-remitting phase varies with low age at onset, good recovery from first relapse, symptoms from afferent fibres only and onset in one region only associated with a better prognosis (Runmarker and Andersen, 1993; Eriksson *et al.*, 2003). However approximately two-thirds of all relapsing-remitting MS patients develop secondary progressive course within 25 years of symptom onset (Runmarker and Andersen, 1993).

1.3.3 Measurements of disability

Objective measurements of clinical dysfunction are important for measurement of disease progression or recovery and determination of efficacy of therapeutic intervention. The first commonly used scale was proposed in 1955, the Disability Status Scale (DSS) (Kurtzke, 1955). This was a graduated scale which, in steps, described the symptom range from normal function to death as a numbered scale. It was revised in 1983 to provide greater sensitivity, creating the Expanded Disability Status Scale (EDSS) (Kurtzke, 1983). The scale is based on the level of clinical

symptoms and/or signs in the following functional systems: (i) visual; (ii) brainstem; (iii) pyramidal; (iv) cerebellar; (v) sensory; (vi) bowel and bladder; (vii) cerebral and (viii) ambulation. From this, a combined score between 0 (normal neurological function) and 10 (death) may be calculated, in steps of 0.5 with increasing severity. From scores of 4.0 and above, the EDSS becomes more dependent on ambulation. The scale is in common usage and a primary outcome measure in treatment trials.

An additional disability assessment is provided by the MS functional composite (MSFC) score, a combined assessment of mobility (25 foot timed walk [TWT]), coordination (nine-hole peg test [PEG]) and cognition (three second Paced Auditory Serial Addition Test [PASAT]) (Cutter *et al.*, 1999). It is often used with the EDSS to provide additive information that is not as strongly influenced by ambulation. A further scale based on an algorithm which relates scores on the EDSS to the distribution of disability in a database of patients with comparable disease durations was also recently devised (Roxburgh *et al.*, 2005) and may offer more sensitive prediction of individual disability prognosis.

1.3.4 Disease progression

Natural history studies show some variability, but generally there is agreement that approximately 15 years from symptom onset most patients require a unilateral walking aid (Weinshenker and Ebers, 1987; Weinshenker *et al.*, 1989a), whilst the median time from onset of CIS (i.e. a single clinical event that is indicative of demyelination) to secondary progression is 19 years (Eriksson *et al.*, 2003). Long term MRI follow-up studies have shown a median EDSS at 14 years from onset of

clinical symptoms to be 3.25, signifying mild to moderate disability (Brex *et al.*, 2002).

A further study has shown that although the time course to reach moderate disability (i.e. limited walking but without aid; EDSS 4) varies and is influenced by factors such as gender, age, symptoms and clinical phenotype at onset, degree of recovery from first relapse and time to second relapse (Weinshenker *et al.*, 1989b); progression from this point to severe disability (i.e. wheelchair bound; EDSS 7) is relatively uniform and not influenced by the above factors (Confavreux *et al.*, 2003). This may suggest that there are at least two pathological substrates in MS, one associated with greater variability and dependent on patient factors, and the other more inevitable regardless of patient type and that they are present at different stages of the disease.

1.3.5 Diagnosis

Clinical history and examination findings remain the cornerstone diagnostic information in MS. Diagnostic criteria in MS have evolved primarily because of the increasing availability of paraclinical investigations such as information from cerebrospinal fluid (CSF) - to show evidence of intrathecal inflammation - visual evoked potentials (VEP) – to reveal altered nerve conduction in keeping with demyelination - and more recently MRI.

In 1983, Poser et al (Poser *et al.*, 1983) devised a 'New Diagnostic Criteria' for MS which had roots in a previously used scheme (Schumacher *et al.*, 1965) but was able to incorporate confirmatory investigations such as VEPs, CSF and neuroimaging (at

the time, this was mainly computerised tomography). The basis of diagnosis was the clinical demonstration of lesions disseminated in time and space between the ages of 10-59 years at onset by a competent neurologist once other possible diseases had been considered. These criteria allowed a patient to be classified as either definite or probable with further subdivision depending on the relative levels of clinical and laboratory supported evidence (see Table 1.2). This scheme gained wide acceptance in clinical and research use.

Table 1.2 *Poser, et al diagnostic criteria (Poser et al., 1983)*

Category	**Relapses**	**Number of CNS sites involved**		**Paraclinical evidence**	**CSF oligoclonal bands**
1. Clinically	2	2			
definite	2	1	and	1	
2. Laboratory	2	1	or	1	+
supported	1	2			+
definite					
3. Clinically	2	1			
probable	1	2			
	1	1	and	1	
4. Laboratory	1	1	and	1	+
supported	2				+
probable					

1.3.6 Typical MRI appearances

Following publication of the Poser criteria (Poser *et al.*, 1983) MRI with its sensitivity to pathological change associated with MS, became available (Ormerod *et al.*, 1987; Miller *et al.*, 1998; Arnold and Matthews, 2002). A typical finding (in greater than 95% of patients with clinically definite MS and 50-70% with a CIS) is multiple hyperintense lesions in the white matter on a T_2-weighted sequence (Ormerod *et al.*, 1987; Miller *et al.*, 2004a). The presence of a gadolinium-enhancing lesion on a post-contrast T_1-weighted scan correlates with disruption of the blood brain barrier (BBB) and signifies an acute lesion (Miller *et al.*, 1998). However, the correlation of both these MRI measures with clinical disability as measured by the EDSS is weak (IFNB Study Group, 1995; Kappos *et al.*, 1999). A further observation on pre-contrast T_1-weighted images are so-called hypointense 'black holes' (Uhlenbrock and Sehlen, 1989) which some but not all investigators have found to correlate more strongly with EDSS over time (Truyen *et al.*, 1996).

Characteristic patterns of T_2-weighted hyperintense lesions have been ascribed to MS. Lesions should be multiple in nature, with at least one greater than 5mm in diameter. Periventricular, infratentorial and spinal cord lesions may be more specific for MS than other neurological conditions that can cause similar appearances (Arnold and Matthews, 2002). Corpus callosum and juxtacortical lesions are also characteristic.

Figure 1.1: *Examples of T1-weighted hypointense lesions (a) and T2-weighted lesions (b). See Figure 2.3 for examples of contrast enhancing lesions.*

Image (a) ***Image (b)***

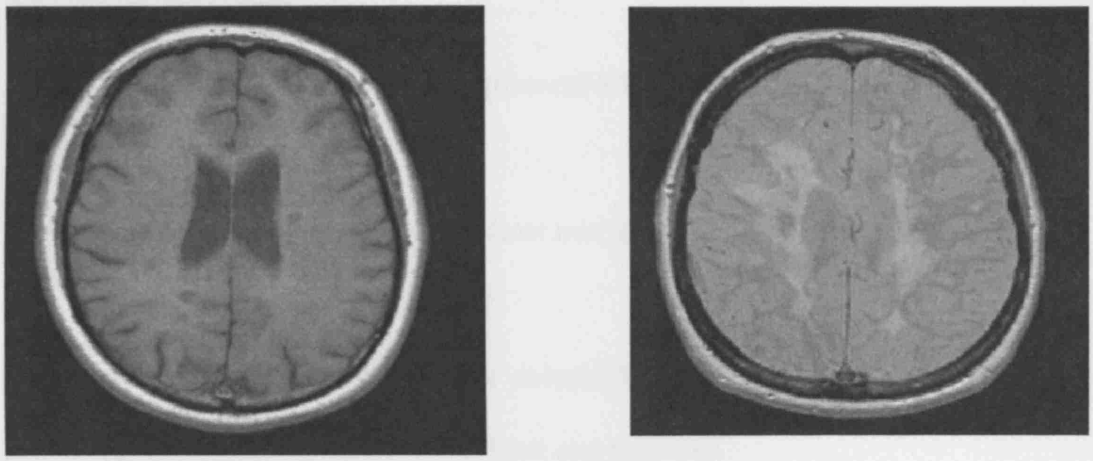

1.3.7 Recent MRI diagnostic criteria

Previous diagnostic criteria did not include primary progressive MS into its classification. To address this and to use the technology of MRI, a position paper for this clinical phenotype was published in 2000 (Thompson *et al.*, 2000). Three categories of certainty were employed - definite, probable and possible - and clinical and paraclinical investigative evidence was incorporated (see Table 1.3). Fluctuations in symptoms were allowed particularly in the context of infections or exercise.

Table 1.3 *Diagnostic criteria for primary progressive MS (Thompson et al., 2000)*

1.Definite diagnosis

(a) Clinical progression for at least one year *and*

(b) Positive CSF evidence *and*

(c) Positive MRI evidence *or* equivocal MRI evidence *and* delayed VEPs

2.Probable diagnosis

Either: (a) Clinical progression for at least one year *and*

(b) Positive CSF evidence *and*

(c) Equivocal MRI evidence *or* delayed VEP

or: (a) Clinical progression for at least one year *and*

(b) Positive MRI *or* equivocal MRI *and* delayed VEP

(CSF either negative or unavailable)

3.Possible diagnosis

(a) Clinical progression for at least one year *and*

(b) Equivocal MRI evidence *or* delayed VEP

Because of the diagnostic difficulty of this form of MS, particularly from conditions resembling it in which unmatched oligoclonal bands in the CSF are absent (Rudick *et al.*, 1986; Fieschi *et al.*, 1995; Zeman *et al.*, 1996), CSF had to be abnormal for a definite diagnosis of primary progressive MS to be made. Positive MRI evidence was considered to be: (i) nine brain T_2-weighted lesions; (ii) four to eight brain lesions and one spinal cord lesion and (iii) two discrete spinal cord lesions regardless of brain MRI findings. Equivocal evidence is provided by less than four brain lesions with one cord lesion; or between four and eight lesions in the brain with normal cord imaging.

McDonald et al criteria

The sensitivity to pathological change of MRI in MS also led to the formulation of new diagnostic criteria (McDonald *et al.*, 2001). Two categories of diagnosis were allowed: 'definite' and 'possible' (Table 1.4).

MRI abnormality criteria in keeping with MS were based on previous studies (Barkhof *et al.*, 1997; Tintoré *et al.*, 2000) and consisted of at least three out of four of: (i) One gadolinium-enhancing lesion or nine T_2 hyperintense lesions if there are no enhancing lesions; (ii) At least one infratentorial lesion; (iii) At least one juxtacortical lesion and (iv) At least three periventricular lesions. One spinal cord lesion may be substituted for one brain lesion. However, diagnosis still requires dissemination in time, which can be determined from MRI by: (i) a gadolinium-enhancing lesion on a scan at least three months after onset of a single attack at a different site *or* (ii) a new T_2 lesion on a scan at least three months after the clinical event.

Clinical evidence from the patient was still considered paramount and a diagnosis without paraclinical investigations possible if objective clinical relapses could be demonstrated that were disseminated in time and space. The new criteria also allowed diagnosis in certain patients with a CIS if they had suitable MRI criteria. Follow-up analysis has shown good specificity and sensitivity for subsequent development of clinically definite MS on clinical grounds alone (Dalton *et al.*, 2002a; Tintoré *et al.*, 2003) with one study showing the development of MS with the new criteria after one year to have a high sensitivity (83%), specificity (83%), positive predictive value

(75%), negative predictive value (89%), and accuracy (83%) for clinically definite MS at three years (Dalton *et al.*, 2002a). The criteria have been widely adopted.

Table 1.4 *McDonald et al diagnostic criteria (McDonald 2001)*

Clinical presentation	**Additional data needed for diagnosis**
Two or more attacks; objective evidence of 2 or more lesions	None
Two or more attacks; objective clinical evidence of 1 lesion	Dissemination in space: demonstrated by MRI *or* Two or more MRI lesions consistent with MS plus positive CSF *or* Await further clinical attack implicating different site.
One attack; objective clinical evidence of 2 or more lesions	Dissemination in time demonstrated by MRI *or* second clinical attack
One attack; objective clinical evidence of 1 lesion (CIS)	Dissemination in space demonstrated by MRI *or* at least two MRI lesions plus positive CSF *and* Dissemination in time demonstrated by MRI *or* second clinical attack
Insidious neurological progression suggestive of MS	Positive CSF *and* Dissemination in space demonstrated by MRI (as per MRI positive criteria in primary progres MS) *and* Dissemination in time demonstrated by MRI *or* continued progression for one year

1.3.8 Differential diagnosis

Other neurological conditions can give rise to multifocal disease and cerebral MRI abnormalities. Lesions associated with aging, migraine and lacunar infarcts tend to be more peripheral and randomly located or in the basal ganglia and are usually not visible on T_1 images and not associated with CSF abnormalities. Acute disseminated encephalomyelitis (ADEM) is a monophasic illness which may present similarly to MS. MRI lesions are, however, all of similar age and follow-up scanning can be useful in determining this: lesions often tend to resolve and new lesions are unlikely to appear (O'Riordan *et al.*, 1999). Devic's disease (neuromyelitis optica) is an inflammatory condition confined to the optic nerves (often bilaterally) and spinal cord. MRI lesions in the brain are rare and spinal cord lesions tend to extend for more than two vertebral bodies (Poser and Brinar, 2004).

Other vasculitides such as systemic lupus erythematosus usually affect white matter more peripherally than MS and often present with a greater degree of psychiatric symptoms. Blood testing for inflammatory markers, and auto-antibodies (especially double-stranded DNA and anticardiolipins) may be helpful in distinguishing between the conditions. Other infectious conditions such as Lyme disease, progressive multifocal leukoencephalopathy and Human Immunodeficiency Virus may also present with evolving central neurological symptoms and often serum and CSF serology is necessary to rule out these diagnoses. Neurosarcoidosis can present similarly to MS, and require Gallium scanning and/or biopsy (Arnold and Matthews, 2002). Serum and CSF angiotensin converting enzyme measurement can have some value in monitoring disease progress but are often unhelpful diagnostically.

1.4 The pathogenesis of MS

1.4.1 Introduction

The most widely recognised pathological feature of MS is the demyelinated plaque. They have a predilection for areas such as the optic nerves, periventricular regions (particularly around the lateral and fourth ventricles), corpus callosum, corticomedullary junction, subpial section of the brainstem and the cervical spinal cord (Weinshenker *et al.*, 1989a). The main histopathological features of demyelination, relative preservation of the axons, gliosis and inflammation have long been described (Charcot, 1868), and a possible relationship between MS lesions and blood vessels recognised (Rindfleisch, 1872).

The variability in presentation and natural history amongst MS patients has lead to speculation as to whether MS is a combination of disease types (Revesz *et al.*, 1994; Compston and Coles, 2002). The evidence of multifocal aetiologies with variable response to present therapies for MS (Lucchinetti *et al.*, 2000) reinforces this possibility. The clinical effect of current therapies in MS shows some efficacy in reducing clinical relapses but little benefit in preventing or minimising increasing progressive disability (Compston, 2004). This implies that a complex pathological mechanism exists in MS, possibily involving a number of processes.

The BBB is the structure which theoretically separates the CNS parenchyma from circulating peripheral molecules and cells (Minagar and Alexander, 2003). It is made up of highly organised junctions between endothelial cells (tight junctions and

adherens junctions) and provides structural integrity in which there is normally no major histocompatibility complex (MHC) expression thus minimising presentation of CNS antigen to circulating T lymphocytes. A highly developed transport system and support network (provided by pericytes, astrocytes and perivascular macrophages) complete the functional barrier (Minagar and Alexander, 2003; Bradl and Hohlfeld, 2003). Within the CNS, oligodendrocytes synthesise and maintain the myelin sheath covering around neuronal axons. Myelin functions as an insulating segmented coating allowing the normal propagation of saltatory axonal conduction.

Disturbances to the BBB are associated with MS (Tofts and Kermode, 1989; Adams, 1989; Kwon and Prineas, 1994; Brück *et al.*, 1997; Lassmann *et al.*, 1998b; Minagar and Alexander, 2003). Once breached damage occurs to the myelin sheath with subsequent delay of saltatory conduction and this leaves the now exposed axon vulnerable to potentially irreversible damage leading to persisting disability (Compston and Coles, 2002).

1.4.2 The inflammatory evolution of lesions

There is strong evidence of an inflammatory chain of events in MS in which the integrity of BBB is disturbed allowing peripheral inflammatory cells to enter the CNS. A secondary inflammatory reaction within the CNS propagated by cytokines and chemokines produced by these inflammatory cells occurs resulting in focal demyelination and subsequent axonal loss with possible recovery or gliosis and neurodegeneration (Compston and Coles, 2002; Minagar and Alexander, 2003). This may be associated with a clinical relapse event. Greater amounts of inflammation are

noted in relapsing-remitting and secondary progressive clinical types in comparison to primary progressive MS (Thompson *et al.*, 1991; Revesz *et al.*, 1994; Lucchinetti and Brück, 2004).

CD8+ T cells dominate the T cell populations involved in the inflammatory response and these show pro-inflammatory Th1-like lymphokine profile (Martino *et al.*, 2002; Bradl and Hohlfeld, 2003). The exact trigger for the initial activation of peripheral inflammatory response is unknown. There is evidence that the frequency of clinical events may be increased in the presence of a clinical infection, possibly suggesting that a virus or toxin precipitant, perhaps displaying a similar antigen profile to a self-antigen within the CNS, is responsible (Bradl and Hohlfeld, 2003).

Activated peripheral T-lymphocytes express adhesion molecules and up-regulate the crossing of the BBB by damaging its integrity. The resulting inflammatory cellular infiltrate into the CNS re-encounters immunologically indistinguishable specific self-antigen and sets up an inflammatory reaction mediated by T-cells, macrophages and microglia (which in-turn express class II MHC molecules which activates antibody production) with the release of factors (such as tumour necrosis factor (TNF)-α) causing the proliferation and propagation of the response and setting up a pro-inflammatory loop (Compston and Coles, 2002). Myelin and its supporting cells (oligodendrocytes) are opsonised by microglia causing demyelination and blocking saltatory conduction of an action potential and a visible lesion (Compston, 2004). In addition, nitric oxide (generated in inflammatory lesions) may act on axons transiently blocking conduction and can also cause irreversible damage by impairing mitochondrial-derived energy supply to axons (Bjartmar *et al.*, 2003; Stys, 2004).

A 'hypoxic' metabolic state may be generated by the inflammatory response due to: (i) toxic metabolites interfering with mitochondrial energy metabolism; (ii) oedema from BBB leakage causing disturbance of the microvasculature; (iii) inflammatory reaction to the vessel wall potentially mediated by the clotting cascade or cytokines produced by inflammatory cells and (iv) direct damage on endothelium by cytotoxic T-lymphocytes. This can cause thrombotic occlusions of microvessels noted pathologically in severe acute MS lesions and in Devic's disease (Lassmann, 2003a); although this is unlikely to be a mechanism of tissue damage in most MS lesions and patients.

A further histological finding in acute lesions is remyelination, the process of recovery from demyelination with structural repair (Compston and Coles, 2002; Brück *et al.*, 2003). This process has been noted to occur early in lesion genesis and can co-exist with ongoing demyelination and is generally more successful in lesions which still retain large numbers of macrophages (Brück *et al.*, 2003). From this, recovery of function may be possible.

1.4.3 Acute inflammatory axonal transection

MS had historically been considered a demyelinating disease where axons were relatively spared. However, evidence now shows that not only does axonal loss occur in MS, but that it starts in the acute setting.

Immunochemistry studies measuring amyloid precursor protein (APP), a marker of axon damage, have revealed axonal transection with subsequent distal degeneration

both in acute lesions and periplaque white matter, with an average axonal loss in lesions of between 30-82% (Ferguson *et al.*, 1997; Trapp *et al.*, 1998; Bitsch *et al.*, 2000; Kuhlmann *et al.*, 2002; Lassmann, 2003b). The highest degree of axonal loss is associated with active demyelination usually within two weeks of its onset (Kuhlmann *et al.*, 2002; Lassmann, 2003b). Evidence of an inflammatory mechanism is given by the correlation between axonal damage and CD8+ cytotoxic T cells and microglia (Trapp *et al.*, 1999; Bitsch *et al.*, 2000; Kuhlmann *et al.*, 2002). Also, axonal loss appears to occur in early disease in the relapsing-remitting and secondary progressive phenotypes in comparison to primary progressive MS (Bitsch *et al.*, 2000; Kuhlmann *et al.*, 2002). It is not clear if the axonal damage indicated by APP positive staining is permanent or transient (Ferguson *et al.*, 1997).

The process of axonal injury is complex and involves disturbance of the axoplasmic membrane causing an influx of calcium molecules leading to disintegration of the axonal cytoskeleton (Lassmann, 2003b). Small fibre loss is most prevalent (Lassmann 2003b; DeLuca *et al.*, 2004). The mode by which this occurs may be from direct immune attack or 'bystander injury' where demyelination leaves the axon exposed to the surrounding inflammatory milieu (O'Connor, 2002).

1.4.4 Acute lesion heterogeneity

From a study in which lesions were sampled from patients at biopsy, histological appearances suggested that acute MS lesions may be classified into different types reflecting the basis of myelin protein loss, the geography and extension of plaques, mechanism of oligodendrocyte destruction and degree of complement activation

(Lucchinetti *et al.*, 2000). Four differing patterns of active lesion are described (see Table 1.5), with individual patients said to express one type of lesion only.

Table 1.5: *Patterns of lesion heterogeneity (Lucchinetti et al., 2000)*

Lesion type	Neuropathological findings
Type I	(a) Active inflammatory demyelination with remyelination
	(b) Sharply defined lesion edge
	(c) Perivenous distribution
	(d) Variable oligodendrocyte loss at lesion border
Type II	(a) As Type I ***with also:***
	(i) Local deposition of immunoglobulin and complement
Type III	(a) Active inflammation but no remyelination
	(b) Poorly defined lesion edge extending into adjacent areas
	(c) Pronounced oligodendrocyte apoptosis
	(d) Not centred around vessels
Type IV	(a) Perivenous inflammation with no remyelination
	(b) Sharply defined lesion edge
	(c) Oligodendrocyte loss in adjacent white matter
	(d) No apoptosis

The reason for lesion differences is unclear, but may be related to disease duration and/or severity, previous lesions and patient susceptibility (Lucchinetti *et al.*, 2000). It should be stressed however, that these lesions were biopsied because of diagnostic

doubt due to atypical appearance and hence it is uncertain how representative they are of MS lesions as a whole.

All lesion types occur in the presence of the inflammatory infiltrate as described earlier. A large degree of similarity exists between the differing patterns. In order of frequency, types II, III, I and IV are the most common, with type IV lesions particularly rare and possibly only seen in primary progressive subjects (Lucchinetti *et al.*, 2000). Types I and II were seen in all clinical phenotypes of MS, whilst type III observed where disease duration was less than two months. It is unknown if the lesion types in a particular patient progress into another type as the lesion becomes more established. Areas of complete remyelination, shadow plaques, were noted to be sharply demarcated with uniformly thin myelin sheaths throughout and no signs of axon destruction (Lucchinetti *et al.*, 2000; Kuhlmann *et al.*, 2002).

A recent report in a severe acute relapsing-remitting case, noted lesions similar to Type III, except that more profound apoptosis of oligodendrocytes and microglial activation were seen with areas of complement activation and evidence of remyelination (Barnett and Prineas, 2004). The authors speculated whether this lesion type was the initial lesion event in the acute development of plaques in MS. It was however noted that the severity of the case made it somewhat atypical and that further studies are required (Trapp, 2004; Barnett and Prineas, 2004).

1.4.5 Grey matter and normal appearing white matter

Macroscopically normal white matter (so-called normal-appearing white matter (NAWM)) has attracted interest particularly in view of the poor correlation between T_2-visible lesions and clinical disability (Miller *et al.*, 1998). This led to speculation that the pathological processes involved are more diffuse than first appreciated. Furthermore, although visible MRI lesions are seen only in white matter, there is evidence of grey matter involvement in the disease.

A histological study of NAWM in patients with established MS revealed abnormalities in 72% of the samples, with the main findings being: (i) astrocytic activation and proliferation leading to gliosis and (ii) unsuspected demyelination (Allen and McKeown, 1979). In patients with clinically less severe MS, milder abnormalities were noted consisting of astrocytic proliferation and gliosis and also sclerosis of blood vessels, perivascular inflammation and some areas of demyelination (Allen *et al.*, 1981). Damage to the BBB with inflamed microvessels is also seen microscopically in the NAWM (Martino *et al.*, 2002). Axonal loss possibly secondary to Wallerian degeneration (destruction in distal areas relating to a demyelinated plaque) has also been noted in NAWM (Evangelou *et al.*, 2000; Lassmann, 2003b; Lucchinetti and Brück, 2004).

The presence of grey matter lesions associated with MS has become widely recognised (Kidd *et al.*, 1999; Peterson *et al.*, 2001). These demyelinating lesions are less obvious macroscopically and histologically than their white matter counterparts,

have fewer inflammatory cells and are noted to have extensive neuroaxonal injury (Peterson *et al.*, 2001; Bjartmar *et al.*, 2003; Trapp, 2004; Lassmann, 2004).

1.4.6 The mechanisms of recovery

Particularly in the early stages of the condition, MS is associated with good functional recovery. A number of factors may be important: (i) damage to axonal fibres may be repaired (remyelination); (ii) neuronal pathways may adapt to compensate (plasticity) (Werring *et al.*, 2000b) and (iii) enough axons in the demyelinated area have remained sufficiently intact that once the transient inflammatory infiltrate has eased and conduction block removed, clinical function may recover by the insertion of sodium channels along the demyelinated membrane thereby facilitating non-saltatory conduction (Compston and Coles, 2002).

Remyelination is the process in which new myelin sheaths are restored to demyelinated axons enabling them to carry action potentials and recover lost function (Franklin, 2002). It is associated with large numbers of remaining oligodendrocytes and new oligodendrocytes derived from pre-cursor cells in the demyelinated area. A sufficient number of these pre-cursor cells must be recruited and adequate differentiation into oligodendrocytes capable of remyelination must occur for the process to be successful. Remyelination occurs acutely in lesions and may need inflammatory cells (macrophages, T cells and released cytokines) to remove myelin debris and promote factors that activate astrocytes to produce myelin growth factors (Franklin, 2002). Successful and complete remyelination is visualised by neuropathologists as a shadow plaque with minimal axonal loss.

Most lesions, however, do not remyelinate (Trapp *et al.*, 1999). Recent studies have noted between 13-42% of lesions show evidence of remyelination and that completely denuded axons were less likely to undergo this process (Barkhof *et al.*, 2003; Schmierer *et al.*, 2004a). Possible causes of failure include: (i) deficiency of sufficient oligodendrocytes and/or their precursors and (ii) a lack of a sufficient stimulating environment to signal these cells and promote their differentiation (Barkhof *et al.*, 2003). It has also been speculated that as animals age or are exposed to repeated insult the ability of recruitment and differentiation of these cells may diminish thereby undermining remyelination (Franklin, 2002). Further, persisting astrocytic reactivity may cause gliosis which forms a seal preventing further remyelination taking place (Brück *et al.*, 2003; Compston, 2004).

1.4.7 Clinical substrates of the pathological processes

The different locations of plaques, variable extent of recovery and the complexity of the neuronal network are factors in how pathological mechanisms in MS reveal themselves clinically.

Demyelinated lesions exhibit blocked saltatory conduction giving rise to neurological deficit if they are in a clinically eloquent area. Additionally, these axons are unable to sustain conduction in 'adverse' conditions such as increase in ambient temperature causing symptoms of conduction failure, Uhtoff's phenomena. Demyelinated axons can also discharge spontaneously and show increased mechanical sensitivity giving rise to Lhermitte's sign (an 'electric-shock' sensation on bending the neck forward). Ephaptic transmission (cross-talk) can also arise between neighbouring demyelinated

axons causing paroxysmal symptoms such as trigeminal neuralgia (Compston and Coles, 2002).

Differing clinical phenotypes of MS have a basis in the pathological mechanisms of that individual subtype. In particular, primary progressive MS is associated with less inflammation and MRI visible lesions than its relapsing-remitting and secondary progressive counterparts, but does show evidence of ongoing axonal destruction (Thompson *et al.*, 1991; Lucchinetti and Brück, 2004; Matthews, 2004). This may explain the lack of clinical relapses and the progressive development of neurological dysfunction associated with the phenotype. It should also be noted that although clinical relapses present a defined neurological deterioration the actual relationship between these and the development of significant disability in relapsing-remitting MS is poor, and may suggest that a further chronic pathological mechanism exists (Confavreux *et al.*, 2003).

1.4.8 Chronic degeneration in multiple sclerosis

The inflammatory cellular infiltrate associated with demyelination decreases with time (Kuhlmann *et al.*, 2002). Strong evidence exists that axonal loss continues during clinical remission and is due to a chronic process in the absence of significant active inflammation (Trapp *et al.*, 1999). Evidence exists suggesting that after an initial inflammatory symptomatic relapsing-remitting course, a level of dysfunction is reached from which an inevitable and increasing level of disability then arises possibly related to a chronic progressive neurodegenerative process (Coles *et al.*, 1999; Rudick *et al.*, 1999a; Confavreux *et al.*, 2003; Maggs and Palace, 2004).

Histologically, chronic MS plaques have: (i) a circumscribed hypocellular central region; (ii) no active myelin breakdown; (iii) prominent fibrillary gliosis; (iv) decreased axonal density; (v) decreased oligodendrocyte numbers and (vi) variable degrees of inflammation (Lucchinetti and Brück, 2004). It has been shown that slow ongoing axonal destruction occurs in inactive demyelinated plaques with little or no inflammation and no remyelination (Lassmann, 2003b). This chronic process may start at disease onset, but because of initially good reparative capacity in patients, only later in the disease course - when the CNS is unable to compensate - a progressive course associated with increasing clinical dysfunction ensues (Confavreux *et al.*, 2003; Lassmann, 2003b; Noseworthy *et al.*, 2000). This 'threshold' for the development of disability may reflect: (i) lesion location; (ii) disease activity and (iii) genetic susceptibility (Bjartmar *et al.*, 2003).

A possible mechanism for axonal loss in chronically demyelinated lesions is the lack of myelin-derived trophic support these axons receive (Bjartmar *et al.*, 2003; Compston, 2004; Trapp *et al.*, 1999). These denuded axons are vulnerable to toxic substances like nitric oxide and TNF-α (Barkhof *et al.*, 2003). Further, a decrease in oligodendrocyte precursor cells present in chronic lesions makes remyelination fail in these areas (Brück *et al.*, 2003). Finally, chronic inflammatory axonal damage may occur due to inefficient clearance of blood borne inflammatory cells in the CNS, perhaps secondary to some persisting stimulus (Martino *et al.*, 2002). There is good correlation between the extent of axonal damage and disability (Davie *et al.*, 1995; Filippi *et al.*, 1995; Losseff *et al.*, 1996a; Losseff *et al.*, 1996b; De Stefano *et al.*, 1998; Wujek *et al.*, 2002).

1.4.9 Potential vascular role in pathogenesis

Interest into the role of blood circulation and perfusion in the pathogenesis of MS exists for several reasons. Lesions in MS have a significant vascular component (Lucchinetti *et al.*, 2000; Kirk *et al.*, 2004). In addition, factors released during the inflammatory cascade are known to promote angiogenesis (the process leading to the development of new blood vessels from pre-existing ones) (Kirk *et al.*, 2004). These include adhesion molecules, TNF-α, nitric oxide and vascular endothelial growth factor (VEGF).

Angiogenesis is involved in a number of inflammatory diseases (for example rheumatoid arthritis). Blood vessels within MS lesions show irregular morphology and proliferation consistent with angiogenesis (Lassmann, 2003a; Kirk *et al.*, 2004). The precise significance of this in MS is not fully understood but provides further avenues of investigation.

1.4.10 Magnetic resonance imaging correlates of pathogenesis

Focal T_2-weighted lesions are seen in greater number in relapsing-remitting and secondary progressive disease than primary progressive subjects (Thompson *et al.*, 1991; Lycklama à Nijeholt and Barkhof, 2003). Pathological correlates of these lesions are heterogeneous and may signify demyelination, inflammation and oedema, axonal loss and remyelination (Miller *et al.*, 1998; Barkhof *et al.*, 2003). Inconsistencies remain regarding T_1 hypointensity in lesions and axonal loss. Some studies have suggested an association (Van Waesberghe *et al.*, 1998; Van

Waesberghe *et al.*, 1999) whilst a recent pathological study showed no significant difference in axonal density between hypo and isointense lesions (Schmierer *et al.*, 2004a).

Gadolinium-enhancing lesions indicate breakdown of the BBB and are correlated with histopathological features of inflammation (Katz *et al.*, 1993; Brück *et al.*, 1997). The size and intensity of enhancement depends on: (i) the intravascular concentration of gadolinium; (ii) the permeability of the BBB and (iii) the volume of the leakage space (Martino *et al.*, 2002). Two patterns of enhancement exist: (i) homogenous; and (ii) ring-enhancing. Eighty per cent of enhancing lesions appear hypointense on pre-contrast T_1-weighted scans (possibly representing demyelination and/or oedema); by 6 months 50% of these are isointense. Ring-enhancing lesions are more likely to remain hypointense after 6 months (Van Waesberghe *et al.*, 1998). Where persisting hypointensity is demonstrated irreversible structural changes are likely.

Lesions in the spinal cord affect both grey and white matter and the main pathological substrates are demyelination and inflammation and possibly gliosis rather than axonal loss (Lycklama à Nijeholt *et al.*, 2003). Cervical cord atrophy has been observed in patients with progressive disease (Losseff *et al.*, 1996b). The lack of correlation between this atrophy and loss of axonal density in cord tracts suggests that factors such as inflammation and oedema and astrocytic proliferation may temporarily mask volume loss. Over time cord atrophy is then revealed as inflammation and oedema decreases (De Luca *et al.*, 2004).

Brain volume MRI studies have shown greater degrees of atrophy in all clinical phenotypes of MS – especially secondary progressive - in comparison to controls, which correlates with axonal loss and disability (Ge *et al.*, 2000; Lycklama à Nijeholt *et al.*, 2003). The poor correlation between MR-visible lesions and atrophy suggests that factors other than degeneration secondary to lesions are involved (Pelletier *et al.*, 2003).

Less inflammation is noted in plaques in primary progressive MS compared with the secondary progressive phenotype (Thompson *et al.*, 1991), whilst secondary progressive MRI abnormalities suggest a greater degree of axonal damage in comparison to both primary progressive and relapsing-remitting patients (Van Waesberghe *et al.*, 1998; Bitsch *et al.*, 2000).

1.4.11 Roles of inflammation and neurodegeneration in pathogenesis

Two over-riding pathological mechanisms have been described, inflammation and neurodegeneration. How these two processes interact is not fully understood.

Inflammation had been thought of as the main mechanism causing disability and progression. A possible mechanism for this is epitope spreading in which T cell autoreactivity against initially a single antigen then spreads and shift to a larger number of secondary autoantigens rendering the body more likely to mount an autoimmune response to a presented antigen (Tuohy *et al.*, 1998; Bradl and Hohlfeld, 2003). Additionally, relapses due to inflammation can cause persisting disability (Lublin *et al.*, 2003). Further evidence for the role of inflammation in disability

includes: (i) inflammatory demyelination is particular to MS; (ii) post-mortem of acute severe cases of MS show florid inflammatory changes; (iii) the extent of axonal injury correlates with the number of activated microglia (Trapp *et al.*, 1999; Bitsch *et al.*, 2000; Kuhlmann *et al.*, 2002) and (iv) diffuse white matter injury is associated with a diffuse inflammatory reaction (Lassmann, 2003b).

The complexity of the role of inflammation is demonstrated by evidence for the beneficial effects of the inflammatory response in MS. Neuroprotective molecules (for example brain derived neurotophic factor (BDNF)) and cytokines (for example interleukin-4) are released by T-cells and macrophages. These promote neuronal survival and suppress the autoimmune response and may help remove toxic substances from the initial response preventing secondary demyelination (Martino *et al.*, 2002; Bradl and Hohlfeld, 2003). Macrophages also promote remyelination by stimulating proliferation of oligodendrocyte precursor cells (Martino *et al.*, 2002). However, initially in a clinical relapse these effects may be too weak to outweigh the harmful effects (Hohlfeld *et al.*, 2000; Bradl and Hohlfeld, 2003). It is possible though that these beneficial effects are partly responsible for maintaining remission following an event (Minagar and Alexander, 2003; Antel and Owens, 2004).

There has been consideration about the actual role of the inflammatory response in MS and how it relates to clinical course and disability (Trapp, 2004). Evidence that non-inflammatory mechanisms cause disability and progression include: (i) inflammatory lesions are poorly predictive of later disability; (ii) progressive phenotypes of MS are often associated with less inflammation but more disability and

(iii) current therapies have a more pronounced anti-inflammatory effect on MRI than clinical benefit for patients (Kappos and Duda, 2002).

In the light of this, a possible hypothesis is that a slow on-going neurodegenerative process starts early in the course of MS, but because of early CNS compensation for this, an inflammatory relapse symptomatology predominates initially which slowly burns out over time. The reparative mechanisms associated with the inflammatory phase and ongoing chronic degenerative losses are eventually exhausted when a 'threshold' of neuronal loss is reached and a symptomatic progressive course then ensues. The 'threshold' is likely to vary between patients depending mainly on the extent of previous disease course and genetic susceptibility. Another hypothesis is that while inflammatory events come first, a point is reached where neuroaxonal loss occurs as a secondary but autonomous problem due to lack of trophic support from widespread and persistent demyelination.

1.5 Current management strategies

Two main approaches exist towards current management: (i) symptomatic/supportive measures and (ii) disease modifying therapies.

1.5.1 Symptomatic and supportive measures

At initial diagnosis, the patient may have little or no clinical dysfunction. At this stage, often the most important intervention is providing information. Contact with a specialist nurse service (if available) and support societies can be helpful.

Depending on the level of disability multidisciplinary services such as occupational therapy, physiotherapy, speech and language therapy and neuro-rehabilitation are useful with an increasing evidence base regarding the efficacy of such strategies (Freeman *et al.*, 1997; Freeman *et al.*, 1999).

Certain common symptoms are partially amenable to pharmacological therapy. These include spasticity, bladder dysfunction, neuropathic pain, fatigue, depression and sexual dysfunction. Corticosteroids have been employed for increasing the rate of natural recovery following clinical relapse. Three or five day intravenous courses of methylprednisolone or oral courses of prednisolone have been shown to be effective in this regard (Milligan *et al.*, 1987; Barnes *et al.*, 1997). However, the use of steroids has not been shown to affect the long-term clinical outcome (Beck *et al.*, 1992).

1.5.2 Disease modifying therapies

Interferon beta (BIFN), in two forms (1a- Avonex, Rebif; 1b- Betaferon), and Glatimer acetate (Copaxone) are licensed for use in relapsing-remitting MS patients who meet set criteria introduced by the Association of British Neurologists in line with trial data, requires the patient to have experienced at least two clinically significant relapses in the last two years and to be sufficiently mobile (Chilcott *et al.*, 2003). These drugs are partially effective, decreasing relapses by a third and having minimal effect on overall disability (IFNB MS Study Group, 1993; IFNB MS Study Group *et al.*, 1995; Johnson *et al.*, 1995; Jacobs *et al.*, 1996; PRISMS Study Group, 1998). Prescribing in the United Kingdom is coordinated under the government's risk-sharing scheme (Phillips, 2004) and annual assessment is taking place to determine the long term efficacy and cost effectiveness of the medication.

Studies investigating these drugs use in progressive clinical forms of MS have been largely negative and hence BIFN is only used if concurrent relapses in these patients are significantly responsible for overall clinical dysfunction (European Study Group, 1998; SPECTRIMS, 2001).

Other potential disease modifying therapies have been investigated. Mitoxantrone has been shown to decrease relapse rate and partially help clinical dysfunction in small scale trials but is associated with significant adverse effects and is therefore only used in cases of substantial worsening and/or treatment failures from first line therapies (Edan *et al.*, 1997; Millefiorini *et al.*, 1997; Hartung *et al.*, 2002).

1.5.3 Emerging therapies

Natalizumab (a humanised monoclonal antibody against the $\alpha 4$ chain of $\alpha 4\beta 1$ integrin) in a phase II trial in relapsing-remitting patients offers promise (Miller *et al.*, 2003). It is thought to interfere with cell adhesion and transendothelial migration and regulate immune-cell activation and reduces the frequency of new MRI lesions. A phase III study has recently been completed and shown impressive efficacy with a two-thirds reduction in relapse rate and a halving of the rate of disability progression. However the future use of this therapy has become uncertain after two patients developed progressive multifocal leucoencephalopathy, a potentially life threatening viral infection of oligodendrocytes.

Campath-1H is a monoclonal antibody which depletes T cells and modulates their activity. A small scale study has suggested a potential anti-inflammatory effect in MS although this may be associated with significant adverse effects (Coles *et al.*, 1999); a phase III trial is in progress comparing Campath-1H versus BIFN.

Anecdotal evidence exists for the use of cannabinoids for symptomatology in MS, particularly spasticity. However, a recent double-blind study showed only subjective rather than objective improvements and the drug is under further assessment (Zajicek *et al.*, 2003).

1.6 Conclusions

MS is a complex disease. Consequently, current treatments are only partially effective and prognostic information given to patients cannot be definitive. An improved understanding of disease development and pathogenesis is essential for furthering clinical understanding and therapeutic options. MRI offers an *in-vivo* tool to help determine this and technological advances have the potential to reflect these disease processes thus providing an insight into possible causation and identify suitable pharmaceutical interventions.

The following chapter provides an explanation of the development of MRI and how new quantitative parameters derived from this technology are offering greater scope in our understanding of the disease and may provide potential surrogate markers.

CHAPTER 2

Magnetic Resonance Imaging

2.1 Basic Principles

MRI is a non-invasive technique that can generate images with a high spatial resolution. It emits no ionizing radiation (unlike x-rays), thereby allowing repeated investigations on the same subject.

MRI is based on Felix Bloch's theory presented in 1946 which stated that any spinning charged particle (i.e. nuclei with an odd number of nucleons [protons and neutrons combined]) creates an electromagnetic field (Bloch, 1946). For instance, a hydrogen nucleus ("proton") is a charged particle, as it contains an unpaired proton, and this acts as though it were spinning to create a magnetic field, a magnetic dipole moment. A full description of this phenomenon is only possible using quantum mechanics, but for the purposes of this thesis a simple, classical, model is employed.

When a proton is placed in a magnetic field it will precess. The rate at which it precesses is given by the Larmor equation:

$$\omega = \gamma B_0$$

where ω = angular precessional frequency of a proton (Hz), γ = gyromagnetic ratio, and B_0 = strength of the external magnetic field (Tesla).

If an object is placed in a MRI scanner, then the magnetic field (B_0) generated by the magnet (usually at 1.5 Tesla) is orientated horizontally. Protons, when placed in this field, will align themselves either parallel (longitudinal) or anti-parallel (transverse) to this. The majority of protons will favour the parallel (lower energy) state with the difference between parallel and anti-parallel producing a small magnetic field (M_0 or longitudinal magnetization). If a radio frequency (RF) wave is then introduced, spins corresponding to the frequency of the RF pulse will change their alignment, thereby generating a NMR signal. Once the pulse has ceased, the signal generated can be measured as they return to their original state. In contrast, out of phase proton precession will cancel out any transverse magnetic fields.

As approximately 60% of the body is water, humans contain an abundant amount of hydrogen and this is used to generate MRI images. A pulse of radiofrequency energy is introduced into a sample in the presence of a magnetic field generated by the MRI scanner followed by the collection of RF signal emitted by the sample; the signal is then transformed into digital data which can be transformed into images. Spatial information is derived by 3 orthogonal gradient coils corresponding to the axes x, y and z in a three-dimensional coordinate system which generate magnetic field gradients, disturbing the overall magnetic field homogeneity. The gradients generated by each coil are referred to as:

(1) Slice select gradient

(2) Phase-encoding gradient

(3) Frequency encoding (readout) gradient

and for axial images these correspond to G_z, G_y and G_x respectively (Hashemi and Bradley, 1997).

2.1.1 Generation of an output signal

The output signal must be received in an oscillating form and must be in the transverse x-y plane. Hence, magnetization must be 'flipped' from the z axis into the (x-y) plane by means of the RF pulse with a magnitude given by the flip angle, α, determined by the amplitude and duration of the RF pulse. This generates an x-y magnetization vector which will precess at the same frequency as the individual protons and induces a voltage (the MR signal) in a receiver coil placed in the transverse plane.

2.1.2 T_1, T_2* and T_2 relaxation times

After the RF pulse has stopped, the protons return to their equilibrium position in alignment with the external magnetic field, termed 'relaxation'. Longitudinal magnetization increases back to its original size, M_0, over time (termed longitudinal relaxation and defined by the time constant, T_1) and the transverse magnetization generated by the RF pulse will reduce back toward zero due to the process of spin dephasing in which spins get out of phase due to either differences in the precession rates of the protons (termed transverse relaxation and defined by the time constant, T_2) or external magnetic field inhomogeneity.

Essentially the T_1 relaxation time describes the time taken for the protons to return back to their equilibrium state by giving back the energy they obtained from the RF pulse to their immediate environment (the 'lattice'). The T_2 relaxation time characterizes the rate at which the transverse magnetization component decays.

Unlike T_1, T_2 doesn't involve any net energy transfer. These two processes are independent of one another, with the rates dependent on tissue composition. The dephasing of protons in the transverse plane is also subject to any inhomogeneities in the main magnetic field; and this increases the rate of decay, described as T_2* ('T_2 star') decay, if not compensated for.

Different tissues have inherent T_1 and T_2 properties and these may be affected by pathological change. In tissues made up of large molecules with tightly bound protons (for example lipids or proteins) spins dephase rapidly due to a large number of spin-spin interactions and therefore have short T_2 relaxation times. A structure which contains large amounts of water has a longer T_2 due to its 'free' hydrogen protons. These variations are used in MRI to preferentially visualize and suppress structures.

2.1.3 Repetition Time and Echo Delay Time and Tissue contrast

The above terms describe the methods used to manipulate the way in which the received signal is generated and collected.

Spin echo sequences

The most common imaging (pulse) sequence is the spin echo sequence. A 90° RF pulse is applied tipping protons into the x-y plane and generating measurable transverse magnetization as described earlier. Phase coherence is then lost due to T_2* decay. To rectify this, a second RF pulse (an 180° refocusing pulse) is introduced to tip the protons by 180° in the transverse plane. The rephasing of protons and

detection of the signal is termed the echo, or echo collection. A variable echo delay time (TE) is introduced to allow manipulation of the amount of T_2 decay seen. The time between successive 90° pulses is the repetition time (TR).

Tissue contrast can be manipulated by varying the TE and TR of a sequence. If the TR is long, more time for T_1 recovery in the longitudinal plane occurs minimizing the effect of differing T_1 properties of tissue. Conversely, a short TR maximizes the difference between those tissues which have a fast T_1 recovery rate (eg lipids and proteins) and those which take longer (eg water). Tissues with a short T_1 appear bright, whilst those with long T_1 appear dark. If a short TE is used the difference between the amount of dephasing by different tissue types (with their inherent T_2 relaxation rates) is decreased, hence there is little T_2-weighting. To generate an image with high T_2 contrast (T_2 weighted) a long TE is used and tissues with a short T_2 (eg lipids and protons) appear dark whilst those with a longer T_2 (eg water) appear bright. A sequence with a long TR and a short TE has neither strong T_1 nor T_2 weighting and the image is predominantly dependent on the concentration (density) of free protons in the tissue, a proton density (PD) weighted image (Hashemi and Bradley, 1997).

Summary: T_1 weighted scan: short TR/ short TE

T_2 weighted scan: long TR/ long TE

Proton density scan: long TR/ short TE

In the brain, CSF contains a large concentration of water and has a long T_1 and T_2. White matter is highly structured and consequently has a short T_1 and T_2. Grey matter is less structured but contains more macromolecules than CSF and therefore has

intermediate T_1 and T_2 relaxation times. MS lesions may have a decrease in structure making them detectable on MR images (see chapter one).

2.1.4 Image Formation

The output RF signal must be interpreted for image formation. Spatial information is imparted using the three gradients, one for each of the x, y and z coordinate directions, as previously discussed.

The bandwidth is a measure of the range of frequencies present in the signal. The slice-select gradient allows excitation of a slice of tissue corresponding to the bandwidth of the gradient RF pulse, exciting those protons with relevant Larmor frequency to the gradient pulse. Doing this sequentially in successive pulse sequences selects slices in a predetermined manner to cover the tissue under examination. The bandwidth and the amplitude of the slice-select gradient determine the slice thickness.

The frequency-encoding gradient is applied after the slice-select gradient when the echo is being received. This causes differing precession frequencies along the axis, such that each column of pixels has a different frequency. It is only applied when the signal is measured, and hence the signal strength at each frequency can be measured.

The phase-encoding gradient is applied after the RF pulse and provides spatial information about rows of pixels by causing a phase shift of the protons, with protons at different positions in the gradient precessing at a different frequency. It is applied prior to the frequency-encoding gradient and the process is repeated with phase-

encoding gradients of increasing amplitude, with a separate TR necessary for each phase encoding step. The number of repetitions of the pulse sequence is equal to the number of rows of pixels in the image. The matrix of an image describes the number of frequency encodes x the number of phase encodes (most commonly 256x256).

The vector of application of the three gradients dictates the plane of imaging undertaken (axial, sagittal, coronal or oblique), for 2D imaging the slice select gradient only determines the plane whilst the other gradients determine the in-plane orientation. The initial received signal – in so-called *k-space* - is a waveform that varies with time. It must be converted from the time domain to the frequency domain using the Fourier transform, devised by an eighteenth century French mathematician. Each TR represents a single phase-encoding step, and each echo fills a line of *k-space*. As the TR is always larger than the TE, more than one slice can be sampled with the same phase encoding gradient per TR. Once *k-space* is filled a Fourier transformation is performed in which data for each pixel is constructed to form an image.

Signal-to-noise ratio (SNR) is a measure of signal strength relative to background noise, and is an estimation of signal magnitude. It is proportional to the pixel volume, the square root of the number of phase encoding steps and number of excitations, and inversely proportional to the bandwidth.

Field of view (FOV) defines the dimensions of the area studied and is directly proportional to the bandwidth and inversely proportional to the readout gradient.

2.2 Basic Imaging Sequences

2.2.1 Conventional Spin Echo

After a 90° RF pulse, a free induction decay (FID) is formed. At a time, TE, after this first pulse (time TE/2 after the first 180° refocusing pulse) the spin echo is received. A subsequent whole train of 180° refocusing pulses can be used to produce further successive echoes, each with diminishing amplitudes due to T_2 decay, used for 'dual-echo' or multi-echo scans. The number of RF pulses and subsequent echoes can be varied, with a differing TE all occurring within the time of one TR.

Figure 2.1: *Spin-echo pulse sequence*

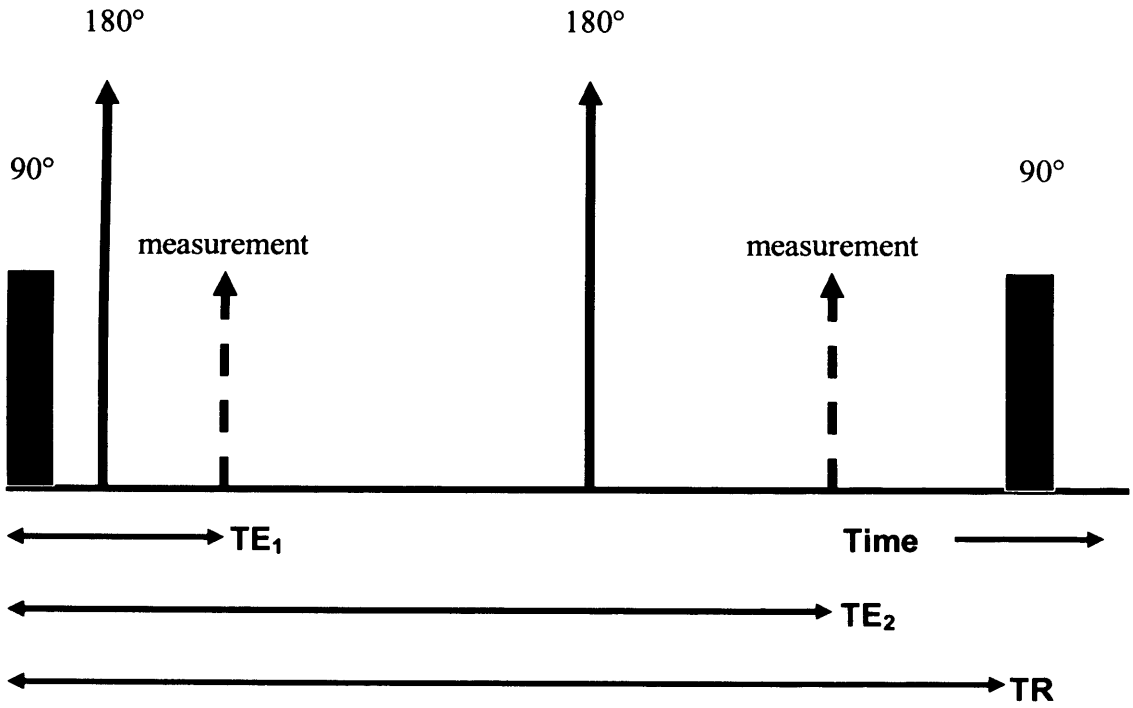

2.2.2 Fast Spin Echo

This variation of Conventional Spin echo (CSE) imaging uses multiple lines, determined by the echo-train length (ETL), to fill more *k-space* within one TR. For each phase-encoding step, the TR is repeated and the ETL dictates the number of images reconstructed. If the ETL=8 and there was 256 phase-encoding steps within *k-space*, then 32 (256/8) TRs are necessary to fill *k-space* rather than the full 256. The longer the ETL, the less number of slices produced due to the relative increase of time it takes to fill *k-space*. An increase in TR can avoid this, but this increases scan time.

Fast spin echo (FSE) decreases scan time without losing SNR allowing high resolution imaging and potentially reducing motion artifact. The trade-offs are: (i) a decrease in coverage and number of slices; (ii) change in contrast (as there is not just one TE) and (iii) 'point spread function' (enhancement or smoothing of small features).

2.2.3 Gradient Echo Imaging

Scan time may be reduced by using a small flip angle, α, thereby allowing a shorter TR. With a smaller α, even with small TR, enough longitudinal magnetization is still generated at the time of the next cycle. No 180° refocusing pulse is used to allow a small α, making the signal susceptible to T_2* rather than T_2 decay. The small α reduces T_1-weighting due to the quicker recovery of longitudinal magnetization associated with smaller pulse angles. Increasing the α, increases the TR and hence increases the T_1-weighting.

High resolution three dimensional gradient echo imaging

In inversion-recovery prepared fast spoiled gradient recall (FSPGR) sequences an inversion pulse can be added and the inversion time (TI) varied to give further control over the degree of T_1 contrast. The degree of T_1-weighting depends on the flip angle and repetition rate of the pulse sequence. The multi-planar nature of the sequence with short TE and TR increases slice number and SNR in a rapid time period allowing good temporal resolution and volume coverage.

2.2.4 Echo Planar Imaging

Echo-planar imaging (EPI) (Mansfield and Pykett, 1978) is a fast sequencing technique which uses high performance gradients to allow rapid on and off switching, to fill *k-space* after a single RF pulse (single shot EPI) with readout gradient during one T_2* decay, or multiple shots (multishot EPI) using multiple excitations.

Contrast depends on the pulsing sequence used. Spin echo-EPI employs an initial 90° RF pulse, then a 180° refocusing pulse, prior to the EPI readout. The technique provides T_1 and T_2 weighting, with contrast determined from the rephasing of the 180° RF pulse. In gradient echo-EPI, the 180° pulse is not used, making it susceptible to T_2* decay. Rapid imaging is possible with this technique. Inversion recovery (IR)-EPI employs a 180° pulse prior to a CSE sequence before EPI is used, and allows additional T_1 contrast.

A disadvantage of EPI is image artifacts, such as geometric distortions, caused by T_2* decay or fat/water chemical shifts and related to the long readout time required to generate the echo train. In addition, the sequence can be associated with tissue and bone artifacts for example at the base of the skull or vertebral column increasing the level of distortions around the posterior fossa of the brain and the spinal cord.

2.3 Quantitative Imaging Techniques

Using the above imaging sequences as a basis, newer MRI techniques have been developed which provide quantitative parameters to infer different structural pathologies. A number of these will now be considered in further detail.

2.3.1 Perfusion Imaging

(i) Introduction

Perfusion is a measure of blood supply to a tissue. It is used to describe the volume of blood passing through an organ normalised to the mass of the organ and is an indicator of tissue health and viability as it is, at least under normal conditions, coupled with parenchymal metabolism, reflecting the delivery of nutrients and oxygen and removal of waste products. The brain receives around 20% of total circulation hence changes in cerebral perfusion may play an important role in disease pathogenesis and monitoring. Perfusion can be determined with MRI by calculating the concentration of a magnetised tracer agent in the target area of interest. It is measured in units of millilitres of blood per gram of tissue per unit time, and requires tracers that diffuse freely between vascular and tissue compartments.

Estimations using single photon emission tomography (SPECT) and positron emission tomography (PET), have been undertaken in patients with MS (Brooks *et al.*, 1984). More recently MRI methods have been developed which potentially have greater spatial and anatomical resolution and do not require the use of ionising

radiation. There are two different techniques based on the type of tracer employed, either using exogenous tracer agents or endogenous arterial water. Perfusion is calculated from the serial measurement of tracer concentration as it passes through the target organ.

(ii) Exogenous bolus MRI methodologies

A paramagnetic substance, such as a gadolinium chelate, is used. Modelling assumes the tracer is wholly intravascular, and that any signal loss that occurs is due to susceptibility effects allowing first-pass kinetics of the agent to be applied (Rosen *et al.*, 1989). Dynamic imaging (high speed acquisition following a rapid injection of contrast) is most often used.

T_2 (spin echo) or T_2* (gradient echo) signal loss due to the intravascular bolus of gadolinium travelling through the capillaries generates a concentration-time curve in the imaging area (Rosen *et al.*, 1990). From this, relative values of cerebral blood flow (CBF), cerebral blood volume (CBV) and mean transit time (MTT) may be calculated (Rosen *et al.*, 1990). The measures are not quantitative but absolute values can be obtained by measuring arterial input function, but this can be prone to partial volume error. The measurement relies on the perfusion being constant and unaffected by the tracer which is well mixed within the blood and can be accurately measured.

The technique has a better spatial resolution and SNR than endogenous contrast methods, allowing smaller regions, such as MS lesions, to be analysed. However a

disadvantage is the need to inject a contrast agent with its implications on patient comfort, frequency and cost.

Possible sources of inaccuracy associated with this methodology include: (i) the delay between contrast injection and image acquisition, which can allow dispersal of the agent before the concentration is measured requires a high speed bolus injection to produce a 'tight' bolus to increase SNR and avoid recirculation; (ii) brain coverage is limited due to the fast image acquisition required and (iii) the assumption that the tracer remains intravascular. If there is loss of BBB integrity, for example in some MS lesions (Tofts and Kermode, 1989), this may lead to leakage of contrast with an increase in T_1 effects and an underestimation of calculated values. Finally, the contribution of tracer in large, non-perfusing vessels can cause an over-estimation of true tissue perfusion.

(iii) Endogenous contrast MRI methodologies

Arterial spin labelling (ASL) is a non-invasive technique that uses magnetically labelled blood water as an endogenous tracer. Measurement can be confined to true capillary perfusion only, ignoring blood flow in larger vessels which may not contribute greatly to tissue oxygenation. The disadvantages are a low SNR and the short lifetime of the label. Also, values of flow rate and blood volume are not possible. Two main ASL techniques exist, continuous ASL (CASL) and pulsed ASL (PASL) and these describe the nature of how the endogenous tracer is magnetically labelled. For both techniques the principle is to collect a labelled and control image,

subtract one from the other to remove static tissue signal to leave only labelled blood signal remaining.

Continuous ASL

First proposed in 1992 (Detre *et al.*, 1992) and refined thereafter (Alsop and Detre, 1998), CASL uses a spatially localised RF field to continuously saturate (Detre *et al.*, 1992) or invert (Williams *et al.*, 1992) the longitudinal magnetisation of protons in arterial blood water as it enters the brain. The continuous RF field is applied for a few seconds, along with a field gradient, as protons move through the field, the magnetisation of their spins becomes inverted. On leaving the field, the longitudinal magnetisation of the arterial blood decreases due to T_1 relaxation. If the image slice is close enough to the inversion plane such that some longitudinal magnetisation still remains, then arterial blood entering this area will reduce the longitudinal magnetisation in the slice. A suitable delay time is incorporated to ensure enough magnetised blood may enter the imaging area and perfuse the brain. Rapid imaging techniques such as EPI are required to perform this.

A control image is necessary to remove non-perfusion scanner effects such as magnetisation transfer effects in the static tissue from the labelled sequence. The control sequence is identical to the labelled sequence except that no net inversion of arterial blood water occurs, for example using a double inversion pulse (Alsop and Detre, 1998). Perfusion may then be calculated by subtracting the tissue magnetisation of the control image from the labelled image (Parkes and Tofts, 2002).

The main disadvantages of CASL are (i) the low SNR; (ii) large power deposition in the tissue due to long labelling time; (iii) the time taken for the labelled blood to reach the area of interest (the transit or arrival time) which is dictated by the T_1 relaxation time of arterial blood water (in pathologies where transit time is delayed complete loss of magnetisation may occur before the tissue target area).

Figure 2.2: *Representation of a CASL sequence*

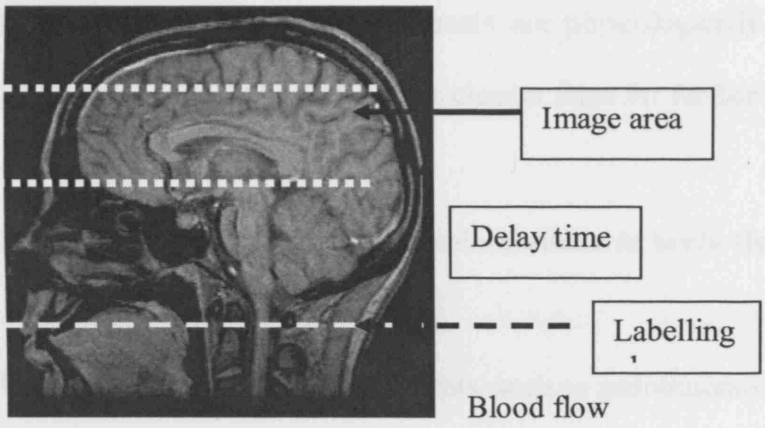

Pulsed ASL

This technique labels a larger volume of spins using a shorter RF pulse in comparison to CASL. A number of methods have been developed, including EPISTAR (echo planar imaging and signal targeting with alternating radiofrequency) (Edelman *et al.*, 1994) and its variation, FAIR (flow-sensitive alternating inversion recovery) (Kwong *et al.*, 1992; Kim, 1995). The disadvantage is a low SNR, approximately half that of CASL, because of the short labelling pulse. However, the shorter RF pulses potentially allow more localised regional perfusion studies.

Modelling the signal

For both methodologies, the difference signal (label minus control) is dependent on: (i) the inversion efficiency; (ii) blood T_1; (iii) tissue T_1; (iv) capillary permeability; (v) arrival time and (vi) perfusion. All these factors can either be assumed or measured, using a number of models. A recent advance attempts to account for the semi-permeable nature of the BBB, as previous assumptions of free diffusion between intra- and extracellular compartments are physiologically inaccurate (Detre *et al.*, 1992; Parkes and Tofts, 2002). See chapter three for further details.

2.3.2 Quantification of contrast enhancement in brain tissue

Using exogenous MR contrast agents, such as gadolinium-chelate, allows delineation of different pathological processes, such as tumours, inflammation and ischaemia. In health, such agents are unable to pass from the circulation into the interstitium due to the BBB and maximal concentration is reached shortly after injection and then declines steadily, predominantly excreted via the kidneys (Silver *et al.*, 2001b). Disruption of this can lead to accumulation of contrast media into the extravascular extracellular space. This can be used to estimate BBB integrity determined largely by a qualitative observation based on visualisation of gadolinium-enhancement of lesions. Gadolinium accumulation may also be measured quantitatively to provide information regarding the structure of the BBB. Gadolinium reduces the T_1 relaxation time of adjacent water protons producing high signal intensity in areas of accumulation on T_1-weighted images (Grossman *et al.*, 1986; Filippi *et al.*, 2000b). Clinical practice has shown gadolinium-chelates to be generally well tolerated.

Areas of contrast enhancement on MRI can be assessed on T_1-weighted images in a number of ways in MS: (i) calculating the volume of enhancing areas on images; (ii) assessing the number of areas of enhancement and (iii) less often, the time course of changes in T_1 signal intensity that arise following injection of gadolinium.

2.3.3 Diffusion imaging

Diffusion imaging illustrates the random molecular displacement of water molecules within a tissue. It is affected by microstructural tissue components such as cell membranes. In the presence of such structures, the direction of diffusion is non-random, tending to preferentially occur parallel to a cell membrane. Estimating the degree of directionality of diffusion therefore offers an insight into the integrity of cellular structure (Pierpaoli *et al.*, 1996). With loss of structure, water diffusion becomes less directional and less restricted. Diffusion imaging provides information to quantify the magnitude and the directionality (anisotropy) of water movement and quantitatively estimate the integrity of the cellular structure within a tissue, which can be affected by disease pathology.

In *isotropic* diffusion, there is no preferred direction for the motion of water and the probability of displacement of a molecule at a certain time is given by a Gaussian distribution (Wheeler-Kingshott *et al.*, 2003). If diffusion is dependent on direction, the tissue has different diffusion properties in different directions, it is said to be *anisotropic*. It may be assumed that the probability of molecular displacement follows a multivariate Gaussian distribution, giving rise to a 3x3 diffusion tensor (DT) matrix

characterised by nine elements (only six elements need to be measured as the matrix is symmetric about the diagonal) proportional to the variance of the Gaussian distribution (Basser *et al.*, 1994).

MRI estimation of diffusion

In the presence of a strong magnetic gradient, diffusion of water molecules causes MR signal loss due to dephasing of spin coherence. The application of a pair of gradients to elicit differences in the diffusivity of water molecules is known as diffusion weighting (DW) (Le Bihan *et al.*, 1988; Turner *et al.*, 1990). For instance, a pair of pulsed magnetic gradients may be added around a 180° refocusing pulse into a spin echo sequence (Westin *et al.*, 2002). The first gradient pulse induces a phase shift for all spins, the second inverts this phase shift, cancelling the phase shift for static spins. Spins which have changed location due to diffusion are not completely refocused by the second gradient pulse, and cause signal attenuation.

If two acquisitions are performed, one without superimposed diffusion gradient ($b = 0$) to eliminate the effects of large vessels and flow, and one with diffusion gradient ($b \neq 0$), where b is a scalar diffusion weighting factor (Le Bihan *et al.*, 1986), an exponential attenuation of the original signal, S_O, occurs. The b value may be increased by diffusion gradients which are stronger, longer or which have a greater length of time between each gradient pulse.

DW in a specific direction is given by the direction along which the gradient is applied and most signal is reduced in the direction where the diffusion coefficient is

higher. For example, in anisotropic areas, such as an axon, most signal attenuation is evident when diffusion gradients are applied along the direction of the axon. Conversely, in isotropic areas signal attenuation is independent of diffusion gradients.

Figure 2.3: *Images generated using a standard diffusion-weighted EPI sequence with different diffusion gradients. Image (a) is a b=0 image with no diffusion gradient and is predominantly T_2-weighted; Image (b) has a large diffusion gradient (700 s/mm^2) and shows suppression of signal in areas of high water concentration.*

Image (a) **Image (b)**

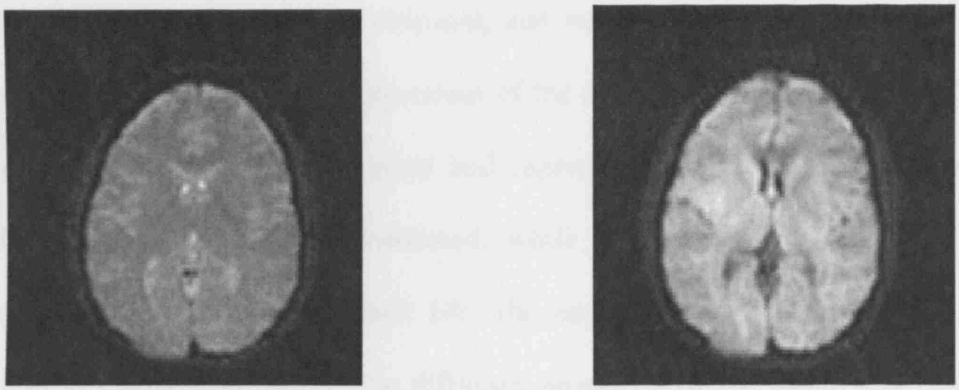

Quantitative diffusion imaging

The apparent diffusion coefficient (ADC) reflects the molecular diffusivity in the presence of tissue restrictions (Le Bihan *et al.*, 1986). A diffusion map may be constructed using ADC information from each voxel measured along the three directions of the diffusion gradients, giving the diffusivity of water in the tissue.

The degree of anisotropy shown by a tissue is dependent on several factors, including orientation of fibre tracts, fibre density and diameter, neuroglial cell packing and

degree of myelination (Pierpaoli *et al.*, 1996). Brain white matter tracts because of its ordered structure, has a higher degree of anisotropy than grey matter.

Diffusion tensor imaging (DTI) gives values independent of the tissue's orientation with respect to the direction of measurements. The tensor is a mathematical construct which can be visualised as an ellipsoid in three-dimensional space. The elements are calculated by simultaneously applying diffusion-weighted gradients in at least six non-colinear directions in addition to a non-diffusion-weighted image (Basser *et al.*, 1994). It is also possible to transform the DT into another tensor D', leaving only three nonzero elements along the main diagonal of the tensor, the eigenvalues (λ_1, λ_2, λ_3). These reflect the shape of the ellipsoid, and when added together reflects the "size" of the ellipsoid, which is independent of the orientation of the ellipsoid. The eigenvectors ($\epsilon 1$, $\epsilon 2$, $\epsilon 3$) are orthogonal and represent the directions along which molecular displacement are not correlated, while the eigenvalues represent the corresponding ADC values. For each DT, the combination of eigenvectors and eigenvalues is unique and reflects the diffusion properties of the tissue and can be measured for each voxel.

From the DT, several rotationally invariant parameters can be defined for each voxel and can be constructed into quantitative maps. The most commonly used are mean diffusivity (MD) and fractional anisotropy (FA). The MD is the average of the eigenvalues in a voxel, whilst FA is equal to the ratio between the square root of the variance of the eigenvalues and the square root of the sum of the squares of the eigenvalues (Basser and Pierpaoli, 1996). FA estimates the proportion of the diffusion

coefficient due to anisotropic diffusion (Pierpaoli *et al.*, 1996; Pierpaoli and Basser, 1996; Papadakis *et al.*, 1999).

Because large gradients are needed, diffusion MRI is sensitive to motion artefacts, due to movements of the head or pulsation of the brain from CSF motion. Fast image acquisitions, such as single-shot DW-EPI are used to counter this, but signal averaging is required to improve the SNR, increasing scanning time.

2.3.4 Spinal cord measurement

Cord imaging is challenging because it is a relatively mobile and pliable structure. Additionally, CSF pulsation alters the position of the cord within the spinal canal and can lead to truncation artefact (Lycklama à Nijeholt *et al.*, 2003). The spinal cord's small diameter and its position surrounded by bone also lowers the SNR. Multi-array coils, a series of individual surface coils linked together to provide a composite image (Roemer *et al.*, 1990), and cardiac gating have improved both the SNR and coverage. Fast three dimensional gradient echo sequences allow volumetric cord sequences which can quantitatively measure cord cross-sectional area and volume.

Quantitative cord atrophy methodologies

Previously, spinal cord cross sectional area measurement required manual outlining on axial images generated by a two-dimensional gradient echo sequence (Kidd *et al.*, 1993). The large degree of operator input impacted on reproducibility. With improved volumetric sequences such as 3D-FSPGR (see section 2.2.3), a semi-automated

measurement technique was developed using images reformatted with slices perpendicular to the cord (Losseff *et al.*, 1996a). Cord images show a signal intensity gradient between the cord (bright) and surrounding CSF (dark).

The basis of the technique is that if the cord and CSF were uniform in their composition then a contour drawn at signal intensity halfway between the signal intensity's of the cord and CSF would be the position of the cord boundary (see Figure 2.4). Area is estimated as an average over five contiguous 3mm axial slices, with the most caudal slice located at the level of the centre of the C2/3 intervertebral disc. This level is used because, the CSF space is wide and it is easier to position the patient such that the cord lies in the middle of the CSF pool, maximising cord/CSF contrast. Also it is an uncommon site for disc protrusion.

Figure 2.4: *Sagittal 3D-FSPGR cord images re-formatted into axial images and contoured using the Losseff technique.*

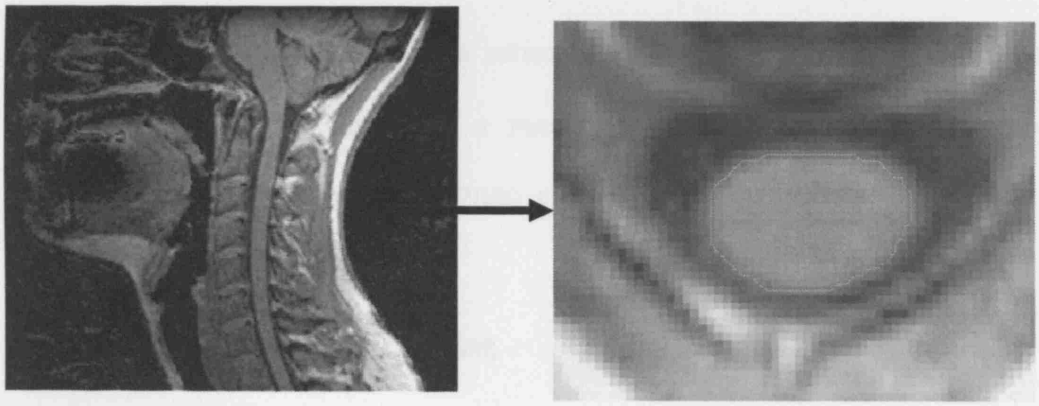

The limitations of the technique are: (i) measurements are restricted to a predefined level of the cord; (ii) significant intensity variations can be caused by surface coils used in the acquisition and (iii) measurements are prone to partial volume error.

A further method, involves calculation of cord volume based on a 3D extraction of the cord surface and the computation of a medial axis (Coulon *et al.*, 2002). It is, at present, under development.

2.3.5 Other quantitative MRI techniques

(i) Brain volume

High resolution, high SNR volume data sets, such as three dimensional IR prepared FSPGR, are often used. Techniques, such as statistical parametric mapping (SPM) (SPM99, Wellcome Department of Cognitive Neurology, Institute of Neurology, London, UK) and SIENA (Structural Image Evaluation, using Normalization, of Atrophy) (Smith *et al.*, 2001), allow estimation of regional and global tissue volume measurements possibly providing a measure of disease effect in a number of conditions, such as MS (Fox *et al.*, 2000; Chard *et al.*, 2002b).

(ii) Magnetisation Transfer Imaging

Magnetisation transfer (MT) imaging enables bound-water (usually NMR-invisible) molecules to be imaged by partly saturating them with a specific RF pulse. The magnetisation transfer ratio (MTR) (Dousset *et al.*, 1992) measures the amount of MT

between bound and free water and represents the fractional (%) reduction in signal intensity following the application of the MT saturation pulse. This is used to give an indication of the integrity of structures such as myelin which is associated with bound-water molecules (Barkhof *et al.*, 2003).

(iii) MR Spectroscopy

This allows the quantitative measurement of concentrations of various brain metabolites. At long echo times four major metabolites: (i) choline containing compounds; (ii) creatine and phosphocreatine; (iii) N-acetyl-aspartate (NAA) and (iv) lactate are estimated. With a short TE, glutamine/glutamate and myo-insositol can be measured. NAA is thought to be a neuroaxonal marker which gives an indication of neuronal function (Tofts and Waldman, 2003); myo-inositol may indicate glial cell content and activity. A number of acquisition methods are employed (Tofts and Waldman, 2003) with metabolite concentration measured using fitting to estimate areas under peaks.

2.4 Data analysis of brain tissue

2.4.1 Registration

To make within-subject or between-subject comparisons, it can be advantageous for images to be in the same anatomical framework. Image registration aligns multiple images into the same geometric space and spatial registration can remove the effects of small movements that take place between image acquisitions during a scanning session. Images of different parameters may be registered, and regions of interest (ROI) on structural images applied to the parametric map and measurements made. Intrasubject registration in longitudinal studies can help to overcome small positioning errors and changes in voxel sizes allowing small measurable changes to be detected over time. Across-subject (inter-subject) registration allows pooling of images from different subjects, so that group comparisons can be made.

Registration is achieved by estimating a mapping between a pair of images, one of which is assumed to be stationary (reference image) and the other (source image) is spatially transformed to match it. Each voxel position in the reference image must be mapped to a corresponding position in the source. The source is then resampled at the estimated positions.

2.4.2 Segmentation

Segmentation is the process of dividing an image into distinct tissue regions. Regarding the brain, the difference in signal intensity between parenchyma and CSF may be enough to drive the process (Ashburner and Friston, 1997), but the signal intensities of grey and white matter vary within the brain, and segmentation of these individual structures is a more complex process. Ideally, the process should be highly automated to improve reproducibility and reduce operator bias. Many methods exist two of which are discussed below.

SPM employs a general linear model with Gaussian field theory to make inferences about regional effects. Brain tissue types are identified by intensity thresholding. Intensities are modelled by a mixture of K Gaussian distributions, parameterised by means, variances and mixing proportions. Segmentation is assisted by overlying prior belonging probability maps derived from segmented images of 151 healthy subjects assumed to be representative (Montreal Neurological Institute brain template). This process requires initial registration to standard space.

Partial volume error may affect the Gaussian distribution, rendering it invalid. A further problem lies in mis-registration with the prior probability images, which are based entirely on relatively young and healthy brains rather than subjects with neurological disease. Because of the intensity difference basis of the segmentation methodology, it works best in images relatively free of artefact which have a good separation of intensities rather than EPI-based sequences. Similarly, other pathological tissue types with differing intensities to the part of the brain they are

within, for example white matter lesions in MS, will be segmented on the basis of the individual lesion intensity potentially causing mis-classification (Chard *et al.*, 2002a).

Another method is clustering, in particular K-means, *'soft'* K-means (Duda and Hart, 1973; Vannier *et al.*, 1985; Taxt *et al.*, 1992) and their fuzzy variant, fuzzy *c*means (Bensaid *et al.*, 1994; Masulli and Schenone, 1999). The technique relies on increasing the orthogonality between the tissue types and enhancing its separation.

Summarising a representative clustering methodology, each voxel of the co-registered images to be segmented is assigned a spatial location and intensity in feature space. These voxels are allocated to separate clusters for the different tissue types within the brain. Each point is dynamically allocated to its nearest cluster until no more reallocations are possible. The confidence of a given allocation depends on the entropy (inversely proportional to the distance of each point from each cluster). This is calculated based on the set of probabilities governing the point to cluster assignment. By minimising the entropy of the system, the confidence of the point-to-cluster arrangement is increased and voxels are maximally segmented (Hadjiprocopis *et al.*, 2003).

The process does not require a prior probability map and because the clustering algorithm can be modified to improve handling of imaging distortions, it may be a more appropriate method for segmenting EPI sequences, such as DTI.

2.4.3 Quantification

(i) Region of Interest Analysis

This is useful for analysis of a particular part or parts of the brain, for example visible lesions or deep grey matter. One or several ROIs may be applied in each subject to the studied images. One method of creating a ROI is using Dispimage (Plummer, 1992) a semiautomated local thresholding technique where the operator moves a cursor to a specific area and the package then contours an area with similar threshold intensity values. The size and shape of the ROI depends on the competing considerations of avoiding introducing extra noise to the measure from structures outside the area intended but including enough voxels to improve the sensitivity of the measure. This process may be time-consuming, cause bias and affect reproducibility. Hence, strict definition and consistency of ROI placement is required.

ROIs should ideally be defined on conventional structural MR images, where greater resolution exists, and then transferred to the parameter map under investigation. Also direct placement onto the parameter map may lead to bias. The images and maps need to be spatially registered. The ROI approach is unable to investigate large areas of tissue which may be especially relevant if one is investigating a disease which diffusely affects the brain.

(ii) Histogram Analysis

Histograms of MR parameter values are increasingly used to characterise subtle disease changes in particular. The histogram is a frequency distribution showing the number of voxels with particular MR parameter values. It may be applicable to any parameter affected by diffuse changes in the brain. An advantage of this approach is possible improved sensitivity by sampling large areas of tissue, particularly useful in diffuse neurological conditions. The technique also avoids the problem of bias from ROI placement, thereby increasing reproducibility aiding longitudinal study (Tofts *et al.*, 2003) and can be used to assess whole brain change or a specific area can be pre-selected and the histogram generated from voxels from this area alone, although this re-introduces possible operator bias.

To generate a MR parameter histogram from data collected, the tissue area studied must be defined from the images acquired and histogram 'spikes' removed (Tofts *et al.*, 2003). An interval, bin width, is then selected for the parameter. As brain volumes differ from subject to subject, histograms are usually normalised by dividing all values by the total number of voxels and a frequency distribution is obtained which represents the fraction of the total brain volume in one interval (Tofts *et al.*, 2003).

Usual histogram variables measured are: (i) the average value; (ii) the peak location (parameter value that is most common in the brain tissue) and (iii) the peak height (corresponding voxel value of the peak location). See Figure 5.2 for an example.

Considerations include: (i) accurate segmentation of the brain to prevent contamination from different tissue types; (ii) differential rates of brain atrophy between subject groups may confound calculations because of the influence of partial volume pixels at the edge of a tissue and (iii) inter-subject brain volume differences (normalisation as described above is usually carried out to minimise this).

(iii) Group mapping

In this mode of analysis, regional inferences are possible without the bias that is associated with ROI placement. (Ashburner and Friston, 2000). Analysis most commonly uses SPM.

Firstly, all image datasets are spatially normalised to the same stereotactic space. A non-uniformity correction is made and images are segmented and smoothed to reduce the effects of incomplete registration and residual inter-subject differences. SPM employs a general linear statistical model with Gaussian field theory to make inferences about regional effects from normalised maps (Friston *et al.*, 1995). In particular, group comparisons and correlations with an external parameter (such as disease severity) can be performed. Voxelwise significance is determined using Gaussian random field theory (Worsley *et al.*, 1996) on inferences with correction for multiple comparisons if required.

Some concerns do exist however (Bookstein, 2001). Nonuniformity (for example local change in voxel size) can cause signal intensity alteration and not all local differences in intrinsic tissue can be recognised.

2.5 Application of quantitative MRI techniques in Multiple Sclerosis

2.5.1 Perfusion MRI

The first study in MS was performed in 1984 using PET imaging (Brooks *et al.*, 1984). Since then, further studies measuring either blood flow or glucose uptake have reported regional decreases in grey matter areas with two studies observing lower CBF in areas of white matter (Lycke *et al.*, 1993; Bakshi *et al.*, 1998; Blinkenberg *et al.*, 2000).

Initial MRI studies have employed gadolinium-bolus methodology. The largest study undertaken investigated 25 subjects and employed a correction algorithm to attempt to control for contrast loss through a damaged BBB (Haselhorst *et al.*, 2000). They found a decrease in relative CBF in frontal lobe grey matter, an increase in acute, enhancing plaques and decreased flow in chronic T_1 hypointense lesions. This may indicate an inflammatory process in acute plaques and degenerative pathological change in hypointense lesions. A further study in seven patients observed a decrease in CBV in all lesion types (Jensen *et al.*, 1995). They hypothesised that oedema may decrease the blood volume in acute inflammatory lesions. Similar findings were noted in a further nine patients with the authors suggesting that interstitial oedema and perivascular inflammation was causing small vessel compression, decreasing capillary capacity (Petrella *et al.*, 1997). Both the last two investigations, however, did not model for contrast leakage through the BBB.

More recent gadolinium-bolus studies have taken place. In concert with DWI and using a similar model to a previous study (Haselhorst *et al.*, 2000) to control for BBB leakage, a regional rise in CBF three weeks prior to the onset of a visible enhancing lesion was demonstrated. This preceded an increase in ADC values in the same area and may suggest increased blood flow and vasodilatation occurs before disruption of the BBB at the onset of the inflammatory process. Following the resolution of enhancement, blood flow decreased particularly in resulting T_1-hypointense lesions (Wuerfel *et al.*, 2004). A further study investigating CBF in NAWM ROIs and fitting a gamma-variate function to the change in relaxation rate T_2* curve to approximate for contrast recirculation and loss reported a significant decrease in blood flow levels especially in peri-ventricular NAWM in relapsing-remitting MS subjects. They postulated that diffuse haemodynamic impairment exists throughout the NAWM in such patients which may relate to a subacute or chronic vasculitis that could precede lesion development (Law *et al.*, 2004).

No previous perfusion investigation in MS has used endogenous contrast MRI methodologies. Further, perfusion in all the clinical subgroups of MS is not known.

2.5.2 Contrast enhancement

Previous serial MRI studies in relapse-onset MS have shown that most new lesions initially enhance with gadolinium (Bastianello *et al.*, 1990; Lai *et al.*, 1996; Tortorella *et al.*, 1999). Such lesions (see Fig 2.5) occur five to ten times more frequently than clinical relapses and persist for approximately one month (Miller *et al.*, 1988; Miller *et al.*, 1991; Barkhof *et al.*, 1992; Thompson *et al.*, 1992; McFarland *et al.*, 1992;

Smith *et al.*, 1993). New gadolinium-enhancing lesions occur more often during clinical relapses and acutely symptomatic lesions frequently enhance (Miller *et al.*, 1988; Grossmann *et al.*, 1986; Kappos *et al.*, 1999; Weiner *et al.*, 2000). There is a moderate association between new gadolinium-enhancing lesions and clinical relapse (Kappos *et al.*, 1999). Additionally, gadolinium-enhancing lesions at baseline are correlated with later lesion counts (Molyneux *et al.*, 1998). However, the correlation with clinical disability over the relatively short term is poor or even absent (Kappos *et al.*, 1999).

The standard dose of gadolinium in clinical practice is 0.1 mmol/kg. Evidence from comparative studies suggests that triple dose gadolinium (0.3 mmol/kg) shows up to an 81% increase in new enhancing lesion detection with the higher dose (Silver *et al.*, 1997; van Waesberghe *et al.*, 1997; Filippi *et al.*, 1998d; Rovaris *et al.*, 1998; Rovaris *et al.*, 1999; Silver *et al.*, 2001a). Lesions which enhance only with triple dose gadolinium persist for less time and are associated with less BBB permeability than single dose enhancing lesions (Filippi *et al.*, 1998c). Ring-enhancing lesions (see Fig 2.5) account for approximately 20% of all gadolinium-enhancing lesions and are thought to be associated with greater axonal loss (Morgen *et al.*, 2001).

Studies in mainly well-established relapsing-remitting MS cohorts report enhancement of between 40-80% subjects (Grossman *et al.*, 1986; Thompson *et al.*, 1992; Wiebe *et al.*, 1992; Stone *et al.*, 1995; Kourdriavtseva *et al.*, 1997; Tortorella *et al.*, 1999; Bagnato *et al.*, 2000). From existing published studies, it is unclear what the level of gadolinium-enhancement is at the earliest stages of relapsing-remitting MS.

Because of the association between gadolinium-enhancement and clinical relapse, phase II clinical drug trials have used the level of enhancement a marker of efficacy (Filippi *et al.*, 1998d; Kappos *et al.*, 1999). But because of the absence of a demonstrable strong correlation between enhancement and disability (Kappos *et al.*, 1999) it is not a primary outcome measure in phase III studies. Possible reasons for the absence of correlation between lesion enhancement and disability include: (i) enhancement does not quantitatively indicate the level of axonal damage within the area; (ii) inflammation may also be associated with mediators which promote tissue repair; (iii) previous studies have not assessed gadolinium lesion development at the clinically earliest stages of MS which may be more significant in determining later disability (Brex *et al.*, 2002) and (iv) a lack of long-term follow up.

Figure 2.5: *T_1-weighted images displaying gadolinium-enhancing lesions. Image (a) depicts ring enhancement; image (b) homogenous enhancement.*

Image (a) **Image (b)**

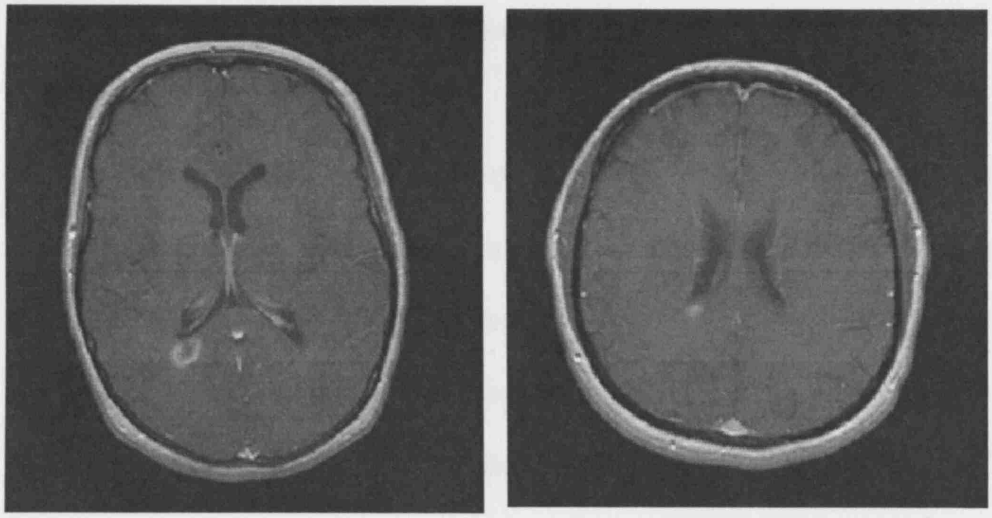

2.5.3 Diffusion MRI

Diffusion-weighted imaging

The first study to investigate MS showed increased ADC values in lesions compared with NAWM (Larsson *et al.*, 1992). A further study demonstrated a significantly raised ADC in NAWM in comparison to controls (Christiansen *et al.*, 1993). Later studies have shown a higher ADC in T_1-hypointense lesions in comparison to non-enhancing T_2-weighted lesions in all subtypes of MS (Horsfield *et al.*, 1996; Droogan *et al.*, 1999; Nusbaum *et al.*, 2000b; Roychowdhury *et al.*, 2000). Some studies have reported a lower ADC in gadolinium-enhancing lesions in comparison to non-enhancing lesions (Nusbaum *et al.*, 2000b; Roychowdury *et al.*, 2000) whilst a further study noted an increase in enhancing lesions in comparison to non-enhancing lesion types (Droogan *et* al., 1999). Lesion heterogeneity may go some way to explain the differing pattern of findings (Luchinetti *et al.*, 2000). All lesion studies show the largest ADC values in T_1-hypointense lesions (Droogan *et al.*, 1999; Nusbaum *et al.*, 2000b; Roychowdury *et al.*, 2000; Castriota Shandberg *et al.*, 2000).

Studies on different clinical MS phenotypes have shown mixed results. No differences were seen in studies comparing secondary and primary progressive and relapsing-remitting MS subjects (Horsfield *et al.*, 1996; Droogan *et al.*, 1999). However, a further study showed differing results between secondary progressive and relapsing-remitting cohorts in comparison to controls (Nusbaum *et al.*, 2000a) whilst another study showed that T_2 visible and T_1 hypointense lesion ADC values were

significantly higher in secondary progressive MS patients in comparison to relapsing-remitting subjects (Castriota Shandberg *et al.*, 2000).

A 12-month study investigating ADC changes prior to and post gadolinium-enhancing lesion formation showed an increase in ADC some months prior to the appearance of the lesion (possibly indicating tissue damage prior to gadolinium visible BBB damage), followed by a slow decay once enhancement has ceased (Werring *et al.*, 2000a). In matched contralateral NAWM regions there was a significant but smaller increase in ADC at time of enhancement possibly due to structural damage in the lesions affecting connected areas of NAWM (Werring *et al.*, 2000a).

Two further 12-month longitudinal studies have been reported. In a cohort with CIS, as the majority developed clinically definite MS, significant changes in ADC were noted in NAWM which correlated to the T_2 lesion load (Caramia *et al.*, 2002). Whilst, in primary progressive patients a longitudinal increase in NAWM ADC correlated with both T_1 and T_2 lesion loads (Schmierer *et al.*, 2004b).

Diffusion tensor imaging

Studies have investigated DTI parameters (MD and FA) in MS. An increase in MD and decrease in FA is noted in all lesion types in comparison to NAWM. T_1 hypointense lesions have the highest MD values amongst all MS clinical phenotypes, whilst gadolinium-enhancing lesions generally have higher MD values than T_2 visible lesions although some heterogeneity exists (Werring *et al.*, 1999; Filippi *et al.*, 2000a;

Bammer *et al.*, 2000; Filippi *et al.*, 2001b; Guo *et al.*, 2001). Regarding FA, gadolinium-enhancing T_1 lesions have shown the lowest values in comparison to control areas, followed by T_1 hypointense lesions and then T_2 visible lesions (Werring *et al.*, 1999; Filippi *et al.*, 2000a; Bammer *et al.*, 2000; Filippi *et al.*, 2001b; Guo *et al.*, 2001). Ring-enhancing lesions have higher MD and lower FA values than homogenously enhancing lesions (Bammer *et al.*, 2000; Nusbaum *et al.*, 2000b; Roychowdury *et al.*, 2000). Lesion and NAWM MD and FA changes are moderately inversely correlated (Filippi *et al.*, 2001b).

In the NAWM, patients with well established MS have raised MD and decreased FA in comparison to controls (Werring *et al.*, 1999; Bammer *et al.*, 2000; Filippi *et al.*, 2000a; Filippi *et al.*, 2001b; Ciccarelli *et al.*, 2001; Guo *et al.*, 2001; Cercignani *et al.*, 2001b; Rovaris *et al.*, 2002b), one study noting larger MD values in peri-lesional NAWM than in NAWM distant from lesions (Guo *et al.*, 2001).

MD histogram analyses have shown a broadening of the shape of the curve with a decrease in peak height. FA histograms have shown a rise in peak height and a shift of the curve to lower values. This may be secondary to white matter disruption causing decreased FA values similar to those of the larger – and more isotropic – grey matter volume of tissue (Cercignani *et al.*, 2001a). All the above changes were seen in cohorts with well established MS. No significant NAWM changes were seen in patients with clinically early relapsing-remitting MS (median disease duration 1.7 years) suggesting that measurable DTI changes outside lesions are not readily apparent at the clinical onset of the disease (Griffin *et al.*, 2001).

A study of grey matter DTI reported significant changes in subjects with secondary progressive disease compared to controls or patients with relapsing-remitting MS (Bozzali *et al.*, 2002). A further study showed raised MD in comparison to controls in secondary and primary progressive MS subjects (Rovaris *et al.*, 2002b). Another ROI study of deep grey matter areas observed a raised FA and decreased MD particularly in the putamen and thalamus (Ciccarelli *et al.*, 2001).

A number of studies have shown no significant changes amongst differing cohorts (Cerciginani *et al.*, 2001a; Ciccarelli *et al.*, 2001; Filippi *et al.*, 2001b). However, lesions in secondary progressive patients have been reported to show raised MD values in comparison to primary progressive disease (Rovaris *et al.*, 2002b).

Two longitudinal DTI studies have been published investigating MS (Cassol *et al.*, 2004; Rovaris *et al.*, 2005). Cassol *et al.* noted no statistically significant longitudinal differences in seven MS subjects compared to seven controls over 12 months, whilst Rovaris *et al.*, observed evidence of a progression of MD abnormalities in a cohort of patients with progressive disease over 15 months.

Clinical and MRI Correlations

Several studies have shown only moderate correlations between clinical disability (EDSS or MSFC) and diffusion parameters (Cercignani *et al.*, 2001a; Filippi *et al.*, 2001b; Castriota Scanderbeg *et al.*, 2000; Filippi *et al.*, 2000a; Ciccarelli *et al.*, 2001; Schmierer *et al.*, 2004b). A study of relapsing-remitting MS subjects showed

moderate correlations between DTI abnormalities in normal appearing tissue and cognitive dysfunction (Rovaris *et al.*, 2002a).

Moderate correlations have been shown between ADC and T_1 hypointensity in a cohort of relapsing-remitting and secondary progressive MS patients (Castriota Scanderbeg *et al.*, 2000) and between an increase in ADC over 12 months and an increase in T_2 visible lesion and T_1 hypointensity lesion loads in primary progressive MS (Schmierer *et al.*, 2004b). Further, a DTI histogram study reported correlations between MD mean, peak height and peak location and T_2 lesion volume and FA mean and peak height and T_2 lesion volume (Cercignani *et al.*, 2001a). This suggests, that only part of the diffusion abnormalities observed are secondary to lesions, and an intrinsic process within normal appearing tissue is also relevant.

Pathological correlations

Possible explanations for the diffusion changes are at present speculative as there are few studies investigating pathological correlates of DTI. Subtle axonal damage in nerve fibre tracts may be expected to decrease anisotropy, and cause a significant increase in MD by expanding the extracellular space or simply by losing axons *per se* (Barnes *et al.*, 1991).

A recent report investigated DTI correlates at post-mortem in eight patients and reported: (i) FA and MD differences between lesions and NAWM; (ii) correlation between MD and myelin content, axonal count and gliosis; (iii) correlation between FA and myelin content only and (iv) correlation between axonal count and myelin

content. The authors suggest that MD is influenced by demyelination, axonal loss and gliosis whilst FA may be more specifically linked to demyelination. It postulated that, as myelin content and axonal count do not correlate with gliosis, MD may be influenced independently by gliosis (Schmierer *et al.*, 2004c). Little other data exists and hence caution must be observed when interpreting *in-vivo* DTI findings in patients.

2.5.4 Spinal cord imaging

Conventional MR imaging

Approximately 75-90% of MS patients have cord lesions visible on T_2-weighted MRI (Kidd *et al.*, 1993; Lycklama à Nijeholt *et al.*, 1998; Bot *et al.*, 2004a). Typically these lesions are: (i) more likely to occur in the cervical cord (Oppenheimer, 1978); (ii) less than two vertebral segments in length although focal lesions may merge giving rise to large areas (Kidd *et al.*, 1993; Thorpe *et al.*, 1996; Lycklama à Nijeholt *et al.*, 1997) and (iii) occupy the lateral and posterior white matter columns and do not spare the grey matter (Tartaglino *et al.*, 1995; Thielen and Miller, 1996). Compared to other sub-groups, primary progressive patients are more likely to develop additional diffuse cord abnormalities (Lycklama à Nijeholt *et al.*, 1997; Lycklama à Nijeholt *et al.*, 1998). T_1 hypointense lesions are rarely seen, possibly due to a denser organisation of spinal cord tissue (Lycklama à Nijeholt *et al.*, 2003). Gadolinium-enhancing lesions are observed less frequently in the spinal cord than the brain but when they occur, are more often associated with clinical relapses (Thorpe *et al.*, 1996).

Cross-sectional studies have shown no association between the number of spinal cord and brain lesions (Kidd *et al.*, 1993; Lycklama à Nijeholt *et al.*, 1998), however, a longitudinal study did demonstrate a relationship between the development of new cord and brain lesions in relapsing-remitting MS (Thorpe *et al.*, 1996). In general, studies have reported little or no relationship between the number of MR-visible cord lesions and disability.

Spinal cord cross-sectional area and volume

Studies have demonstrated significant decreases in upper cervical cord area (UCCA) particularly in patients with progressive forms of MS in comparison to controls (Losseff *et al.*, 1996a; Filippi *et al.*, 1996a; Filippi *et al.*, 1997; Lycklama à Nijeholt *et al.*, 1998; Stevenson *et al.*, 1998; Edwards *et al.*, 1999; Liu *et al.*, 1999; Rovaris *et al.*, 2001; Vaithianathar *et al.*, 2003; Lin *et al.*, 2003b; Lin *et al.*, 2004). Further, a strong correlation has been found in some studies between cervical cord atrophy and disability (Losseff *et al.*, 1996a; Filippi *et al.*, 1996a; Edwards *et al.*, 1999; Lin *et al.*, 2004). However, it is unclear how early in the course of MS this loss of area starts to occur.

A cross-sectional study in CIS patients demonstrated a slight loss in area in those who had brain T_2 lesions, but showed no longitudinal changes over one year (Brex *et al.*, 2001). However, most other cross-sectional studies have observed no UCCA differences between relapsing-remitting MS and controls (Losseff *et al.*, 1996a; Stevenson *et al.*, 1998; Vaithianathar *et al.*, 2003; Lin *et al.*, 2003a) although longitudinal loss has been demonstrated (Stevenson *et al.*, 1998; Lin *et al.*, 2003a).

Cervical cord volume studies have shown significantly lower values in combined populations of relapsing-remitting and secondary progressive MS studies in comparison to controls which correlated to the EDSS (Liu *et al.*, 1999; Edwards *et al.*, 1999) whilst a further study, with larger cohort sizes, showed volume loss only in secondary progressive patients rather than in relapsing-remitting subjects (Lin *et al.*, 2003b). A recent report using the *Coulon* technique (Coulon *et al.*, 2002) appeared to be relatively insensitive to progressive change over 12 months (Hickman *et al.*, 2003).

An association between the calculated cord values and the total intracranial volume has been suggested (Edwards *et al.*, 1999; Vaithianathar *et al.*, 2003) and also a possible effect of subject gender (females having smaller cross-sectional areas than males) (Blatter *et al.*, 1995). Subject height and weight has also shown a possible relationship with UCCA (Kameyama *et al.*, 1994; Losseff *et al.*, 1996a). Correlations between the cord atrophy and clinical functional systems suggestive of cord pathology, such as sphincter function (Losseff *et al.*, 1996a; Lycklama à Nijeholt *et al.*, 1998) and the pyramidal system (Losseff *et al.*, 1996a) have also been reported.

2.5.5 Other quantitative MRI techniques

(i) Brain volume

Brain volume reductions in MS patients may be due to axonal loss and demyelination, whilst acute inflammation and gliosis may increase volume (Miller *et al.*, 2002; Miller, 2004b). Studies have shown that brain atrophy is present at an early clinical stage of relapsing-remitting MS and affects both grey and white matter (Chard *et al.*, 2002b; De Stefano *et al.*, 2003). Further, in CIS patients who developed clinically definite MS over the course of a one year study ventricular enlargement suggestive of cerebral atrophy was also observed (Dalton *et al.*, 2002b). Some studies have shown a link between increasing cerebral atrophy and disability (Losseff *et al.*, 1996b; Paolillo *et al.*, 1999). Whilst, in an eight year follow-up study, there was a suggestion that greater amounts of brain atrophy early in the clinical course may increase the likelihood of later significant disability (Fisher *et al.*, 2002).

Comparative studies have shown a greater degree of atrophy in secondary and primary progressive forms of MS in comparison to relapsing-remitting patients (Stevenson *et al.*, 2000; Kalkers *et al.*, 2001a; Lin *et al.*, 2003b). No significant difference was noted between secondary and primary progressive subjects in one comparative study (Kalkers *et al.*, 2001a). These changes were only weakly correlated with T_1 and T_2 lesion loads.

Because of the sensitivity of brain volume measurement and its correlation to disability, increasingly therapeutic drug trials are evaluating cerebral atrophy as an

outcome measure. At present, it is uncertain if disease modifying therapies reduce the rate of volume loss in comparison to controls. Two previous papers revealed BIFN does not effect brain volume (Molyneux *et al.*, 2000; Jones *et al.*, 2001), in a third study slowing of atrophy was seen only during the second year of treatment (Rudick *et al.*, 1999b) whilst a further recent study reported a possible 30% reduction in the rate of brain atrophy over two years in CIS patients on BIFN (Filippi *et al.*, 2004). In particular, the possible increase in volume associated with inflammation and its subsequent reduction following BIFN – due to its anti-inflammatory effect – invites a cautious interpretation of these studies.

(ii) Magnetisation Transfer Imaging

MS lesions have lower MTR values than corresponding NAWM areas, with T_1 hypointense lesions having the least values (Cercignani *et al.*, 2000; Filippi *et al.*, 1999). Patients with secondary progressive MS have lower average lesion MTR than less disabling phenotypes of MS (Gass *et al.*, 1994), suggesting a link between MTR and clinical disability (Filippi *et al.*, 2000c). Larger gadolinium-enhancing lesions and ring-enhancing lesions are associated with lower MTR values than smaller homogenously gadolinium-enhancing lesions (Filippi *et al.*, 1998c; Filippi, 2001a). Longitudinal studies of new gadolinium-enhancing lesions show decreases in MTR values as they start to enhance and a partial or complete recovery in the subsequent 6 months (Filippi, 2001a).

Significant MTR changes in NAWM are present in all clinical subgroups of MS and have been correlated with physical disability and cognitive impairment (Filippi *et al.*,

1999; Tortorella *et al.*, 2000; Filippi *et al.*, 2000d; Kalkers *et al.*, 2001b). These changes are only modestly correlated to lesion load, suggesting the presence of intrinsic NAWM pathology. MTR studies in grey matter show lower MTR values with possible association with cognitive symptoms (Rovaris *et al.*, 2000; Cercignani *et al.*, 2001b; Ge *et al.*, 2001).

Two pathological studies investigating correlates of MTR have shown a highly significant association between myelin score or content and MTR and also significantly increased MTR values in remyelinated lesions compared with demyelinated lesions (Barkhof *et al.*, 2003; Schmierer *et al.*, 2004a). Further, correlation was also noted in one study between MTR and T_1-relaxation time but no association was observed between MTR and gliosis (Schmierer *et al.*, 2004a).

(iii) MR Spectroscopy

Reductions in NAA have been reported in MS lesions and NAWM, with greater magnitudes of loss in progressive cohorts in comparison to the relapsing-remitting subjects (Fu *et al.*, 1998; Leary *et al.*, 1999). Studies have also demonstrated a correlation between disability and reduced NAA in MS (Davie *et al.*, 1995; Davie *et al.*, 1997; Sarchielli *et al.*, 1999) and also between reduced NAA and atrophy (Cifelli *et al.*, 2002). At present because of low SNR and modest reproducibility the use of this technique in clinical trials as a surrogate marker of MS is limited.

2.6 Aims of this thesis

The aims of the series of studies outlined in the remainder of this thesis are to use quantitative MR techniques to evaluate their sensitivity and elucidate further the pathophysiology of MS. From this, the potential feasibility of such MR parameters for future use as surrogate *in-vivo* markers both in terms of prognosis and as outcome measures in drug treatment monitoring trials may be inferred.

2.6.1 Evaluation of a new MRI technique in multiple sclerosis

Presented in this thesis is a study with patients from all four of the clinical phenotypes of MS, measuring cerebral perfusion using a MR technique not previously employed (CASL with two compartment correction) which attempts to model for the effect of BBB permeability and thus may not be subject to inaccuracy due to pathological BBB leakage (Parkes and Tofts, 2002). A recent analysis on normal controls using the technique produced promising results (Parkes *et al.*, 2004). Because of advantages such as: (i) non-invasiveness; (ii) modelling for BBB permeability and (iii) the stability of the measure when there is BBB disruption, the investigation in MS may be revealing.

As perfusion is a marker for metabolic state, different pathological correlates may be inferred on the basis of the results found, potentially opening avenues for investigation in more specific cohorts investigating particular clinical correlates, especially cognition.

2.6.2 MRI findings in clinically early relapsing-remitting multiple sclerosis

Often, previous studies investigating the differing quantitative MRI parameters have tended to use cohorts with well established MS and wide variations of disease duration. Hence it remains unclear, particularly in the evaluation of gadolinium-enhancing lesions, diffusion tensor imaging and spinal cord atrophy, what degree of sensitivity these parameters show in clinically early relapsing-remitting MS and how they change longitudinally. The evaluation of quantitative MRI parameters longitudinally in patients with minimal disability may give insights in to the evolution of pathology. Determining the sensitivity of various MRI sequences and their association with clinical markers of disease progression over time will help to assess the relative strengths and weaknesses of individual quantitative MRI parameters and their suitability for use as an *in-vivo* surrogate marker in MS.

Such an evaluation is on-going in the NMR Research Unit at the Institute of Neurology; it includes a cohort of relapsing-remitting MS patients recruited within three years of first symptom onset. The majority of the studies presented in this thesis relate to the evaluation of gadolinium-enhancing lesions, DTI parameters and spinal cord area in this cohort to examine MR sensitivity and potential clinical relevance.

2.6.3 Use of MRI as a clinical surrogate marker

The possibility of using MRI derived metrics in concert with clinical measures to evaluate disease prognosis and response to potential treatments in clinical drug trials holds promise. Reliance on clinical measures alone increases follow-up periods and

cohort sizes as clinical events can be relatively rare and subjective. The use of clinical scales such as the EDSS, although helpful, is weighted towards locomotor function and its reproducibility and sensitivity to change are poor (Filippi *et al.*, 1998e). Even when the MSFC is combined with the EDSS, this may not be sensitive enough to accurately represent clinical change such is the complex and variable nature of MS.

MRI can provide objective measures which are reproducible. Hence, the use of MRI variables as a surrogate marker is an attractive possibility. However, for such a role to exist requires demonstration of correlation between the MR parameter and clinical outcome with a robust prediction of clinical effect on the MR outcome studied. Possible criteria for the use of a paraclinical measure as a potential surrogate endpoint in a clinical drug trial has been suggested: (i) that a given treatment is effective on the surrogate endpoint; (ii) the treatment is effective on the clinical endpoint of interest; (iii) that the surrogate and clinical endpoints are significantly correlated and (iv) the effect of a given treatment on the clinical endpoint is mediated through an effect on the surrogate endpoint (Prentice, 1989).

At present in phase III studies MRI parameters are used only as secondary endpoints. With the increasing range of quantitative MRI parameters and improvements in sequence methodology, further evaluation of cohorts in systematic cross-sectional and longitudinal studies and in well defined population groups may improve correlations with clinical disability and suggest a future role for MRI as a primary endpoint. The benefit of this is a likely increase in statistical power of clinical trials and a possible improvement in the clinico-pathological understanding of the condition.

CHAPTER 3

Cerebral perfusion in multiple sclerosis

3.1 Investigation of cerebral perfusion in multiple sclerosis using continuous arterial spin labelling

3.1.1 Introduction

As discussed in chapter two, perfusion is the term used to describe the volume of blood passing through an organ normalised to the mass of the organ, particularly that part of the circulation responsible for delivery of nutrients and removal of waste products at parenchymal level in the tissue. Hence, the measurement of cerebral perfusion may offer an insight into cerebral metabolism, especially tissue health and viability.

CASL (Detre *et al.*, 1992) has never previously been used to investigate MS. Such a study might be advantageous because CASL is non-invasive and, unlike exogenous contrast methods, may be less susceptible to inaccuracy in diseases like MS which can affect BBB permeability (Tofts and Kermode, 1989) as the methodology does not assume the "contrast agent" - which in this instance is the pool of labelled, endogenous, flowing water protons - remains intravascular.

The technique generates labelled and control images, as described in section 2.3.1. Consequently, subtraction images from these two data sets have signal from labelled protons only as static tissue signal has been removed (Parkes and Tofts, 2002). A T_1

map is also collected at the same resolution and slice positions using a gradient echo EPI inversion technique in order to segment the tissue into grey and white matter regions using appropriate T_1 relaxation times. These images have the same image distortions as do the perfusion images (Parkes and Tofts, 2002).

The two-compartment theory

Previous CASL models have assumed that water is freely diffusible between the vascular and extracellular compartments (Detre *et al.*, 1992). However, the BBB is known to selectively impede flow across capillary membranes (Minagar and Alexander, 2003). Permeability of the BBB to water dictates the amount of exchange that occurs. The assumption of free permeability has the potential to overestimate measured perfusion values, with one simulation study reporting the magnitude of overestimation to be 62% in white matter and 17% in grey matter at 1.5 T (Parkes and Tofts, 2002). The over-estimation is due to the assumption that the labelled protons move directly into the extravascular space, experiencing faster T_1 relaxation than if they had remained in the blood. The difference in T_1 relaxation between blood and extravascular space is much larger for white matter, resulting in the much larger over-estimation in this case.

A two-compartment methodology (blood and extravascular compartments) was devised to address this inaccuracy (Parkes and Tofts, 2002). An extra model parameter is introduced, the permeability surface area product (PS), to account for labelled water crossing between the two compartments. The total magnetisation in the difference image is the sum of the magnetisation from each compartment multiplied

by their relative volumes. This can be simplified to leave only one extra parameter (PS/v_{bw}) where v_{bw} is the fractional blood water per unit volume of tissue. Modelling for errors in the model parameters revealed the T_1 relaxation time of water in blood and the equilibrium magnetisation of blood as those necessary to estimate most accurately (Parkes and Tofts, 2002).

Evaluating the technique

A recent study on 34 normal controls was undertaken with the above CASL sequence to assess its validity (Parkes *et al.*, 2004). Comparable results were obtained when considering other methods, with a whole brain perfusion reproducibility of 8% [PET 12% (Matthew *et al.*, 1993); SPECT 11% (Podreka *et al.*, 1989)]. Grey matter was noted to exhibit approximately twice the perfusion of white matter whilst grey matter perfusion decreased by 0.45% per year (mainly due to loss in the frontal lobes) and females had approximately 13% higher whole brain perfusion than males (Parkes *et al.*, 2004).

Because of the evidence of a vascular role in the pathogenesis of MS as described in section 1.4.9, CASL investigation may be revealing. Cerebral perfusion is a fundamental biological function which, at least under normal conditions, is coupled with parenchymal metabolism, hence potential exists for it to be a quantitative marker for pathological processes that alter metabolism.

A possible consequence of inflammation is local change in cerebral blood flow and volume which serve to transport cells and nutrients to the inflammatory site (Jackson

et al., 1997). Angiogenesis and vascular remodelling have been proposed as factors in the pathophysiology of cancer and certain chronic inflammatory diseases such as rheumatoid arthritis and psoriasis (Folkman 1995; Stromblad and Cheresh, 1996). Promotion of angiogenesis secondary to factors released in the inflammatory cascade associated with MS (such as nitric oxide, VEGF, interferon-γ and TNF-α) has also been reported (Van Meir, 1995; Ziche and Morbidelli, 2000; Giovannoni *et al.*, 2001; Kirk and Karlik, 2003). Further, angiogenesis has been detected in lesions in animal models of MS (Proescholdt *et al.*, 2002; Kirk and Karlik, 2003). This suggests that inflammation in MS may be associated with raised cerebral blood flow and volume.

Decreases in regional cerebral blood flow and volume have been reported in a variety of CNS diseases, such as cerebrovascular disease, Alzheimer's disease and other forms of dementia which would be consistent with decreased metabolic activity secondary to neurodegeneration (Keir and Wardlaw, 2002; Lojkowska *et al.*, 2002; Varrone *et al.*, 2002; Pasquier *et al.*, 2002).

As stated in section 2.5.1, previous perfusion investigations have generally sampled small numbers of mainly relapsing-remitting or secondary progressive MS subjects and not used CASL (Brookes *et al.*, 1984; Lycke *et al.*, 1993; Jensen *et al.*, 1995; Petrella *et al.*, 1997; Haselhorst *et al.*, 2000; Wuerfel *et al.*, 2004; Law *et al.*, 2004).

In this presented work, cerebral perfusion was estimated using CASL. Absolute measurements of perfusion were obtained in 60 MS subjects of all clinical phenotypes and 34 healthy volunteers in order to investigate: (i) the potential of a non invasive *in vivo* method to detect cerebral perfusion abnormalities in MS; (ii) regional patterns of

perfusion abnormality in both grey and white matter in the clinical MS subgroups with a hypothesis that decreased perfusion would, in reflecting neuronal and axonal loss, be associated with progressive and disabling forms of MS.

3.1.2 Methods

Subjects

Sixty subjects (mean age 48.1 [range 17-69] years; median EDSS 4; 21 male, 39 female) from four different subgroups (Lublin and Reingold, 1996) of clinically definite MS (Poser *et al.*, 1983) (21 relapsing-remitting, 14 secondary progressive, 13 benign and 12 primary progressive) were compared with 34 healthy controls (mean age 40.7 [range 20-67] years; 15 male, 19 female). The relapsing-remitting cohort was subdivided into those who were on BIFN (n=11; median treatment 1.6 years [range 0.15-2.05]) and those not (n=10), full details in Table 3.1. No subject had a previous history of any other significant central nervous or systemic autoimmune conditions. Because of the potential effect on cerebral perfusion, subjects with a history of cerebrovascular disease, psychomotor depression, illicit drug use, poorly controlled hypertension and ongoing medication with an immunosuppressant other than BIFN were also excluded. Subjects were scanned at least thirty days after a relapse or steroid treatment.

MRI protocol

All scans were acquired on a GE Signa 1.5T system (General Electric, Milwaukee, USA). A CASL pulse sequence using gradient EPI was performed (see figure 3.1) (Parkes and Tofts, 2002). The scanning parameters were: labelling duration=1.73 s, post-labelling delay=0.75 s, TR=4000 ms, TE=34 ms, 45 averages, matrix=64x64, FOV=240x240 mm, eight 6mm thick slices with a 3mm inter-slice gap covering inferiorly from just above the tentorium to the superior margin of the centrum semiovale, with axis aligned to the infracallosal line. The slices were acquired in an interleaved, ascending order and the in-plane resolution was 3.75x3.75 mm^3. The labelling plane was positioned 4cm inferior to the most caudal imaging slice. Double inversion labelling (with identical scanning parameters) was used for the control sequence as this had no net effect on arterial water longitudinal magnetisation, but matches the magnetisation transfer effects in the labelled image. Control and labelled image collection was interleaved. A T_1 map was also acquired using a three point inversion recovery technique in order to match the distortions of the perfusion images (TI=1s, 1.6s and one measure without inversion to calculate the equilibrium tissue magnetisation [M_0]), TR=7.2s). A gradient echo EPI sequence was used with the same resolution as the perfusion scan in order to exactly match the distortions of the perfusion images.

Table 3.1: *Entry stratification of all recruited subjects*

MS subtype	N	M	F	Mean Age	Median EDSS (range)	Median disease duration (range) yrs
Controls	34	15	19	40.7	0	-
All MS groups	60	21	39	48.1	4.0 (0-8.5)	16 (1-40)
Relapsing Remitting	21	8	13	38.9	2.5 (0-6.5)	10 (1-31)
-no treatment	10	3	7	37.9	3.0 (0-6)	7 (2-31)
-on BIFN	11	5	6	39.8	2.5 (1-6.5)	10 (1-17)
Secondary Progressive	14	3	11	51.2	6.0 (2-8)	18 (7-40)
Primary Progressive	12	5	7	55.7	6.5 (3.5-8.5)	16 (8-34)
Benign	13	5	8	52.6	2.5 (1-3)	24 (20-36)

Figure 3.1: *Diagramatic summary of CASL sequence used (Alsop and Detre, 1998)*

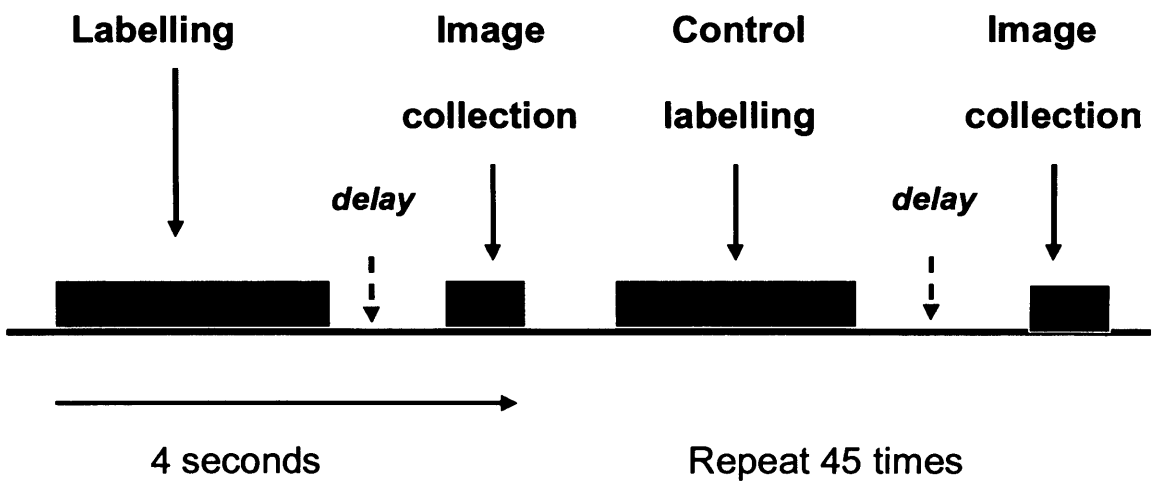

All MS subjects had conventional spin echo PD and T_2-weighted images (TR=3000 ms, TE=15/90 ms, matrix=256x256, FOV=240x240 mm, 46 contiguous slices of 3mm thickness) and 2D T_1-weighted images (TR=620 ms, TE=20 ms, matrix= 256x256; 46 contiguous slices of 3mm thickness) acquired prior to the CASL sequence. Total scanning time was about 35 minutes.

Quantitative perfusion maps (see Figure 3.2) were calculated from the CASL images and T_1 map using a two compartment methodology (Parkes and Tofts, 2002). The model assumed the following parameters: inversion efficiency=0.7; T_1 of blood=1.4 s; arrival time (from the labelling plane to the imaging slab)=0.32-0.83 s (increasing with slice distance, assuming a linear path, with a blood velocity of 14cm/s); permeability surface area product/blood water content (PS/v_{bw})=1.5/0.05 min^{-1}.

Figure 3.2: *Examples of quantitative perfusion maps produced by the CASL sequence (lighter contrast denotes higher perfusion; 0 to 150 ml/min/100ml)*

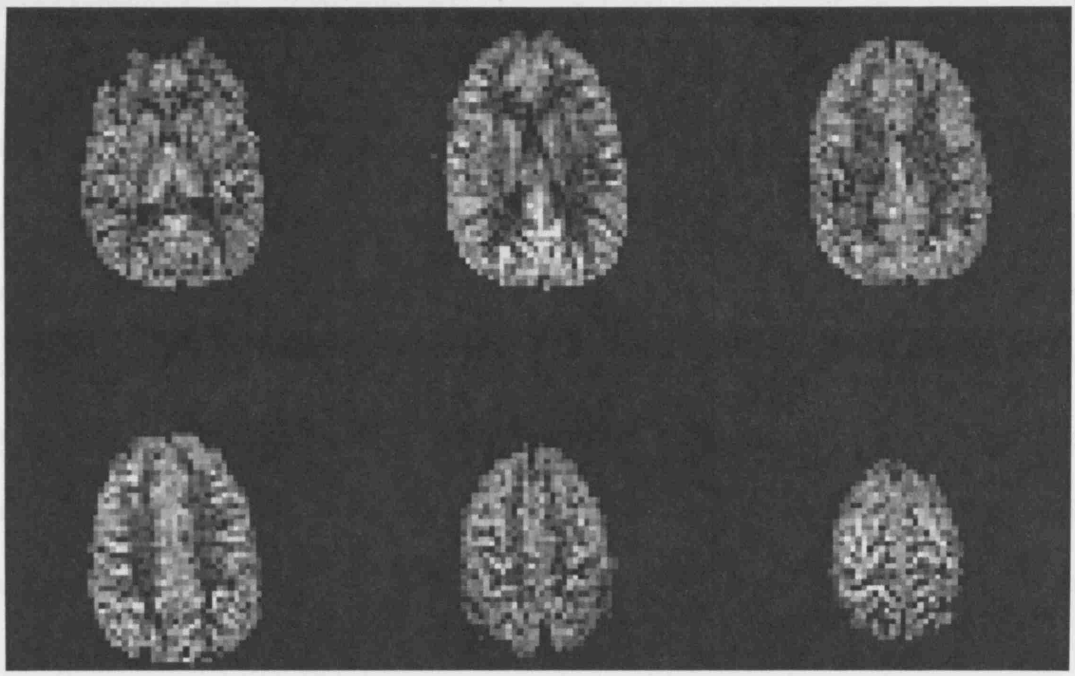

Perfusion image spatial pre-processing

To allow regional quantification within white and grey matter, perfusion maps were spatially pre-processed using SPM99 (Wellcome Department of Cognitive Neurology, Institute of Neurology, London, UK). Initially, non-labelled images were normalised to the EPI template (Montreal Neurological Institute) and then the normalisation parameters were applied to the subtracted labelled perfusion maps. Images were subsequently smoothed with a 12mm full width half maximum kernel. Extracerebral vascular contributions were minimised using a whole brain mask and absolute lower limit perfusion threshold of 5mls/min/100ml to avoid reporting results of doubtful relevance.

Global evaluation of white matter perfusion only

In-house software (Symms *et al.*, 1995) based on Automated Image Registration (AIR) (Woods *et al.*, 1998) was used to register the T_1 map to the perfusion images by rigid body registration to correct for in-plane shifts and rotations. T_1 values derived from previous studies (Steen *et al.*, 1994; Alsop and Detre, 1996; Vymazal *et al.*, 1999) were used to segment perfusion maps (Parkes *et al.*, 2004). Narrow limits were used to ensure high specificity (500-800 ms for white matter). This gave typical volumes of approximately 500 voxels (42 cm^3) of white matter in each subject. Quantitative perfusion values for each slice were averaged and weighted for voxel number, to give an average white matter perfusion value (ml/min/100ml) for each subject. Grey matter perfusion values were not used because T_1 segmentation could

not reliably avoid white matter lesion contamination due to similarities between grey matter and focal lesion T_1 relaxation times (Miller *et al.*, 1989).

All images were displayed on a Sun workstation (Sun Microsystems, Mountain View, CA, USA) using the Dispimage display software package (Plummer, Dept of Medical Physics, University College Hospitals NHS trust, London). Lesions were outlined using a semi-automated contouring technique (Filippi *et al.*, 1998a) on the PD and T_1-weighted images and lesion volumes calculated.

Statistical Analysis

For all statistical models employed, a P value of < 0.05 was considered significant and in the analyses of perfusion maps all P values were corrected for multiple comparisons. Individual MS subgroups were compared to all controls, with the potential covariate of age included and accounted for in each model.

(i) SPM analysis of perfusion maps: SPM employs a general linear model with Gaussian field theory to make statistical inferences, from the normalised SPM perfusion maps, about regional effects (Friston *et al.*, 1995). The statistical model included age and gender, and disease status all as covariates of interest to correct for any differences between control and patient groups. The subjects were included as random effects with each subject contributing one pre-processed perfusion image. The design matrix also included the global mean intensities as confounds which ensured that the results reflected regionally specific differences in perfusion. Following model estimation, 'T contrasts' were specified to test the statistical significance of particular linear combinations of parameter estimates. Voxelwise

significance was determined by using Gaussian random field theory (Worsley *et al.*, 1996) and the resulting statistical maps (SPM(t) maps) corrected for multiple comparisons over the whole perfusion volume. Contrasts compared controls with MS subgroups and different MS subgroups with each other. To avoid reporting areas of doubtful physiological relevance, only local maxima coordinates with a cluster volume > 50 voxels are quoted.

(ii) WM Perfusion values using T_1 segmentation: A further multiple linear regression model evaluated white matter perfusion values derived from T_1 segmentation. In the model, white matter perfusion was the dependent variable, gender and disease subgroup were included as categorical variables, and age as a continuous covariate to assess absolute disease effects allowing for these factors. To quantify the associations between perfusion and clinical status, models included age and gender as before, along with either MSFC as a continuous covariate or dichotomised EDSS values (mild 0 to 3, moderate or severe 3.5 and above) as a categorical variable.

3.1.3 Results

SPM based perfusion analysis

Smoothed, normalised perfusion maps were generated in 33 controls and 59 MS subjects. Maps from one control and one secondary progressive subject were not included due to inadequate normalisation to the EPI template.

The most prominent abnormalities were seen in primary and secondary progressive subgroups, who exhibited regions of reduced perfusion that involved both cortical and

deep grey matter structures and adjacent white matter areas (Table 3.2, figure 3.3), when compared with controls. Smaller regions of decreased perfusion were seen in patients with benign disease, and no areas of reduced perfusion were seen in the relapsing-remitting group.

Compared with controls, there was one small region of increased perfusion (69 voxels, p=0.001) in the secondary progressive group in right frontal subcortical white matter, and another small area of increased perfusion (78 voxels, p=0.003) in ten relapsing-remitting patients not receiving BIFN in a predominantly white matter region adjacent to the left precentral and superior temporal gyrus.

White matter perfusion results using segmentation based on T_1 range

As some white matter lesions have T_1 relaxation values of above 800 ms, the resulting masks will have excluded such lesions. Table 3.3 lists the results using this technique. The values in healthy subjects compare well with other studies (Leenders *et al*, 1990). A significant increase in white matter perfusion was observed in all MS subjects compared to controls (p=0.007). In the subgroup analysis, a significant white matter perfusion increase was seen in the pooled relapsing-remitting cohort (p=0.03), the relapsing-remitting group not on BIFN only (p=0.04) and secondary progressive subjects (p=0.02) compared to controls. There was weak evidence for increased white matter perfusion in benign MS subjects compared to controls (p=0.08). Statistical significance was not reached in those subjects on BIFN (p=0.14). No perfusion differences were detected between primary progressive subjects and controls or when comparing the MS subtypes directly with each other.

Table 3.2: *SPM analysis: Regions of hypoperfusion (voxel clusters with significance of patient groups compared with controls) in the combined cohort and clinical subgroups of MS. No regions of hypoperfusion were detected in the relapsing-remitting subgroup. (SP= secondary progressive; PP= primary progressive; Ben= benign; G= grey matter; W= white matter; NS=No significance)*

Region	**All MS**	**SP**	**PP**	**Ben**
Deep grey matter and adjacent white matter (1) R and L thalamus, caudate and extranuclear areas	**50% G 50% W 2399; p= <0.001**	**50% G 50% W 473; p= 0.001**	**52% G 48% W 2214; p= <0.001**	**43% G 57% W 143; p= 0.004**
Cortical grey matter and adjacent white matter	**66% G 34% W**	**56% G 44% W**	**56% G 44% W**	**76% G 24% W**
(1) R and L middle frontal and precentral and postcentral gyri and inferior parietal areas	1450; p= <0.001	1469;p= <0.001	1802; p= <0.001	526; p= <0.001
(2) R and L superior frontal and medial gyrus	1049; p= <0.001	614; p= <0.001	4668; p= <0.001	NS
(3) R and L precuneus and cingulate gyri	390; p= <0.001	NS	824; p= <0.001	NS
(4) R and L paracentral lobule	259; p= 0.001	NS	NS	NS
(5) L superior parietal lobule and subgyral areas	185; p= 0.007	NS	210; p= 0.010	NS

Figure 3.3: *Regions of perfusion decrease in primary progressive subjects compared to normal controls. The colour bar indicates the T score.*

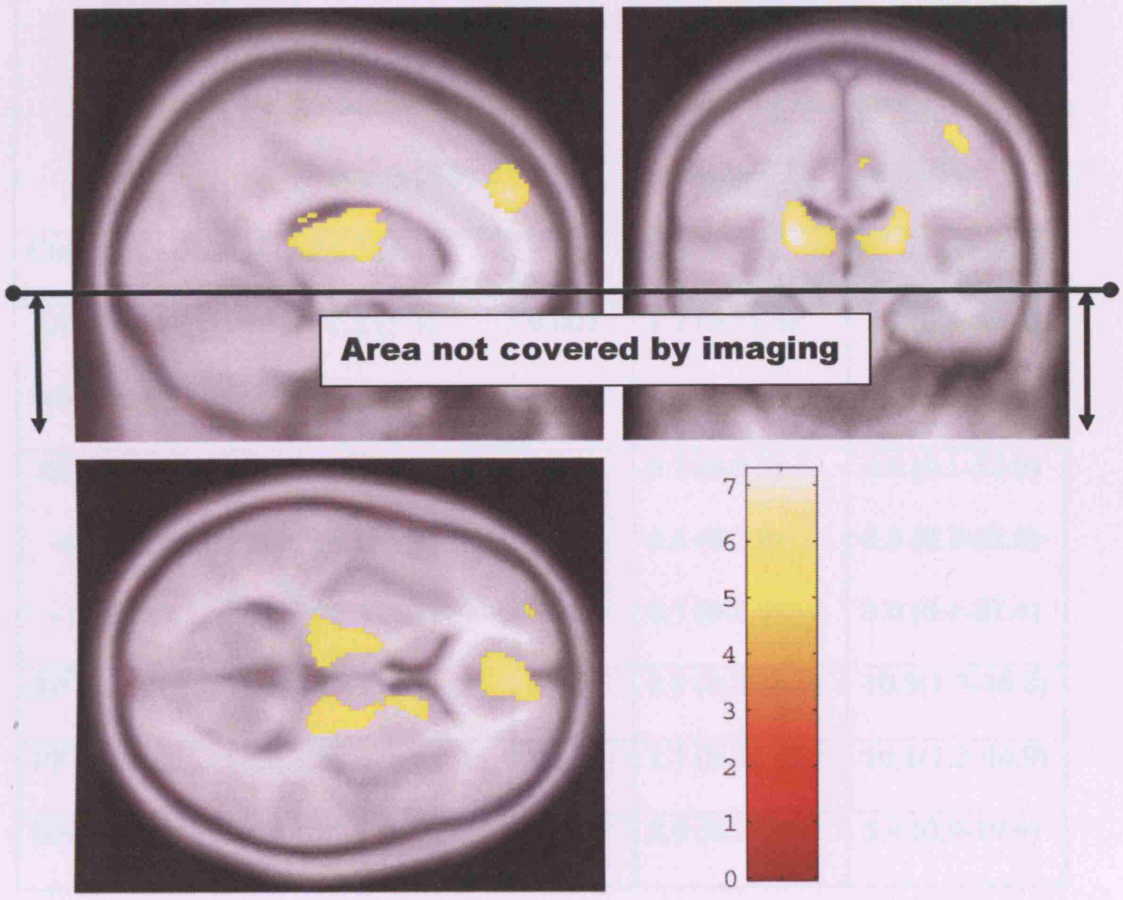

Table 3.3: *White matter perfusion results (ml/min/100ml) based on T_1-segmentation methodology in all subjects.*

[a]Difference adjusted for gender. p-value is for difference in comparison to controls.

Subject Type	No	WM perfusion ml/min/ 100mls (SD)	P value[a]	Median T_1 lesion vol (mls) (range)	Median PD lesion vol (mls) (range)
Controls	34	24.2 (4.2)	-	0	0
All MS subjects	60	27.2 (5.3)	0.007	1.2 (0-15.3)	5.7 (0.1-52.6)
All RR	21	27.4 (4.7)	0.03	0.7 (0-8.3)	4.6 (0.1-52.6)
- no BIFN	10	28.1 (5.3)	0.04	0.6 (0-7.9)	5.5 (0.3-52.6)
- on BIFN	11	26.7 (4.1)	0.14	0.7 (0-8.3)	3.0 (0.1-22.4)
SP	14	28.3 (5.7)	0.02	2.8 (0.2-15.3)	10.3(1.3-36.8)
PP	12	25.8 (5.0)	0.33	1.7 (0-10.4)	10.1(1.3-44.9)
Benign	13	27.1 (6.2)	0.08	2.0 (0.3-9.8)	5.4 (0.9-19.4)

Correlations between perfusion and MRI or clinical measures

In the SPM analysis there was no evidence of a correlation between perfusion measures and either lesion load or clinical outcomes. In the T_1 segmented white matter perfusion analysis, there was evidence that white matter perfusion may be

increasing more with PD lesion volume in the secondary progressive group than in other subtypes (p=0.03). There were no other significant correlations.

3.1.4 Discussion

The presented study is the first to quantify cerebral perfusion in MS using a non-invasive method. The main findings were a reduction of grey matter perfusion, especially deep grey matter, and an increase in white matter perfusion in certain clinical MS phenotypes.

Decreased grey matter perfusion

There were a large number of regions with lower perfusion located in both cortical and deep grey matter and adjacent white matter regions. This is generally concordant with previous studies (Brooks *et al.*, 1984; Pozzilli *et al.*, 1991; Lycke *et al.*, 1993). Neuronal and axonal dysfunction and loss in grey matter, with a corresponding reduction in local metabolic activity, may be the most likely cause of decreased grey matter perfusion. Another possible explanation for perfusion inhomogeneity could be due to a 'steal phenomenon' in the local vascular network caused by the redistribution of perfusion due to abnormalities of brain activity in other regions. Additional, more localised, perfusion studies are required to investigate this further.

The primary progressive subjects exhibited the largest areas of reduced perfusion, possibly consistent with axonal loss being a prominent neuropathological feature in this subgroup (Lucchinetti and Brück, 2004). Secondary progressive subjects also

revealed substantial areas of reduced perfusion, which is again consistent with neuroaxonal loss or dysfunction observed using other putative MR markers of axonal integrity at this stage of disease (Matthews *et al.*, 1996; Fu *et al.*, 1998). Benign MS subjects showed only limited areas of decreased perfusion, which could reflect a generally less severe underlying pathology, mirroring the clinical phenotype. No regions of reduced perfusion were seen in the relapsing-remitting group possibly consistent with less neuroaxonal damage reflecting the lower disability and shorter disease duration of this cohort.

Hypoperfusion in MS patients relative to controls was apparent in both cortex and deep grey matter, and was especially striking in the thalamus and caudate nuclei. A recent MR study in secondary progressive MS has reported a decrease in thalamic volume and NAA (Cifelli *et al.*, 2002). Furthermore, evaluations of glucose uptake in MS using PET have revealed areas of low metabolic function in the thalamus (Paulesu *et al.*, 1996; Blinkenberg *et al.*, 2000). The decreased thalamic perfusion observed in our pooled MS cohort is consistent with neuronal loss or dysfunction in this structure. The decreased perfusion in cortex and deep grey matter structures might also be indicative of disconnection between cortical regions and subcortical relay systems due to demyelination. The observation of decreased perfusion in the primary and secondary progressive subgroups of MS suggests that CASL has the potential to investigate the effects of neuroaxonal damage on brain metabolism in MS. As PET studies have suggested a possible correlation between areas of low function and cognitive (Blinkenberg *et al.*, 2000) or memory disturbance (Paulesu *et al.*, 1996), CASL may provide a potentially useful, non-invasive, evaluation into these symptoms in MS studies.

Increased white matter perfusion

Global assessment, using segmented T_1 maps, revealed raised perfusion in MS white matter compared with controls only in relapsing-remitting (particularly those not on BIFN) and secondary progressive subgroups.

Increased white matter perfusion might reflect higher metabolic activity due to an increase in cell number and activity in NAWM or lesions (lesions with a T_1 relaxation time of less than 800 ms will have been included in the globally segmented WM). In MS NAWM, such features include astrocyte proliferation and microglial activation (Allen *et al.*, 1981). In lesions, especially of recent onset, inflammatory features include perivascular cuffs of lymphocytes and macrophage infiltrates (Lassman, 1998a). PET studies (using benzodiazepine agonists as a microglial marker) showing increased activity in gadolinium-enhancing lesions and NAWM in MS subjects with greater disease progression (Banati *et al.*, 2000; Debruyne *et al.*, 2003) provide further evidence of the potential role of inflammation in white matter in MS.

Although gadolinium enhanced scans were not obtained to investigate the presence of inflammatory lesions, previous studies have shown that they occur more often in relapsing-remitting and secondary progressive MS rather than other subtypes (Thompson *et al.*, 1991; Thompson *et al.*, 1992) and are less common in patients on BIFN (Li and Paty, 1999). Our observation with the relapsing-remitting subgroup not treated with beta-interferon should, however, be interpreted cautiously, as there were only 10 subjects in this cohort and the increase was only marginally significant.

The SPM analysis of white matter perfusion suggests a complex regional pattern. Although small foci of increased perfusion were observed in relapsing-remitting and secondary progressive subgroups, areas of decreased perfusion were also seen, especially adjacent to areas of decreased deep grey matter perfusion in patients with primary or secondary progressive MS. Axonal loss is described in white matter lesions and NAWM (Trapp *et al.*, 1998; Evangelou *et al.*, 2000) and if extensive, might result in decreased metabolic activity and hence perfusion. An additional explanation may be that a vasculitic process possibly associated with regional hypoxia – either as a primary or secondary event - may be occurring as proposed by in a recent exogenous contrast MRI perfusion study (Law *et al.*, 2004).

Methodological considerations

A two-compartment model (Parkes and Tofts, 2002) was used to quantify perfusion to correct for the selective permeability of the BBB, producing a technique with greater physiological accuracy. With CASL and two-compartment modelling, an increase in BBB permeability to water in MS, in comparison to controls, could result in a small underestimation of perfusion, possibly contributing to some of the perfusion reductions noted, but not the white matter increases. However, simulations of the two-compartment model show that even relatively large changes in the permeability constant would result in minimal changes to the perfusion measurements (Parkes and Tofts, 2002). Also, it would be difficult to model exactly for permeability differences between MS subjects and controls as it could be influenced by the between subject variability of inflammatory activity. It is theoretically possible that a specific effect on the blood T_1 relaxation time due to MS may significantly alter the measured

perfusion result. However there is little evidence to suggest that MS has such an effect. Hence, this technique offers a potentially more accurate evaluation of perfusion in MS than previous approaches.

It should also be noted that statistical inferences based on Gaussian field theory (SPM) may be problematical if the normality of residuals cannot be guaranteed. One possible method of overcoming this - not done in the study detailed in this chapter - is to test each control versus the rest of the group and establish a false positive rate (Jones *et al.*, 2005). It should be noted, however, that the present study was exploratory both in terms of the feasibility of CASL in assessing MS and also determining the best means of analysis. Future, more defined, investigations should take this consideration further into account when using SPM.

Potential sequence improvements include: (i) the acquisition of a T_2-weighted sequence that is fully registered with the perfusion images to improve focal lesion segmentation on the perfusion maps; (ii) an increased number of signal averages to improve resolution (but at the cost of increased scan time). Image acquisition must be achieved within the time frame of the blood T_1 relaxation time necessitating high speed EPI acquisition lowering the resolution and limiting brain coverage. Higher field strength scanners would increase the T_1 relaxation time and SNR, although specific absorption rate limitations may occur.

This study confirms that a new non-invasive perfusion methodology (CASL with two compartment modelling) is capable of reliable quantitative measurement in MS and from the results pathophysiological mechanisms may be hypothesised.

CHAPTER 4

Contrast enhancement in clinically early relapsing-remitting multiple sclerosis

4.1 Introduction

Clinical and pathological challenges remain regarding the evolution of MS. Greater understanding regarding this may: (i) offer patients more accurate information regarding clinical course; (ii) identify those who may benefit most from disease modifying therapy and (iii) aid development of new and more effective therapies.

With this in mind, the evaluation and longitudinal follow-up of patients at the clinically earliest stages of relapsing-remitting MS is relevant to allow delineation of pathogenesis from the onset of disease to later clinical development. This may improve the understanding of whether pathological processes early in MS influence the magnitude of later disability. Using quantitative MRI measures in such a cohort would provide an opportunity to explore pathological evolution using these *in vivo* imaging measures at a stage when patients are likely to have minimal disability. The sensitivity of the MR measures to detect pathological change can be evaluated and - as longitudinal observation continues – the relationship of the imaging changes with the future clinical course can also be studied.

The potential role of the early clinical course *per se* in MS is shown by previous studies demonstrating that the degree of recovery from first relapse and time to second relapse may have later prognostic value (Confavreux *et al.*, 2003). Additionally the observation that cerebral atrophy occurs at the earliest stages of MS

with correlation to disability (Chard *et* al., 2002b; De Stefano *et* al., 2003) indicates that early axonal loss does occur in MS and that it is clinically relevant.

The possibility that early MR lesion development may influence later prognosis in MS was illustrated by a long-term MRI study in CIS patients which noted that change in T_2 lesion load within the first five years of onset was more strongly related to disability at 14 years than later lesion volume measures (Brex *et al.*, 2002). Possible explanations for this are that: (i) axonal damage within new inflammatory lesions may occur to a greater degree within the first year after disease onset (Kuhlmann *et al.*, 2002); (ii) acute inflammation early in the course of MS may expose further potential autoantigens to immune surveillance, known as epitope spreading (Tuohy *et al.*, 1998); (iii) it is possible that widespread early demyelination may render exposed axons more liable to later damage due to loss of trophic support, and (iv) extensive early tissue damage may establish more complex pathophysiological processes that are subsequently harder to regulate.

To address the relationship of early MRI findings with clinical evolution a cohort of patients with clinically definite (Poser *et al.*, 1983) relapsing-remitting (Lublin and Reingold, 1996) MS was recruited at the NMR Research Unit at The Institute of Neurology, London using the following criteria: (i) they were within three years of first symptom onset; (ii) they were not on disease modifying therapy at baseline and (iii) there was a minimum of one month since last relapse and/or course of steroids at baseline.

Previous quantitative MR studies in this cohort have shown: (i) metabolite changes in both grey matter and NAWM in patients demonstrated by MR spectroscopy (Chard *et al.*, 2002c); (ii) both cross-sectional and longitudinal MTR abnormalities observed in comparison to controls (Davies *et al.*, 2004; Davies *et al.*, 2005); (iii) significant detectable baseline grey and white matter atrophy in patients (Chard *et al.*, 2002b) and progressive grey matter tissue loss over follow up for 18 months (Chard *et al.*, 2004) to two years (Tiberio *et al.*, 2005).

The next two chapters of this thesis focus on the findings of three MRI measures in this patient cohort: (i) the number and volume of gadolinium enhancing lesions (Chapter 4); (ii) measurements of diffusion parameters from the analysis of DTI scans using whole brain and normal appearing brain tissue histograms (Chapter 5), and (iii) the measurement of spinal cord cross-sectional area (UCCA) (Chapter 5).

The studies of gadolinium-enhancing lesions provide an indication of the extent of early inflammation since such lesions have been correlated in post mortem and biopsy studies with histopathological features of active inflammation in MS (Katz *et al.*, 1993; Brück *et al.*, 1997). DTI provided a potential assessment of more global changes involving normal appearing brain tissues and UCCA measurement evaluated the development of atrophy that could potentially reflect axonal loss in functionally important longitudinal tracts or grey matter within the cord. All studies reported in chapters four and five investigate patients from the clinically early relapsing-remitting MS cohort and also – in chapter five – an age-matched control cohort recruited in parallel to the MS cohort.

4.2 Intensive evaluation of contrast enhancement in clinically early relapsing-remitting multiple sclerosis: a six month follow-up study

4.2.1 Introduction

As discussed in section 2.5.2, gadolinium-enhancement of MS lesions on MRI are seen more often during relapses but can occur in clinically stable patients and occur five to ten times more frequently than clinical relapses (Miller *et al.*, 1988; Miller *et* al., 1991; Barkhof *et* al., 1992; Thompson *et* al., 1992; McFarland *et* al., 1992; Smith *et* al., 1993). To directly investigate if inflammation early in the course of MS is relevant to the later clinical outcomes, it is necessary to determine the extent of gadolinium enhancing lesions at the earliest stages of MS and follow patients prospectively over time assessing their clinical function. In this section, the extent of enhancing lesions detected using an intensive scanning protocol over six months is reported. Longer term follow up and its relationship to this period of intensive monitoring is detailed in section 4.3.

4.2.2 Methods

Subjects

Forty patients from the early relapsing-remitting cohort described earlier (mean age 36.2 [range 24.1-55.6] years; 29 female, 11 male; median disease duration 1.7 [range 0.5-3] years; median EDSS 1.5 [range 0-3]) underwent baseline MRI and clinical assessment (EDSS (Kurtzke, 1983) and MSFC (Cutter *et al.*, 1999)). Of the original

40 subjects, 31 had MRI and clinical assessment at six months. Intensive observation of inflammatory (i.e. gadolinium-enhancing) lesions was undertaken in 21 subjects scanned at baseline and again after 1, 2, 3 and 6 months. Informed consent was obtained from all subjects and the study had approval by the joint ethics committee of the Institute of Neurology and National Hospital for Neurology and Neurosurgery, Queen Square, London.

MRI protocol and Image analysis

Scans were performed on a GE Signa 1.5 Tesla machine (General Electric Medical Systems, Milwaukee, Wisconsin, USA). At all scanning time points, subjects had a 2D T_1-weighted CSE images of the brain (TR=540ms; TE=20ms; matrix=256x256; FOV 240x240 mm; 28 contiguous 5mm slices covering the whole brain) and spinal cord (TR=500ms; TE=14ms; matrix 512x512; FOV 480x240 mm; 13 contiguous 3mm sagittal slices) in the same scanning session immediately prior and then approximately 15 minutes following an injection of triple dose gadolinium (0.3 mmol/kg). Also following contrast injection, conventional spin echo PD and T_2-weighted images (TR=2000ms; TE=30/95 ms; matrix=256x256; FOV=240x180 mm; 28 contiguous 5mm axial slices covering the whole brain) were acquired.

Enhancing lesions were identified by an experienced observer (DHM). These areas were contoured on a SUN workstation using DispImage (Plummer, Dept of Medical Physics, University College Hospitals NHS Trust, London) (Plummer, 1992) and volumes calculated using a semiautomated contouring technique (Filippi *et al.*, 1998a).

Statistical Analysis

Spearman rank correlation coefficients were used to assess correlations between gadolinium-enhancing lesion volumes and other quantitative variables. Wilcoxon rank sum tests were used for between group comparisons of lesion volumes, EDSS and changes in EDSS over six months, and time since last relapse (prior to study entry). Changes from baseline for any of these variables were assessed using Wilcoxon sign rank tests. Association between pairs of binary variables were assessed using Fisher's exact test. Comparisons of MSFC, and its changes over six months, were analysed using regression to adjust for baseline and to investigate potential confounding by age, gender or disease duration; change in MSFC was analysed by paired t-test. Analyses were carried out in Stata 7.0 (Stata Corporation, College Station, Texas, USA). A p value of < 0.05 was considered significant.

4.2.3 Results

Prevalence and pattern of Gadolinium-enhancing lesions

Tables 4.1 and 4.2 outline cohort demographics, clinical and MRI characteristics and pattern of gadolinium enhancement at baseline and six months. No relationship was found between the time since last relapse prior to study recruitment and baseline gadolinium-enhancement (median 241 days post relapse to recruitment of subjects without enhancing lesions [1 of 8 had a relapse within 3 months prior to baseline]; median 200 days in subjects with enhancing lesions [4 of 32 had a relapse within 3 months prior to baseline]; p=0.772). 121 enhancing lesions were identified (mean

lesion number per subject 3.02 [SD 3.89]) in 32 out of 40 subjects (80%) at baseline (in 22 patients in the brain only; in 2 in the cord only; 8 patients had enhancing lesions in both regions).

From the original 40 subjects, two had possible allergic reactions to gadolinium (both consisted of a mild, non-specific rash only) and seven declined to undergo the scan at 6 months. There was no significant difference in terms of clinical demographics or gadolinium-lesion enhancement at baseline between the nine subjects who did not complete the study and the remaining 31 subjects. Twenty (64.5%) out of the 31 subjects studied at six months had gadolinium-enhancing lesions (13 in the brain only; 7 in both brain and cord), compared with 25 (80.6%) of the same 31 subjects at baseline. A total of 64 gadolinium-enhancing lesions were observed at month six (mean number in all subjects was 2.06 (SD 2.41)). At baseline the same 31 patients had 101 gadolinium-enhancing lesions (85 brain; 16 cord). However, the decrease in overall number of gadolinium-enhancing lesions comparing month six with baseline was not significant (Wilcoxon sign rank test; $p=0.244$). The presence of brain enhancement at six months and the presence of baseline enhancement was significantly associated (Fisher's exact test; $p=0.013$). Including data of 21 subjects from the original cohort who had additional scans at months 1, 2 and 3, only 2 out of 40 patients (5%) had no gadolinium-enhancing lesions at any time point.

Table 4.1: *Gadolinium-enhancing lesions for all subjects (Pt) (new lesions (persisting lesions in brackets); * ring lesion; ND=Not done; B=brain; C=cord).*

Pt	Mth 0		Month 1		Month 2		Month 3		Month 6	
	B	C	B	C	B	C	B	C	B	C
1	0	0	0	0	ND	ND	ND	ND	ND	ND
2	0	0	0	0	ND	ND	1	0	0	0
3	0	0	0	0	0	0	0	0	0	0
4	0	0	0	1	0	0	0	0	0	0
5	0	1	0	0 (1)	0	1	ND	ND	ND	ND
6	0	0	1	0	0	0	1	0	ND	ND
7	0	0	2	0	0 (1)	0	0	0	0	0
8	0	0	0	0	0	0	0	0	1	0
9	0	0	0	1	0	0	0	0	0	0
10	0	1	ND	ND	ND	ND	ND	ND	ND	ND
11	1	0	ND	ND	ND	ND	ND	ND	ND	ND
12	1	0	ND	ND	ND	ND	ND	ND	ND	ND
13	1	0	0	0	1	2	0 (1)	1 (2)	0	0
14	1	1	2	1	0	0 (1)	0	0	1	1
15	1	0	1	0	2 (1)	0	0 (3)	0	2	0
16	1	0	1 (1)	0	0 (1)	0	ND	ND	3	0
17	1	0	0	0	ND	ND	0	0	1	0
18	1	0	1	1	ND	ND	1	0	3	0
19	1	0	2	0	6 (1)	0	ND	ND	5	1
20	1	1	0	2 (1)	ND	ND	1	1	ND	ND
21	2 *	0	1 * (2)	0	4 * (2)	0	1 * (2)	0	2	0
22	2	0	2 (2)	0	1 (2)	0	1 (1)	0	0	0
23	2	0	ND	ND	ND	ND	ND	ND	ND	ND
24	2	0	8 (2)	0	5 (7)	0	4 (10)	0	5	0
25	2	1	ND	ND	ND	ND	0	0	5	1
26	3	0	2 (1)	0	0 (2)	0	ND	ND	0	0
27	3	1	1 (2)	1	1 (2)	0 (1)	18 (1)	0	8 *	2
28	3	0	1 (2)	0	ND	ND	ND	ND	1	0
29	3	0	1 (3)	0	1	0	1 (1)	0	1	1
30	3	0	5 (1)	0	2	0	4 (1)	1	2	0
31	3 *	0	1 (1)	0	1 (1)	0	0	0	1	0
32	3	0	3 (1)	0	2 * (2)	0	3	1	2	3
33	4	0	2 (2)	0	1	0	0 (1)	0	2	0
34	5 *	0	2 (2)	0	1 (3)	1	0 (2)	0 (1)	1	1
35	6	0	3 (2)	0	5 (4)	0	3 (3)	0	5 *	0
36	7	1	4 (1)	0	2 (3)	0	ND	ND	0	0
37	8	0	ND	ND	3	1	4	0	3	0
38	9	4	0 (1)	0 (1)	1 (1)	0 (1)	0 (1)	0	1	0
39	10	8	8 (5)	2 (2)	10 (5)	1 (1)	ND	ND	0	0
40	11	1	ND	ND	ND	ND	ND	ND	ND	ND

Table 4.2: *Clinical and MRI features of patients with and without gadolinium (Gd)-enhancing lesions at baseline and 6 months. (mean values unless stated otherwise).*

	Non-enhancing 0 mths (n=8)	**Enhancing 0 mths (n=32)**	**Non-enhancing 6 mths (n=11)**	**Enhancing 6 mths (n=20)**
Age (years)	39.31	35.44	40.42	35.10
Gender (male:female)	2: 6	9: 23	2: 9	5: 15
Disease duration (yrs)	1.68	1.85	2.33	2.36
EDSS Median (range)	1.75 (1-2)	1.0 (0-3.5)	2.0 (1-3.5)	1.50 (0-3)
PD load (ml) Median (range)	6.22 (1.12-19.61)	4.71 (0.50-40.78)	4.27 (0.95-14.29)	6.54 (1.57-29.16)
T1 load (ml) Median (range)	0.98 (0.27-3.75)	0.61 (0-9.87)	0.71 (0.13-3.23)	0.72 (0-7.89)
Gd load (ml) Median (range)	No lesions	0.34 (0.04-4.30)	No lesions	0.27 (0.03-2.87)

Associations between Gadolinium-enhancement and clinical and MRI outcomes

Nineteen subjects had had a total of 21 relapses during the study. Symptomatic enhancing lesions were seen in seven of these relapses (two brain; five cord). Patients

with baseline gadolinium-enhancing lesions were (non-significantly) more likely to experience relapses in the following six months (risk of relapse = 0.63 in those with enhancing lesions; 0.25 in subjects without enhancement [relative risk 2.52; 95% confidence interval {CI} 0.73, 8.66; p=0.11]). There was an increase in EDSS from 0 to 6 months (median EDSS=1.5 at baseline; 1.75 at 6 months; p=0.039) but the EDSS change was not correlated with the number of gadolinium-enhancing lesions. There was no change in MSFC from 0 to 6 months (p=0.417).

Four subjects required a course of steroids within the study time period due to a relapse, whilst four of the 31 subjects who completed the study had commenced BIFN by six months. There was no significant difference in the levels of gadolinium-enhancement at baseline or six months between the four patients commenced on BIFN and the remaining 27 patients not on the medication. When these subjects treated with BIFN are removed from the whole cohort 6 month analysis (leaving 27 subjects not on disease modifying therapy who had both baseline and 6 month scans), there were 83 gadolinium-enhancing lesions (mean 3.07 lesions per subject [SD 3.73]) at baseline and 57 (mean 2.11 lesions per subject [SD 2.45]) at month 6, a 31.3% decrease. However, the apparent decrease was not significant when considering either the number of subjects with at least one gadolinium-enhancing lesion (p=0.102) or the overall number of gadolinium-enhancing lesions (p=0.293). No other statistically significant differences were found in subjects regarding gadolinium lesion frequency pre-versus post treatment.

4.2.4 Discussion

A high degree of gadolinium-enhancing lesion activity was apparent in this cohort of early relapsing-remitting MS subjects none of whom were having a concurrent relapse at the commencement of the study.

The proportion of patients with gadolinium-enhancing lesions (in brain and cord) was 80% at baseline, and 95% exhibited one or more enhancing lesions at some time during the six months of observation. Previous studies investigating relapsing-remitting MS subjects with longer disease durations with either triple or single dose gadolinium have reported generally lower baseline enhancement rates ranging between 40-78% (Thompson *et al.*, 1992; Wiebe *et al.*, 1992; Stone *et al.*, 1995; Koudriavtseva *et al.*, 1997; Tortorella *et al.*, 1999; Bagnato *et al.*, 2000).

The high level of activity observed could have several explanations. Firstly, relapsing-remitting MS subjects with short disease durations may have higher levels of enhancement. Secondly, as the subjects were required to have had at least two relapses within three years, it may have been a more 'active' cohort (although, no relationship was found between the time of last relapse prior to study entry and baseline gadolinium-enhancement). Thirdly, triple dose gadolinium (rather than single or double dose) will have increased the number of enhancing lesions (van Waesberghe *et al.*, 1997; Silver *et al.*, 1997; Filippi *et al.*, 1998d; Rovaris *et al.*, 1998; Rovaris *et al.*, 1999; Silver *et al.*, 2001a) and active scans (Filippi *et al.*, 1996b; van Waesberghe *et al.*, 1997; Silver *et al.*, 1997; Filippi *et al.*, 1998b; Filippi *et al.*, 1998d; Silver *et al.*, 2001a), although it has less of an effect on the latter. On the other

hand, 5mm MRI slice thickness was used in this study, and thinner slices (e.g. 3mm) might have further increased the detection of gadolinium-enhancing lesions (Filippi *et al.*, 1995; Filippi *et al.*, 1997; Firbank *et al.*, 1999).

Although not statistically significant, in the 27 patients who did not receive BIFN the total number of gadolinium-enhancing lesions decreased by almost one-third between baseline and month six. This might have occurred by chance alone, although conceivably it could also reflect a trend for regression to the mean to occur in such studies or for there to be a natural decline in enhancing lesion activity in the very early stages of relapsing-remitting MS; however, in the absence of monthly scans between months three and six, we do not rule out the possibility that it is simply a part of natural fluctuations in disease activity.

Clinically, there was a slight increase in EDSS over six months with no change seen in MSFC. These findings might be explained by the fact that at the low levels of EDSS studied, a subtle increase could reflect the emergence of new physical signs without an associated alteration of function.

In summary, we observed a high initial degree of inflammatory activity in early relapsing-remitting MS with a trend to decrease over the following six months. Having determined short term activity early in the course of MS, the next section now details longer term follow-up and its relationship with the period of intensive monitoring of enhancing lesions.

4.3 Longitudinal investigation of the levels of contrast enhancement and clinical dysfunction in clinically early relapsing-remitting multiple sclerosis

4.3.1 Introduction

Previous studies of gadolinium-lesion enhancement and its relationship to relapses, disability or atrophy have shown that although an association between such enhancing lesions and the development of clinical relapse exists, the correlation with long term disability is poor (Miller *et al.*, 1988; Miller *et* al., 1991; Barkhof *et* al., 1992; Thompson *et* al., 1992; McFarland *et* al., 1992; Smith *et* al., 1993; Khoury *et al.*, 1994; Stone *et al.*, 1995; Koudriavtseva *et al.*, 1997; Kappos *et al.*, 1999; Losseff *et al.*, 2001). However, these investigations have often investigated patient groups with varying disease durations and have tended to use standard dose gadolinium (0.1 mmol/kg) which is less sensitive than triple dose in detecting active lesions. In addition, studies investigating cerebral atrophy in MS - which may in part result from neuroaxonal loss in inflammatory lesions (Trapp *et al.*, 1998; Kuhlmann *et al.*, 2002) potentially indicating a possible underlying progressive pathological process in the disease – have not revealed a consistent relationship between the level of gadolinium-enhancing inflammatory lesions early in the clinical course of the disease and brain volume loss (Saindane *et al.*, 2000; Zivadinov *et al.*, 2002). Presently, it is unclear to what extent early inflammation may influence the long term clinical and MR course. By performing such a study on a cohort of clinically early relapsing-remitting MS patients with a relatively homogenous disease duration range and using triple dose gadolinium, more robust associations with long term clinical outcome may be achieved.

This section presents a prospective two-year longitudinal study documenting the extent of gadolinium-enhancement and its relationship to clinical and other MR changes in the clinically early MS cohort described earlier. The aims of this study were to: (i) describe the pattern of gadolinium-enhancement over time; (ii) investigate whether early enhancement is associated with concurrent or subsequent clinical relapse frequency, clinical impairment and disability and (iii) investigate the relationship of early gadolinium-enhancement to later brain atrophy.

4.3.2 Methods

Subjects

Twenty-six patients from the early relapsing-remitting MS described earlier (mean age 37.3 [range 25.9-55.6] years; 19 female, 7 male; median disease duration 1.7 [range 0.5-2.9] years; median EDSS (Kurtzke, 1983) 1.25 [range 0-3]) were scanned from baseline at approximately six month intervals over two years. At six and 12 months, 25 patients were imaged; whilst at 18 months 23 patients were included. At study completion at two years, all 26 patients were scanned. Additionally data from the early intensive six-month study (see section 4.2) was incorporated for scans at 1, 2 and 3 months post baseline – with 25 out of 26 patients undertaking at least two of these monthly scans – in order to provide an indication of the extent of early inflammatory lesions in the brain and cord. The mean number of gadolinium-enhancing lesions in the first six months per patient was then used to determine if associations existed with later clinical and MR parameters over the study course. The median length of time from study start to completion was 733.5 days.

During the study follow up period, 10 of the 26 original MS patients received BIFN treatment, four of whom had started the medication within the first six months of the study. The EDSS and MSFC (Cutter *et al.*, 1999) were assessed in each patient at all time-points and any clinical relapses recorded. Informed consent was obtained from all subjects and the study had approval of the Joint Medical Ethics Committee of the Institute of Neurology and National Hospital for Neurology and Neurosurgery, Queen Square, London.

MRI protocol and image analysis

Scans were performed on a GE Signa 1.5 Tesla machine (General Electric Medical Systems, Milwaukee, Wisconsin, USA). At all time points, MR sequences in each subject were acquired in identical fashion as detailed in section 4.2. Additionally, a 3D inversion-prepared FSPGR sequence (TR 13.3ms; TE 4.2 ms; TI 450 ms; matrix 256x144; FOV 240x180 mm [zero filled to give an image pixel size of 1.2x1.2 mm]) providing 124x1.5 mm slices covering the whole cranium was obtained yearly during a separate scanning session (median 4.5 days (baseline); 7 days (one year); 8.5 days (two years) from the other session). From these images fractional brain volumes were measured using a method described previously (Chard *et al.*, 2002b).

Enhancing lesions were identified by an experienced observer (DHM) and classified as either homogenous or ring-enhancing. Images were transferred to a Sun workstation (Sun Microsystems Inc, Mountain View, CA, USA). T_2 and pre- and post-contrast T_1–weighted lesion volumes were calculated as in section 4.2. The mean number of gadolinium-enhancing lesions within the first six months was calculated

for each patient using data from all scans that the patient had participated in during the first six months of the study.

A recent study investigating brain volume in 21 of the patients taking part in this study showed progressive grey matter tissue loss over two years in comparison to controls (Tiberio *et al.*, 2005). This data was used along with the segmented brain tissue volumes from the remaining five patients in this study not included in the original brain volume cohort - calculated using identical methodology (Chard *et al.*, 2002b) – to investigate any association of change in whole brain volume [WBV]; brain parenchymal fraction [BPF]; grey matter fraction [GMF]; white matter fraction [WMF] over two years with gadolinium-enhancing lesion number over the first six months.

Statistical Analysis

Spearman rank correlation coefficients were used to assess correlations between the mean gadolinium-enhancing lesion number in the first six months of the study and other quantitative variables (including number of clinical relapses, brain tissue volumes, T_1 and T_2 lesion volumes and EDSS) at each time point or their changes over the two years of the study. Wilcoxon sign rank tests were used to assess within group or whole group changes from baseline over two years for these variables. Wilcoxon rank sum tests were used for between group comparisons of lesion measures (particularly mean gadolinium-enhancing lesion number in the first six months and ring lesion enhancement) and the occurrence of a clinical relapse event at different study time-points. Change in MSFC and its three components (25-foot timed

walk test [TWT]; nine hole peg test [PEG] and three second paced auditory serial addition test [PASAT]) were analysed by paired t-tests. Between group comparisons of MSFC - and the three components contained within it - with the mean gadolinium-enhancing lesion number over six months and changes in MSFC over two years, were analysed using regression to allow potential confounding by age, gender or disease duration. Analyses were carried out in Stata 8.2 (Stata Corporation, College Station, Texas, USA) and SPSS 11.0 (SPSS Inc., Chicago, IL, USA). A p value of < 0.05 was considered significant.

4.3.3 Results

Table 4.3 shows the cohort demographic details, lesion volumes, mean gadolinium-enhancing lesion number, brain tissue volumes and frequency of relapse occurrence with p-values testing two-year changes in the whole group of patients. No significant difference was observed between subjects commenced on BIFN in the first six months of the study (n=4) and those not on the medication either in gadolinium-enhancing lesion number in the first six months or on subsequent levels of enhancement over the remainder of the study. Ring gadolinium-lesion enhancement was not associated with the overall frequency of gadolinium-lesion enhancement and later clinical and MRI parameters over the study course. Of all gadolinium-enhancing lesions detected, 7.5% were identified to be ring-enhancing.

Table 4.3: *Demographic, clinical and MRI variables for all patients at each time-point of the study. Mean values unless stated. ([a] p value represents difference between baseline and 2 year values) (Gadolinium=Gd)*

	Mth 0	6 mths	12 mths	18 mths	24 mths	P-value[a]
Patient number (male: female)	26 (7: 19)	25 (6:19)	25 (7:18)	23 (6:17)	26 (7:19)	N/A
Median EDSS	1.25	1.50	1.50	2.0	2.0	**0.006**
MSFC	0.0	0.02	-0.01	-0.04	-0.09	0.299
No of pt relapses in the preceding 6 months	N/A	11	9	7	10	0.705
PD lesion vol (mls)	7.81	8.69	8.79	8.12	9.59	**0.008**
T_1 lesion vol (mls)	1.80	1.57	1.64	1.46	1.82	0.849
Gd-enhancing lesion vol (mls)	0.65	0.33	0.51	0.32	0.19	**0.015**
Number of Gd-enhancing lesions	2.65	1.84	2.56	1.56	1.42	**0.033**
WBV (mls)	1085.32	N/A	1079.86	N/A	1071.87	**<0.001**
BPF	0.811	N/A	0.803	N/A	0.800	**0.004**
GMF	0.544	N/A	0.534	N/A	0.533	**0.001**
WMF	0.268	N/A	0.268	N/A	0.267	0.829

Figure 4.1: *Number of gadolinium-enhancing lesions detected at each time-point during the study.*

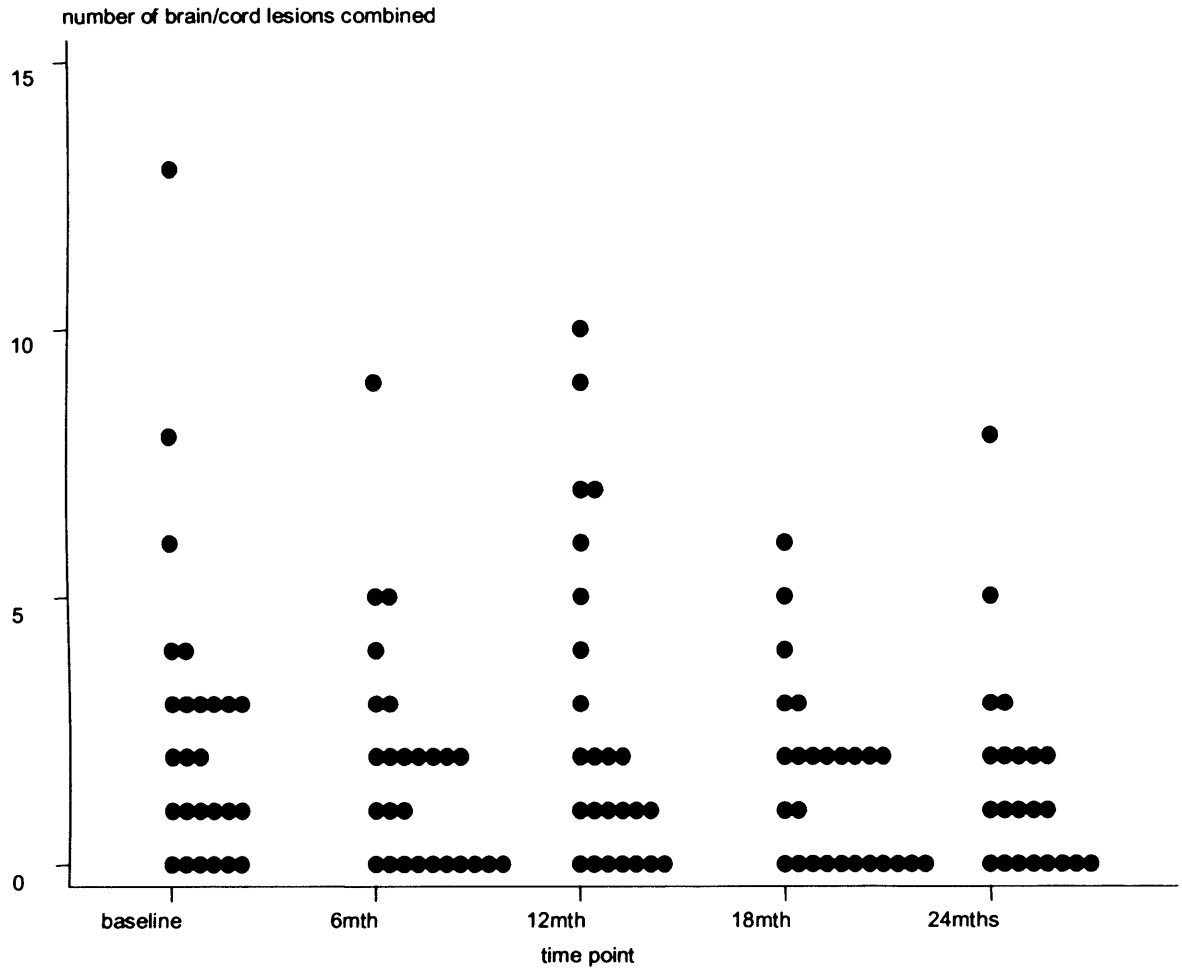

Longitudinal pattern of lesion enhancement

Figure 4.1 illustrates the pattern of gadolinium-enhancement (brain and cord combined) in each patient at all time-points. Age, gender and disease duration were not observed to have significant effects on the development of such lesions. The time of last relapse prior to study entry was not related to the presence of a gadolinium-enhancing lesion at baseline (median 180 days post relapse in patients with no gadolinium-enhancement at baseline; 241 days with baseline gadolinium-

enhancement; p=0.555). A total of 252 (223 brain; 29 cord) gadolinium-enhancing lesions were identified counting all six-monthly time-points (baseline: 69; six months: 46; 12 months: 64; 18 months: 36 and 24 months: 37), with no significant longitudinal trend for change in the number of gadolinium-enhancing lesions at each six-month time-point during the study (p=0.191). A greater mean number of gadolinium-enhancing lesions per patient in the first six months was correlated with greater combined total number of gadolinium-enhancing lesions per patient at the later time-points (12, 18 and 24 months) of the study (r_s=0.561; p=0.003). Only one patient showed no gadolinium-enhancing lesions at all study time-points.

Associations with clinical outcomes

Thirty-nine clinical relapses occurred in the study period (mean 1.50 per patient [SD 1.48]). Table 4.4 illustrates the associations between mean gadolinium-enhancing lesions in the first six months of the study (brain; cord; total i.e. brain and cord) and relapse events in the first six months of the study and during the whole two-year study course. During the first six months there were significantly more total gadolinium-enhancing lesions in patients expressing concurrent relapses than in those who were relapse free (median 1.75 per patient in relapsing group [n=11] versus 1.20 per patient in non-relapsing group [n=15]; p=0.041). Increasing EDSS was correlated with relapse frequency (p=0.048; r=0.392); see Figure 4.2.

Table 4.4: *Association between mean number of gadolinium (Gd)-enhancing lesions per patient over the first six months and occurrence of clinical relapse in the first six months and over the whole study (all patients and those not on BIFN only).*

	Mean six month Gd-enhancing lesions (brain only) (p value)	**Mean six month Gd-enhancing lesions (cord only) (p value)**	**Mean six month Gd-enhancing lesions (brain and cord) (p value)**
Relapse in first six months of study (all patients; n=26)	0.061	0.148	**0.041**
Relapse over two years (all patients; n=26)	0.238	0.457	0.160
Relapse over two years (patients not on BIFN; n=16)	0.313	0.492	0.313

Table 4.5 details associations between the mean gadolinium-lesion number (brain; cord; total) in the first six months of the study in comparison to clinical measures during the study. In the whole cohort, a significant increase in EDSS was noted by 24 months (p=0.006) however this was not associated with the extent of gadolinium-lesion enhancement in the first six months (see Table 4.5). The MSFC did not change significantly in the whole cohort during the study (see Table 4.3), and whilst there

was a suggestion of relative improvement in MSFC in patients with higher mean gadolinium-lesion enhancement during the first six months (r_s=0.401; p=0.047) this was not a consistent finding over time, see Table 4.5.

Figure 4.2: *Graph showing correlation between number of relapses per patient (RELAP_NO) over two years and change in EDSS (EDSS_2YR) during the study.*

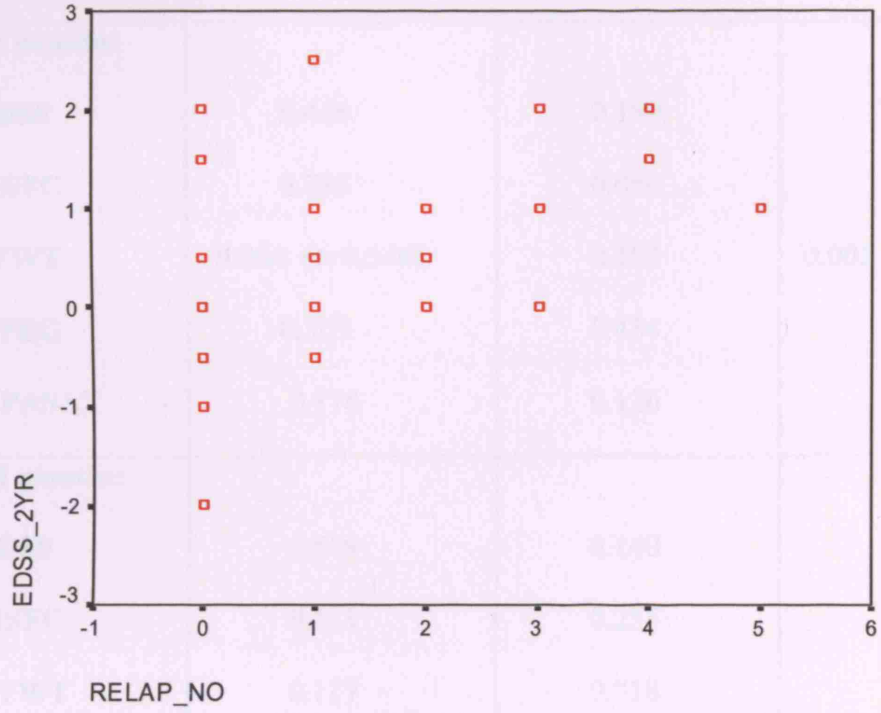

In all subjects over the study course there was an improvement in the PEG (p=0.041) whilst the TWT and PASAT showed no significant change (p=0.095 and p=0.113 respectively). There was evidence of a relative preservation of the TWT over 12 months and 24 months, but not over 18 months in those patients who had higher levels of gadolinium-lesion enhancement in the first six months of the study. No associations were seen between gadolinium-enhancement and the PEG or PASAT (Table 4.5).

Table: 4.5: *Associations between mean six-month gadolinium (Gd)-enhancing lesions per patient and subsequent change in clinical measures during the study.*

	Mean six month Gd-enhancing lesions (brain only) (p values)	**Mean six month Gd-enhancing lesions (cord only) (p values)**	**Mean six month Gd-enhancing lesions (brain and cord) (p values)**
12 months:			
EDSS	0.466	0.199	0.368
MSFC	0.285	0.064	0.153
TWT	0.004 (r=0.546)	0.193	0.003 (r=0.567)
PEG	0.303	0.434	0.260
PASAT	0.176	0.126	0.268
18 months:			
EDSS	0.609	0.140	0.435
MSFC	0.111	0.255	0.068
TWT	0.117	0.718	0.101
PEG	0.359	0.093	0.546
PASAT	0.771	0.105	0.557
24 months:			
EDSS	0.305	0.144	0.512
MSFC	0.064	0.517	0.047 (r=0.401)
TWT	0.018 (r=0.462)	0.391	0.015 (r=0.472)
PEG	0.981	0.181	0.809
PASAT	0.888	0.425	0.772

Associations with other MRI parameters

Apart from a correlation between a higher level of cord gadolinium-enhancement in the first six months and greater amount of BPF atrophy over 12 months (r_s=-0.413; p=0.045) no other significant associations were noted between gadolinium-enhancement in the first six months and subsequent changes in brain volume for all patients and also in those subjects who did not continue BIFN throughout the whole study (n=16) only.

A correlation was observed between a higher mean number of brain (but not cord) gadolinium-enhancing lesions in the first six months and greater T_2 lesion volume increase over 12 months (r_s=0.442; p=0.027) but not at later time-points.

4.3.4 Discussion

The main findings were: (i) a relatively high degree of inflammatory activity existed throughout the two years of this study; (ii) there was a moderate association between mean gadolinium enhancement and relapse events in the first six months and (iii) inflammation was not associated with a consistent pattern of clinical deterioration or brain atrophy over the study course.

The high degree of inflammatory activity noted during this study (20/26 patients [77%] had gadolinium-enhancing lesions at baseline) illustrates the sensitivity of this MR parameter. Additionally this amount of inflammation did not significantly decrease longitudinally over the study course. It should be noted, however, that cord

gadolinium-enhancement alone was a relatively uncommon event during the study and this may be an explanation for the lack of an association between mean values of this measure over six months and study outcomes.

The suggestion of relative preservation of MSFC in those subjects with greater degrees of early gadolinium-lesion enhancement should be treated with caution since, (i) there was no overall change in MSFC; (ii) the relationship with MSFC was not observed at all time-points; (iii) the strength of the statistically significant associations given that multiple comparisons were made are relatively weak and (iv) the MSFC is susceptible to improvement due to practice learning (Cohen *et al.*, 2001) and the relative improvement in PEG findings in the cohort during the study may be due to a learning effect. The TWT is less affected by practice effects (Cohen *et al.*, 2001), but, as for the overall MSFC, caution is advised interpreting the associations given the marginal level of significance and multiple testing. The finding of a deterioration of clinical function in the EDSS but not the MSFC in the whole cohort suggests that the EDSS was more sensitive to change than the MSFC in this cohort. This may in part be due to the practice effect associated with the MSFC (Cohen *et al.*, 2001) and if the components of the MSFC (particularly the PASAT and PEG) had been done several times at baseline, then this effect may have been minimised (Solari *et al.*, 2005).

The presence of gadolinium-enhancing lesions was not found to consistently correlate with the development of later cerebral atrophy. Some previous studies have shown a relationship (Simon *et al.*, 1999; Leist *et al.*, 2001; Gasperini *et al.*, 2002; Paolillo *et al.*, 2004) but this finding is not universal (Saindane *et al.*, 2000). The complexity of

the association between gadolinium-enhancement and brain volume measures is further illustrated in a recent study using a sub-set of the cohort described in this investigation which showed that higher degrees of ongoing gadolinium-enhancing lesion volume was associated with a significant increase in WMF, whilst baseline gadolinium-lesion volume correlated with WMF and BPF tissue loss at two years (Tiberio *et al.*, 2005). A number of different pathological mechanisms are likely to be present in patients with clinically early relapsing-remitting MS that have opposing effects on brain volume. Inflammatory gadolinium-enhancing lesions are associated with oedema and cellular infiltrates that may increase brain volume (Compston and Coles, 2002). On the other hand, axonal loss occurs in acute inflammatory lesions (Trapp *et al.*, 1999; Kuhlmann *et al.*, 2002) and may cause tissue loss (Lassmann, 2003b). Additional inflammation and axonal loss occurs in NAWM (Allen *et al.*, 1981; Evangelou *et al.*, 2000). These competing effects on brain volume may be masking a relationship between inflammatory lesions and brain atrophy at least over the period of study in a cohort that has a high inflammatory lesion load.

Interpretation of the potential relationship between gadolinium-lesion enhancement and long term clinical function is complex. Whilst inflammatory relapses and also neuroaxonal loss secondary to inflammation may be detrimental to clinical outcome, inflammation is also associated with – or closely followed by - remyelination and possible neuronal repair (Compston and Coles, 2002). There may also be other mechanisms for progressive disability that are independent of the inflammatory (gadolinium-enhancing) white matter lesions e.g. progressive axonal loss in post-inflammatory (non-enhancing) white matter lesions or in the NAWM, as well as

regions of grey matter demyelination and axonal loss (Evangelou *et al.*, 2000; Peterson *et al.*, 2001; Miller *et al.*, 2002; Lassmann, 2003b; Bjartmar *et al.*, 2003).

Ring enhancement of lesions has previously been associated in some studies with greater degrees of demyelination and axonal destruction ultimately giving rise to a poorer clinical outcome (Morgen *et al.*, 2001). In contrast, a recent analysis showed a large degree of remyelination and resolution of T_1 hypointensity associated with this lesion type (Lucchinetti, 2003). Investigation of such lesions in this study did not yield any consistent significant associations and suggest that such lesions have little if any influence on the intermediate clinical course in patients with RR MS.

Overall, the results suggest that in clinically early relapsing-remitting MS inflammation was prevalent but a consistent relationship of this with clinical disability and neuroaxonal loss (inferred by the development of brain atrophy) over a two year period was not apparent. The concurrent association between gadolinium-enhancing lesions and clinical relapse confirms the findings in many previous studies (Miller *et al.*, 1988; Barkhof *et* al., 1992; Smith *et* al., 1993; Stone *et al.*, 1995; Koudriavtseva *et al.*, 1997; Kappos *et al.*, 1999) and suggest that using this MR parameter as a primary outcome in phase II treatment trials of the relapsing-remitting phase of MS is appropriate. While the absence of a consistent correlation with longer term clinical function raises legitimate doubt that gadolinium enhancing/inflammatory lesions affect the long term prognosis for disability, it should be noted that the follow up period was still relatively short and there was relatively little disability change. Continued investigation by long term follow up is required to

determine the relationship between early gadolinium-lesion activity and the long term clinical course.

CHAPTER 5

Diffusion tensor and upper cervical cord MR imaging studies in clinically early relapsing-remitting multiple sclerosis

5.1 Introduction

In addition to the extent of early inflammation inferred from the measurement of the number and volume of gadolinium enhancing lesions on MRI, other factors are likely to be relevant in determining later clinical outcomes in MS. For instance, measuring gadolinium-enhancing lesions does not give a quantitative assessment of inflammation outside these lesions (NAWM and grey matter). Also, gadolinium-enhancing lesions usually persist for approximately one month only (Thorpe *et al.*, 1996), or sometimes for as little as one week (Lai *et al.*, 1996); hence, it is possible that areas of resolving inflammatory activity following previous gadolinium-enhancement may be missed, even if scanning at intervals of one month. Finally, as ongoing neurodegeneration is likely to be a key mechanism for progressive clinical dysfunction, and because its relationship with inflammation is complex and the two are not necessarily or inevitably always linked, the measurement of inflammatory lesions alone may not be sufficient. Additional quantitative MR parameters may complement gadolinium-enhancing lesion measures to provide a more complete overview of the level of pathological change – including both inflammation and neurodegeneration - present in both grey and white matter.

Diffusion tensor imaging (DTI) can provide an indication of parenchymal structural integrity by measuring water movement in normal appearing brain tissue (NABT)

(see section 2.3.3); whilst UCCA gives an indication of pathological damage resulting in tissue loss – and by implication loss of myelin and axons - at a clinically eloquent location. Studies of these measures in clinically early relapsing-remitting MS are presented in the remainder of this chapter and with those detailed in chapter four; inferences may be derived regarding the sensitivity of these parameters and their suitability in monitoring the clinico-pathogenic evolution of MS.

5.2 Diffusion tensor imaging in early relapsing-remitting multiple sclerosis: cross-sectional analysis

5.2.1 Introduction

Quantitative DTI studies in MS have shown measurable abnormalities in both lesions and NABT in all clinical subtypes of MS (see section 2.5.3). However it remains unclear how early in the disease course these occur. A study using part of the early relapsing-remitting MS cohort described in chapter four (median disease duration of 1.7 years) detected significant abnormalities only in lesions but not NABT using ROI analysis (Griffin *et al.*, 2001). Other recent DTI studies using whole brain histogram analysis have suggested greater pathological sensitivity (Cercignani *et al.*, 2000; Nusbaum *et al.*, 2000a; Cercignani *et al.*, 2001a). However, histogram analysis may be liable to partial volume edge effects between CSF and brain tissue thereby contaminating the results (Maldjian and Grossman, 2001).

In this study, an automated segmentation algorithm was employed which may improve the precision and accuracy of segmentation of CSF and NABT and allow greater brain coverage (Hadjiprocopis *et al.*, 2003). Using quantitative DTI parameters – FA and MD - histogram analysis of both NABT and whole brain tissue (WBT) was undertaken in a subgroup of the cohort investigated previously (Griffin *et al.*, 2001). The aims were: (i) to determine if DTI observable disease effects could be detected early in the clinical course of MS using a potentially sensitive and accurate methodology; (ii) to investigate the potential for partial volume edge effects to

contribute to NABT histogram abnormalities by analysing the results with and without adjustment for inter-subject differences in brain volume.

5.2.2 Methods

Subjects

Twenty-eight patients from the early relapsing-remitting MS cohort (mean age 36.2 [range 26-56] years; 6 males, 22 females; median disease duration 1.6 [range 0.5-3] years; median EDSS 1.5 [range 0-3.5]) were recruited and compared with 20 healthy volunteers (mean age 38 [range 24-54] years; 7 males, 13 females). The EDSS (Kurtzke, 1983) and MSFC (Cutter *et al.*, 1999) were assessed in each patient. Informed consent was obtained from all subjects and the study had approval by the joint ethics committee of the Institute of Neurology and National Hospital for Neurology and Neurosurgery, Queen Square, London.

MRI protocol

Scans were performed on a GE Signa 1.5 T scanner (General Electric Medical Systems, Milwaukee, Wisconsin, USA). The diffusion protocol was acquired with a single shot diffusion weighted (DW) EPI sequence (TE=78 ms; TR=2.5-3 s; acquisition matrix=96x96 reconstructed as 128x128; FOV=240x240 mm and 4 b values, increasing linearly with G^2 (G=gradient amplitude) from 0 to 700 s mm^{-2}, applied in each of seven non-collinear directions to determine the diffusion tensor) (see section 2.3.3). Cardiac gating was used to reduce motion artefacts associated

with blood and CSF pulsation. From this, 21 contiguous 5mm slices covering most of the brain were compiled after reconstruction. On-line time averaging of the complex signal can cause disruption of the averaged signal due to large phase changes caused by motion between successive acquisitions in the presence of large diffusion gradients. Therefore, a minimum of four identical acquisitions were collected and stored separately for subsequent off-line magnitude averaging, which is insensitive to phase differences, to improve the SNR.

In the same scanning session, high resolution IR-prepared single shot EPI images were acquired (TR=6 s; TE=105 ms; TI=200 ms; matrix=256x256; FOV=240x240 mm; 28 contiguous 5mm slices covering the whole brain, consisting of 21 slices matching the DW-EPI sequence plus an additional four slices superiorly and three slices inferiorly). In a separate scanning session within four weeks of the DTI session, all subjects had conventional dual spin-echo T_2 and PD images (TR=2000 ms; TE=30/95 ms; matrix=256x256; FOV=240x180 mm; 28 contiguous 5mm axial slices covering the whole brain) and pre and post-contrast (triple dose gadolinium [0.3 mmol/kg]) T_1-weighted images (28 x 5mm contiguous axial slices covering the whole brain; TR=540 ms; TE=20 ms; matrix 256x256; FOV 240x240).

As subjects with MS exhibit increased brain atrophy when compared with healthy controls (Chard *et al.*, 2002b) this may influence histogram analysis. Therefore, brain volumes were measured from a 3D inversion-prepared FSPGR sequence (TR=13.3 ms; TE=4.2 ms; TI=450 ms; matrix=256x144; FOV=240x180 mm [zero filled to give an image pixel size of 1.2x1.2 mm]; NEX [number of excitations]=1, with

124x1.5mm coronal slices covering the whole brain) obtained in the same scanning session as the diffusion images.

Image Analysis

Using a method described previously (Chard *et al.*, 2002b) brain parenchymal volumes (BPV) (defined as whole brain volume excluding CSF) were calculated for each subject. BPV has been shown to have favourable reproducibility with a coefficient of variation of 0.8% (Chard *et al.*, 2002a). The diffusion data was processed to determine the diffusion tensor on a voxel by voxel basis for each slice (Basser *et al.*, 1994). From the diffusion tensor the FA and MD were calculated (Basser and Pierpaoli, 1996; Pierpaoli and Basser, 1996).

NABT diffusion data was extracted firstly by excluding lesions, then extra-cerebral tissue and finally segmenting the remaining voxels into NABT and CSF. Using Dispimage (Plummer, Dept of Medical Physics, University College Hospitals NHS trust, London) (Plummer, 1992) lesions were outlined using a semi-automated contouring technique (Filippi *et al.*, 1998a) on the PD-weighted images. The lesion ROIs were then applied to the b=0 mainly T_2-weighted images of the diffusion data set and – with visual reference to the corresponding high resolution IR images - excluded from further analysis. Extracerebral tissues were extracted from the b=0 and IR data sets using Dispimage (Plummer, 1992).

Segmentation of CSF and NABT using the b0 and IR images (see figure 5.1)

Firstly, the b=0 image set was interpolated to matrix=256x256 to match that of the IR data set. Seven slices not covered by the b=0 images (4 from below and 3 from above the b=0 image slab) were removed from the IR image set, leaving 21 slices exactly corresponding to the b=0 brain coverage.

A new automated segmentation algorithm which uses an adaptive clustering technique with entropy minimisation (Hadjiprocopis *et al.*, 2003) incorporating the use of the standard K-means algorithm (Duda and Hart, 1973) and simulated annealing (Kirkpatrick *et al.*, 1983; Aarts and Korst, 1989) was used to segment the resulting b=0 and IR data sets into NABT and CSF. A brief description of the segmentation process now follows.

Clustering is a process in which a set of points (voxels of co-registered images to be segmented i.e. the b=0 and IR data sets) are positioned in feature space and allocated to separate clusters, in this case defined for CSF and NABT, depending on the Euclidean distance between each other and each cluster's centre. K-means dynamically allocates each point to its nearest cluster until the system reaches equilibrium and no more re-allocations are necessary. Each point is associated with a set of probabilities governing the point-to-cluster assignment; the probability that a point belongs to a given cluster is inversely proportional to its distance from the cluster's centre. The confidence of a point-to-cluster assignment depends on the said set of probabilities; it increases if one probability is predominant and significantly larger than the others in the set and decreases when all probabilities are

approximately equal. The entropy of the set of probabilities is a notion that helps to quantify the confidence of assignment; the lower the entropy of a given set, the higher the confidence of assignment.

By minimising the total entropy of the system (using 'simulated annealing' (Kirkpatrick *et al.*, 1983; Aarts and Korst, 1989) [which introduces small random perturbations to the point positions and recalculates the entropy]) the overall confidence of a particular point-to-cluster arrangement is increased and voxels are maximally separated into CSF and NABT. The algorithm used (Hadjiprocopis *et al.*, 2003) attempts to account for artefacts associated with EPI data sets by repeating the segmentation process as above on the NABT mask only with a larger number of clusters. Point-to-cluster allocations with values closest to the CSF, as derived from the first stage of the segmentation, are discarded, removing partial volume voxels. The extent of partial volume removal is determined by the number of iterations performed using this part of the process and this was carried out until, by visual inspection, the operator was confident that the NABT mask remaining did not contain significant amounts of CSF. For all subjects in this study seven iterations were used as, using control subjects not included in this study, this had previously been viewed to be satisfactory to remove enough partial volume and still leave a representative brain tissue mask.

The outer voxel of the segmented image in each slice was eroded to minimise partial volume effects between the outer margin of the cortex and surrounding CSF. The diffusion parameters (MD and FA) were then calculated over the NABT mask and the remaining voxels used for histogram analysis. In addition, regions classified as

lesions were added separately to the NABT FA and MD maps to allow analysis of WBT. Each histogram was smoothed and normalised by dividing the height of each bin count by the total number of voxels included in the histogram. The following variables were derived for each DTI parameter: (i) the mean; (ii) the peak location (parameter value that is most common in brain tissue) and (iii) the peak height (corresponding voxel value of the peak location).

Figure 5.1: *A representative example of CSF segmentation achieved using information from b=0 and IR-EPI sequences (image (a) and (b) respectively) to generate a segmented brain tissue mask (image (c)).*

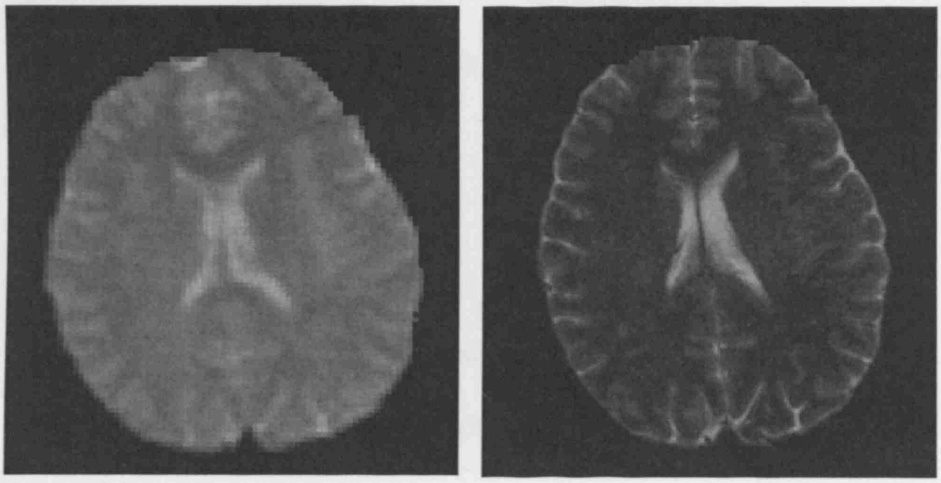

Image (a) **Image (b)**

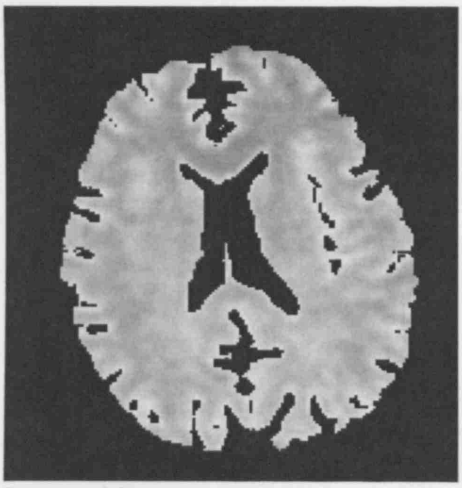

Image (c)

Statistical Analysis

Statistical analyses were performed using SPSS 11.0 (SPSS Inc., Chicago, IL, USA). MS effects on DTI parameters were estimated using multiple linear regression models, which included gender and disease status (MS or healthy control) as categorical variables and age and BPV as continuous covariates. Linear regression using the above model was also used to assess the effects of disease duration and MSFC on the measured DTI parameters. The relationships between the DTI parameters and lesion volumes were assessed by Pearson correlations. The associations between EDSS and all DTI parameters were investigated using Spearman correlations. Two-tailed significance values were estimated for all correlations. A p value of < 0.05 was considered significant.

5.2.3 Results

For MS subjects the median T_2-weighted lesion load was 6.5 (range 1.6-21.2) mls; median T_1 hypointense lesion load was 1.3 (0-6.6) mls and median gadolinium-enhancing lesion load was 0.5 (0-1.4) mls. The mean BPV for controls was 1090 mls (range 920-1380) and for MS subjects the mean was 1060 (range 860-1340) mls. No significant difference in BPV was noted between the MS subject and control groups ($p=0.27$). Table 5.1 illustrates the histogram results for each DTI parameter.

Table 5.1: *mean DTI parameter results in subjects and controls in NABT and WBT. Statistical comparison (p values) between MS subjects in comparison to controls. Effect of BPV noted on the p values.*

	Controls	MS (NABT)	MS (WBT)	P value (with BPV)	P value (without BPV)
FA mean	0.33	0.31	0.31	0.17	**0.04**
FA peak location	0.21	0.20	0.20	0.73	0.33
FA peak ht (normalized voxel count)	139.0	150.06	150.29	**0.02**	**0.005**
MD mean ($mm^2/sx10^{-3}$)	0.96	0.99	0.99	0.20	0.14
MD peak location ($mm^2/sx10^{-3}$)	0.82	0.85	0.85	0.11	**0.06**
MD peak height (normalized voxel count)	142.07	137.66	137.10	0.37	0.42

DTI parameters

Fractional Anisotropy: BPV but not disease duration had a statistically significant effect on all the histogram variables. In models accounting for any BPV, gender and age differences, there was a significant increase in FA peak height in MS subjects in comparison to controls (p=0.02) (see Figure 5.2). When BPV is excluded, in addition to an increased FA peak height in MS subjects (p=0.005), a significant decrease was also noted in the mean FA in MS subjects in comparison to controls (p=0.04).

Mean Diffusivity: BPV did not have a significant effect on any of the MD histogram variables. An increase in disease duration was noted to have a negative correlation with MD peak height (p=0.04). When BPV was excluded there was weak evidence of

an increase in MD peak location in MS subjects in comparison to controls (p=0.07). But when BPV was included in the model this diminished (p=0.11).

Clinical and MRI Correlations

The EDSS was observed to have a negative correlation with BPV in MS subjects (r_s = -0.468, p=0.01). There was weak evidence of significant correlation between a raised mean MD (r_s = 0.322, p=0.09) and increased MD peak location (r_s = 0.343, p=0.07) and increasing EDSS in MS subjects. No other correlations were observed.

Figure 5.2: *Normal appearing brain tissue FA histogram for all patients (dashed line) in comparison to controls (solid line). Normalised voxel count values ($x10^3$).*

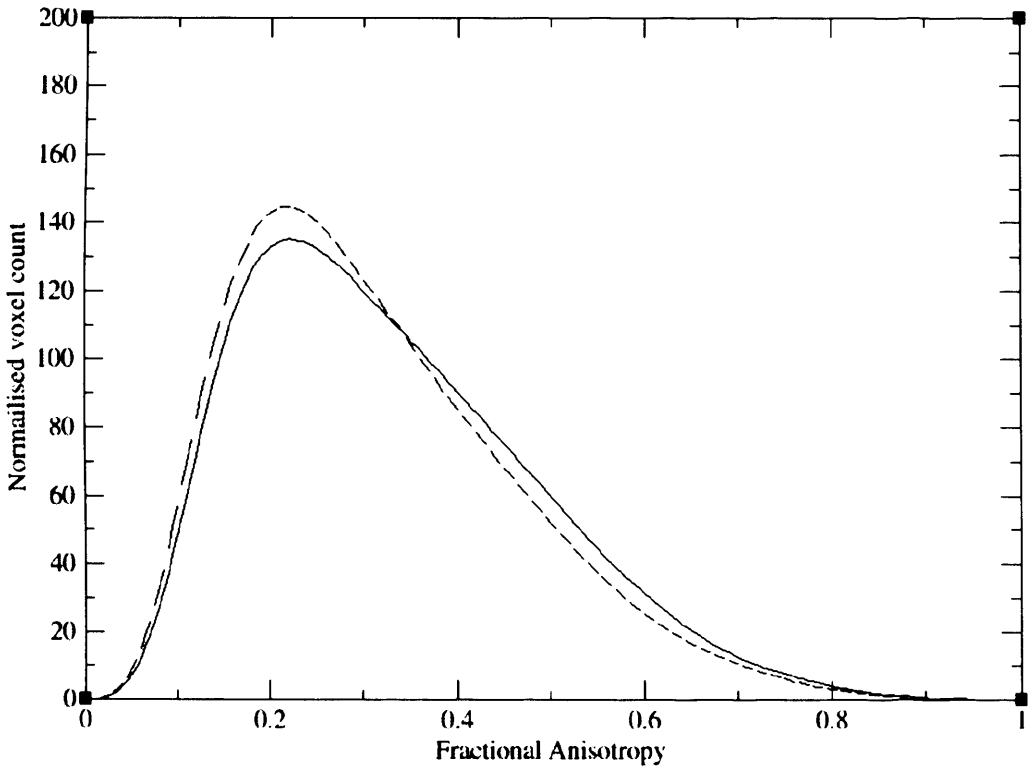

5.2.4 Discussion

The results suggest that subtle measurable DTI abnormalities in NABT and WBT were present early in the clinical course of MS and that including BPV as a covariate in the analytical model is necessary to evaluate accurately how robust these abnormalities are.

DTI and pathology

Quantitative DTI parameters allow estimation of the directionality of water (FA) and the restriction of water movement (MD) (Basser and Pierpaoli, 1996). An increased FA peak height in MS subjects in comparison to controls is the only significant variable in statistical models including BPV. This suggests that water diffusion is less directional. A possible explanation for a rise in FA peak height is a decrease in fibre tract integrity in white matter which may give rise to a pattern of lower anisotropy similar to that of the grey matter. Hence there will be an increased proportion of voxels within this lower defined FA range (Cercignani *et al.*, 2001a). The fact that no significant change is observed in the other FA variables suggests that these changes may be in their earliest stages. The results also suggest that FA may be the most sensitive DTI parameter to early pathological changes in MS.

The inclusion of BPV as a covariate attempts to correct for inter-subject volume variations that may introduce partial volume errors. As diffusion values differ significantly between brain parenchyma and CSF, even small admixtures of CSF into a voxel nominally containing pure tissue could result in significant diffusion changes.

The extent of this partial volume effect depends on the number of voxels in which significant contamination occurs. This in turn depends on the surface area of the brain and its proportion to deeper lying brain tissue which will be less affected by partial volume considerations. Hence, the proportion of pure tissue voxels likely to be contaminated with CSF may be dependent upon brain volume, therefore differing inter-subject brain volumes within a cohort may confound the measured results if not adequately corrected for. While the geometry of the brain surface is too complex to allow this effect to be directly modelled, BPV measurement does give statistical allowance for this possible influence.

Furthermore, it has been suggested that brain volume loss may be a result, at least partially, of axonal loss (Chard *et al.*, 2002b). Hence, the loss of significance in the mean FA and MD peak location when BPV is included in the analysis suggests that these results may reflect either axonal loss or the presence of partial volume error, or both. The increase in FA peak height remains after inclusion of BPV. This suggests that a true intrinsic tissue change is present. The lack of correlation between lesion load and NABT FA peak height suggests there is a primary disease process in the NABT rather than an effect secondary to lesions. The significant relationship observed between increased disease duration and decreased MD peak height suggests that MD changes may occur later in the clinical course of MS than FA. The lack of correlation between the DTI parameters and lesion loads and clinical status measures may be in part due to the cohort's relatively low lesion loads and EDSS.

The pathological basis for the NABT FA abnormality is speculative given the current lack of direct correlation between diffusion measures and histopathological data.

Subtle damage to neuronal fibre tract coherence is suggested by the FA changes and this may be secondary to demyelination (Trapp *et al.*, 1998). We can not exclude the possibility that other subtle changes reported in MS NABT, such as astrocyte hyperplasia, microglial activation and regions of cortical demyelination, might contribute to the abnormal FA. It is at present uncertain why ongoing disease processes in this cohort appear to cause significant change to FA only.

Methodological considerations

Diffusion sequences are at risk of patient movement artefact as the DTI sequence may take up to 30 minutes to acquire and although intra-dataset registration is performed as part of the DT calculation, any such motion may not be fully accounted for. For the validity of the results to be optimal, partial volume errors must be minimised. In the current study, these were addressed in three ways: (i) the utilisation of an automated segmentation methodology; (ii) the erosion of the outer voxels from the derived segmentations and (iii) the incorporation of BPV in the statistical models employed to model for inter-subject differences in brain volume. Hence, the method used represents a potential advance in comparison to other histogram analyses (Nusbaum *et al.*, 2000a; Cercignani *et al.*, 2001a; Tourbah *et al.*, 2001). The observation of diminishing significance of some NABT abnormalities after including BPV as a covariate raises the possibility that studies which do not use this covariate may sometimes identify positive results as a result of partial volume edge effects rather than true intrinsic NABT changes. With the relatively large pixel sizes acquired in DTI, these effects are more liable to occur.

5.3 Diffusion tensor imaging in early relapsing-remitting multiple sclerosis: longitudinal analysis

5.3.1 Introduction

As detailed above, subtle measurable DTI abnormalities are present in clinically early relapsing-remitting MS. However, the ability of DTI to detect longitudinal progressive abnormalities and, if present, how they relate to the clinical and pathological evolution of MS remains unclear.

Accurate longitudinal DTI measurement is problematical particularly due to the registration and segmentation difficulties associated with EPI sequences. Nevertheless, the longitudinal evaluation of DTI parameters in MS is important to assess the potential of such parameters to monitor and quantify aspects of disease pathology including those which occur in NABT.

As noted in chapter two there have been few previous longitudinal DTI studies in MS published (Cassol *et al.*, 2004; Rovaris *et al.*, 2005) and although both investigations suggested that progressive MD abnormalities may accrue, neither included patients with clinically early relapsing-remitting disease. Three DWI studies – i.e. without the rotationally invariant DTI parameters - have also been reported (Werring *et al.*, 2000a; Caramia *et* al., 2002; Schmierer *et* al., 2004b). Caramia *et al.* observed a significant increase in ADC in NAWM in CIS subjects, the majority of whom subsequently developed MS. Schmierer *et al.* reported a longitudinal increase in NAWM ADC in a cohort of primary progressive patients. Finally, Werring *et al.*

detected ADC changes in acute lesions before and after their appearance and also noted significant abnormalities in contralateral NAWM regions.

In this study, we present a longitudinal investigation of the clinically early relapsing-remitting MS cohort employing a similar methodology to the cross-sectional study (section 5.2) with the addition of a registration algorithm between structural and DTI parameter images to improve the methodology. The aims were: (i) to detect any measurable progressive DTI abnormalities over time in clinically early relapsing-remitting MS in comparison to healthy controls and whether this relates to clinical or conventional MRI change and (ii) to infer, from the results, whether quantitative DTI parameters have potential in following the course of MS from its earliest stages.

5.3.2 Methods

Subjects

In this two year study, at baseline 28 patients (mean age 37.7 [range 24.1-55.6] years; 20 female, 8 male; median disease duration 1.9 [range 0.5-3] years; median EDSS 1.5 [range 0-3]) and 15 healthy volunteers (mean age 35.7 [range 29.8-52.7] years; 9 female, 6 male) were scanned at yearly intervals. At one year (median 373 days controls; 363 days patients), 24 patients and 13 controls were imaged whilst at two years, all 28 of the patients and 14 of the controls completed the study (median time from baseline 746.5 days in controls and 728 days in patients).

No patients were on BIFN at recruitment; whilst 9 of the 28 original patients had commenced treatment by the end of the study. The EDSS (Kurtzke, 1983) and MSFC (Cutter *et al.*, 1999) were assessed in each patient at all time-points. Informed consent was obtained from all subjects and the study had approval of the Joint Medical Ethics Committee of the Institute of Neurology and National Hospital for Neurology and Neurosurgery, Queen Square, London.

MRI protocol

This was identical to the cross-sectional study (section 5.2).

Image analysis

This was identical to that described in the cross-sectional analysis (section 5.2) except that extracerebral tissue was removed using Brain Extraction Tool (BET) (Smith *et al.*, 2001) part of the FSL-FMRIB's Software Library; www.fmrib.ox.ac.uk and the b=0 and IR images were registered using a normalised mutual information algorithm (Studholme *et al.*, 1999). Both measures were introduced in order to: (i) minimise operator input and (ii) maximise registration between the b=0 and IR images.

Statistical Analysis

For the longitudinal comparison between patients and controls, the mean, peak location and peak height values of both MD and FA over the three time points were modelled using random intercepts regression (Goldstein, 1995) with random subject-

specific intercepts and common linear slope on time from study baseline; MS indicator and MS x time interaction terms were used to estimate patient versus control differences. Potential confounding by BPV, age and gender was examined by adding those terms singly as covariates, retaining each in the model if significant at p=<0.1. Multiple regression models were used to estimate baseline and two-year cross-sectional patient versus control differences with MS indicator and potential confounder covariates (gender, age and BPV) included if any of these contributed to the model at p=<0.1. In patients only, a similar random intercepts model was used with a BIFN indicator and interaction with time and disease duration as an additional covariate to assess the effect of the medication in patients. Multiple linear regression models with change in DTI parameters over the study period and corresponding change in MSFC and lesion volumes as covariates were used to examine associations between these covariates and BPV in patients only. Two-tailed Spearman rank correlations were used to assess correlations between change in DTI parameters and change in the EDSS over the study period. These analyses were implemented in Stata 8.2 (Stata Corporation, College Station, Texas, USA).

Paired t-tests were used to compare changes within a single parametrically analysable variable over the study course, whilst the Wilcoxon sign rank test was used for variables not parametrically analysable. For parametrically analysable variable comparisons between two cohorts at a single time-point, the independent-samples T-test was used, whilst the Mann-Whitney U test was used if the variables were not parametrically analysable. These analyses were implemented in SPSS 11.0 (SPSS Inc., Chicago, IL, USA). A p value of < 0.05 was considered significant.

5.3.3 Results

Demographic, clinical and non-DTI MRI parameters over the study course are detailed in Table 5.2. In MS subjects, significant increases were seen in lesion volume on PD-weighted scans (p=0.039) and EDSS (p=0.015) and decreases in gadolinium-enhancing lesions (p=0.012). Regarding BPV, patients had a significantly increased rate of atrophy over the study course (annual rate (mls): -10.051; p=<0.001; 95% CI: -15.245, -4.856) with borderline evidence of a difference in rate BPV loss between patients and controls by the study's conclusion (annual rate patient-control (mls): -7.471; p=0.085; 95% CI: -15.968, 1.027).

DTI measures in both NABT and WBT in patients and controls over the study course are reported in Table 5.3 together with p values for comparison between the longitudinal rates of change of the two cohorts from baseline to study conclusion. BPV was included in all longitudinal DTI variable analyses.

Normal Appearing Brain Tissue Fractional Anisotropy

At baseline in patients, there was a significantly lower mean (difference patient-control [$x10^3$]: -15.129; p=0.042; 95% CI: -29.688, -0.570) and higher peak height (difference patient-control: 10.41; p=0.008; 95% CI: 2.847, 17.973) than controls. No significant peak location difference was observed (p=0.398).

No significant rate of change difference over time was noted between patients and controls for any of the FA variables (see Table 5.3). There was borderline evidence of

an increase in mean FA in patients only over two years (annual rate [$x10^3$] 4.870; p=0.050; 95% CI: 0.008, 9.733), controls showed no such increase (p=0.984). There was evidence of an increase in peak location in patients only over the study course (annual rate [$x10^3$]: 8.622; p=0.029; 95% CI: 0.895, 16.349) (see Figure 5.3) but not in controls (p=0.601). Intra-cohort peak height rate of change in both patients (p=0.320) and controls (p=0.509) were not significant. Two year cross-sectional analysis reveals no significant difference between patients and controls (mean: p=0.346; peak location: p=0.817; peak height p=0.293).

Normal Appearing Brain Tissue Mean Diffusivity

At baseline, there was weak evidence that patients had a higher peak location (difference patient-control [$x10^3$]: 27.155; p=0.078; 95% CI: -3.141, 57.450) than controls. No significant mean (p=0.111) and peak height (p=0.115) differences were noted. For all MD variables, there was no significant rate of change difference over time between patients and controls (see Table 5.3) or within cohorts: patients (mean=0.187; peak location=0.429; peak height=0.152) or controls (mean=0.845; peak location=0.901; peak height=0.625).

Cross-sectional analysis at two years revealed a significantly higher patient mean (difference patient-control [$x10^3$]: 64.941; p=0.008; 95% CI: 19.190, 118.693) and peak location (difference patient-control [$x10^3$]: 44.387; p=0.024; 95% CI: 6.205, 82.570) but not peak height (p=0.120) in comparison to controls (see Figure 5.4).

Table 5.2: *Demographic, clinical and non-DTI MRI parameters in patients (MS) and controls (NC) over the study course. Mean values unless stated, N/A=not applicable.*

	Baseline		**Year one**		**Year two**		**P-value for study change**	
	MS N=28	***NC N=15***	***MS N=24***	***NC N=13***	***MS N=28***	***NC N=14***	***MS***	***NC***
Age (years)	37.73	35.73	37.87	37.17	39.66	38.01	N/A	
male: female	8:20	6:9	5:19	6:7	8:20	6:8	N/A	
Median EDSS	1.5	N/A	1.5	N/A	2.0	N/A	**0.015**	N/A
PD lesion volume (mls)	7.60	0	10.06	0	8.92	0	**0.039**	N/A
T_1 lesion volume (mls)	1.61	0	1.81	0	1.74	0	0.501	N/A
Enhancing lesion vol (mls)	0.52	0	0.47	0	0.14	0	**0.012**	N/A
MSFC	0.001	N/A	-0.055	N/A	-0.043	N/A	0.593	N/A
BPV (mls)	1071.3	1121.1	1060.2	1127.5	1064.3	1118.3	**<0.001**	0.452

Table 5.3: *Quantitative DTI MRI parameters in patients (MS) and controls (NC) over the study course. Mean values unless stated, N/A=not applicable.*

	Baseline		**Year one**		**Year two**		**P value for rate of change**
	MS N=28	***NC N=15***	***MS N=24***	***NC N=13***	***MS N=28***	***NC N=14***	***MSv controls***
NABT MD:							
Mean	1.0	0.96	1.0	1.0	1.02	0.96	0.337
Peak location	0.85	0.83	0.84	0.85	0.87	0.83	0.702
Peak ht ($x10^3$)	131.3	138.0	128.4	126.5	123.2	133.3	0.628
WBT MD:							
Mean	1.0	0.96	1.0	1.0	1.03	0.96	0.325
Peak location	0.86	0.83	0.84	0.85	0.87	0.83	0.741
Peak ht($x10^3$)	130.7	138.0	127.8	126.5	122.2	133.3	0.598
NABT FA:							
Mean	0.31	0.32	0.31	0.32	0.32	0.33	0.224
Peak location	0.20	0.21	0.20	0.21	0.22	0.22	0.358
Peak ht($x10^3$)	153.4	142.6	155.8	149.4	151.3	145.6	0.258
WBT FA :							
Mean	0.31	0.32	0.31	0.32	0.32	0.33	0.221
Peak location	0.20	0.21	0.20	0.21	0.22	0.22	0.348
Peak ht($x10^3$)	153.5	142.6	155.4	149.4	154.9	145.6	0.252

Figure 5.3: *Combined fractional anisotropy histogram showing change in mean and peak location in MS patients from baseline (solid line) to two years (dashed line). Normalised voxel count values ($x10^3$).*

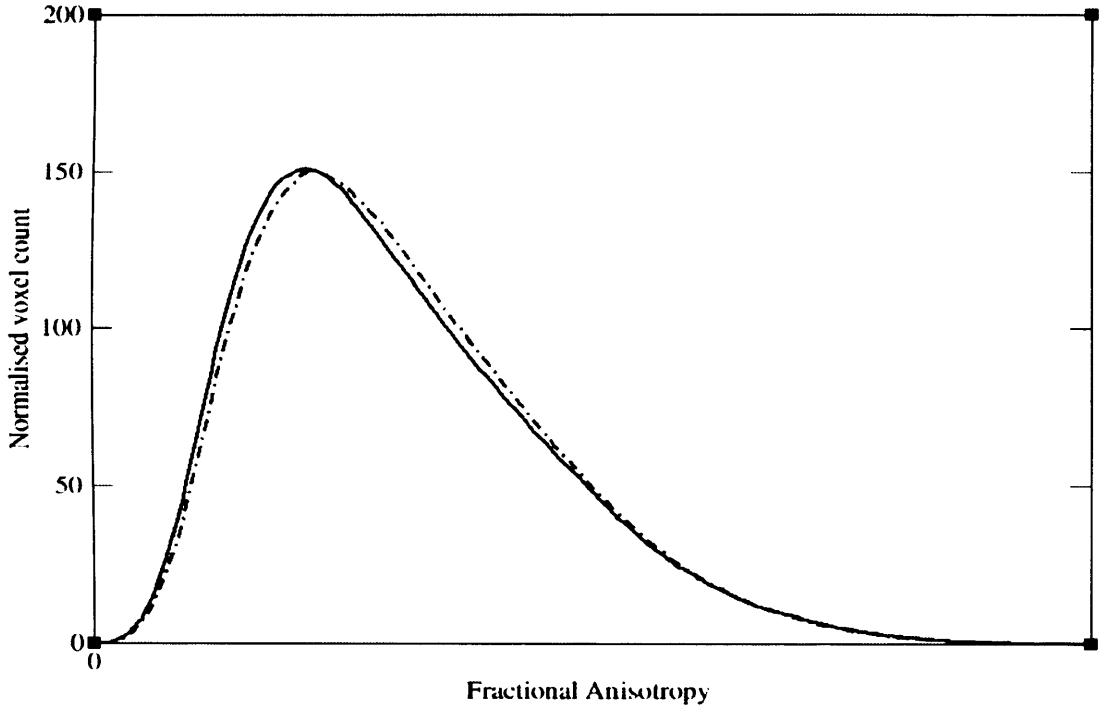

Figure 5.4: *Combined mean diffusivity histogram for all MS subjects (dashed line) and controls (solid line) at two years from study baseline. Normalised voxel count values ($x10^3$).*

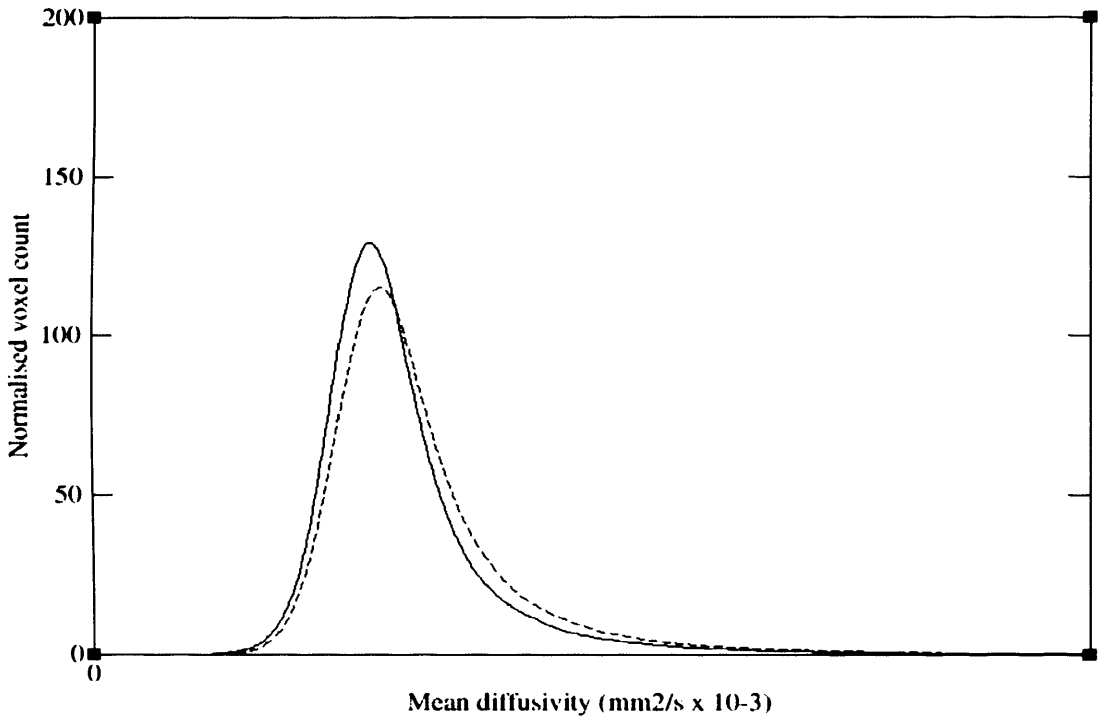

Whole brain tissue results

Including lesions in the analysis minimally affected the significance of the observations and did not provide any new significant findings.

Clinical and MRI correlations

There were no significant correlations between change in EDSS or MSFC and rate of change of any of the DTI variables. Baseline EDSS and MSFC, baseline BPV (and change in BPV over two years), baseline age and disease duration were not noted to

be associated with rates of change of any of the DTI variables. In the nine subjects on BIFN at the study end, the only significant observations were a raised NABT FA mean ($p=0.018$) and NABT FA peak location ($p=0.013$) in comparison to those patients not on the medication. There was weak evidence that an increase in T_1 lesion volume was associated with relative preservation of MD peak height ($p=0.047$). No other associations were seen.

5.3.4 Discussion

The results indicate that although DTI parameters detected subtle abnormalities in MS, no significant differences in longitudinal rates of change between patients and controls in NABT were observed in the clinically early stages of the disease.

Interpretation of DTI parameter results

Baseline findings in this study are similar to a cross-sectional analysis as detailed in section 5.2 and again show FA to be a potentially more sensitive DTI parameter at this stage. The evidence for FA change over time in patients is weak with values tending to return towards those of normal controls. This may suggest a partial resolution of a pathological process thereby increasing anisotropy, potentially indicating an initial abnormality and subsequent recovery in fibre tract integrity. Another possible mechanism might be a decrease in oedema; however, this is uncertain, especially since the MD did not change and also given the marginal level of significance of the finding and the present lack of comparative diffusion MRI and histopathological studies.

The detection of significant cross-sectional patient versus control difference in MD at two years was not, however, associated with significant longitudinal change in MD, and there was considerable variability of the parameter values both within and between the cohorts over each time-point in the analysis. The apparent absence of differences between WBT and NABT values suggests that, in this cohort of early relapsing-remitting MS with a generally low lesion volume, the contribution of lesions to brain tissue DTI histograms as a whole is minimal.

This study was not designed to investigate the effect of disease modifying therapy on DTI parameters. While it is conceivable that a higher NABT FA may reflect an anti-inflammatory effect of BIFN, prospective, randomised and adequately powered studies are required to investigate treatment effects on DTI measures.

The absence of detectable clinical correlations in the analysis may reflect several factors including the limited disability manifested by the MS patients in this study, the relatively small size of the cohort, the limited study duration and possible methodological issues related to the DTI measures themselves (see below).

Methodological considerations

Analysis of DTI data has a number of particular considerations because of the nature of acquisition such as: (i) image distortions; (ii) patient motion artefact; (iii) SNR limitations and (iv) possible partial volume errors during segmentation and analysis. These are accentuated in a longitudinal study as registration between time-points becomes a further consideration – difficult to achieve accurately given the limited

spatial resolution of DTI scans - in addition to the increased number of scans that are used in the analysis. Hence in this investigation, our image and statistical analyses tend to err on the side of caution and this may mask the emergence of a subtle disease effect, even when a robust methodology is used. This may be particularly magnified in clinically early relapsing-remitting MS, where abnormalities are likely to be more subtle than those found in other MS sub-types with greater disability and disease duration (Castriota Scanderbeg *et al.*, 2000; Nusbaum *et* al., 2000a; Griffin *et* al., 2001).

By using an automated segmentation routine (Hadjiprocopis *et al.*, 2003), registration (Studholme *et al.*, 1999) and BPV as a covariate, potential sources of methodological error in the analysis have been at least partially addressed. However, the largely negative results show the possible limitations that exist using DTI as a quantitative parameter to monitor the evolution of NABT abnormality *in-vivo* in early MS. Other quantitative MRI techniques such as brain volume (Chard *et al.*, 2004) and MTR (Davies *et al.*, 2005) have found significant progressive changes in normal appearing grey and/or white matter in a similar early relapsing-remitting MS and control cohort, suggesting these techniques may hold more promise as markers of pathological evolution of NABT at this early clinical stage of the disease.

In recent years, new DTI acquisition sequences have been developed with improved SNR allowing higher spatial resolution (Jones *et al.*, 2002; Wheeler-Kingshott *et* al., 2002). Also, acquisition sequences are becoming faster decreasing possible motion artefacts by incorporating sequence improvements, and future longitudinal investigation of DTI parameters may provide more stable measures better able to

detect subtle or progressive quantitative abnormalities. Rather than global evaluation of NABT, application of tractography measures to evaluate diffusion abnormalities in specific white matter tracts, may yield additional insights (Ciccarelli *et al.*, 2003).

5.4 Cord cross-sectional area in early relapsing-remitting multiple sclerosis: cross-sectional analysis

5.4.1 Introduction

Involvement of the spinal cord in MS, both pathologically and clinically, is common and relevant in the development of disability (see section 2.5.4). Extensive axonal loss in the cord has been documented in post mortem studies and is likely to make an important contribution to the locomotor disabilities and sphincter disturbances that are experienced by many patients (Oppenheimer, 1978; Kidd *et al.*, 1993; Lycklama à Nijeholt, 1998; Ganter *et al.*, 1999; Bjartmar *et al.*, 2000; Lovas *et al.*, 2000; Bergers *et al.*, 2002; DeLuca *et al.*, 2004).

Axonal loss and demyelination will cause loss of tissue. It might therefore be anticipated that when imaging measures of tissue loss are acquired in a clinically eloquent location such as the spinal cord, an association between atrophy and clinical dysfunction would emerge. MRI offers an *in-vivo* method for measuring atrophy and a number of studies have revealed significant cord atrophy cross-sectionally in patients with progressive forms of MS, some with a strong correlation between cervical cord atrophy and disability (Losseff *et al.*, 1996a; Filippi *et al.*, 1996a; Lycklama à Nijeholt, 1998; Edwards *et al.*, 1999; Rovaris *et al.*, 2001; Vaithianathar *et al.*, 2003; Lin *et al.*, 2003a).

It is unclear how early in the course of MS this loss of cord tissue starts to occur. A study in CIS patients demonstrated cross-sectional area loss in subjects with an

abnormal MRI, but showed no longitudinal changes over one year (Brex *et al.*, 2001). However, most other cross-sectional studies have showed no UCCA differences between relapsing-remitting MS and controls (Losseff *et al.*, 1996a; Stevenson *et al.*, 1998; Lin *et al.*, 2003a; Vaithianathar *et al.*, 2003). The somewhat variable findings might reflect differences in cohort size, recruitment and disease duration.

Total intracranial volume (TICV) and gender variations may be relevant. TICV has been correlated with UCCA (Kameyama *et al.*, 1994; Vaithianathar *et al.*, 2003) and differs between males and females (Blatter *et al.*, 1995). The aim of this study was to determine if UCCA loss can be detected cross-sectionally with a sizeable cohort of clinically early relapsing-remitting MS subjects using a sensitive and established technique (Losseff *et al.*, 1996a), with TICV and gender accounted for in the analysis.

5.4.2 Methods

Subjects

Thirty-nine patients from the early relapsing-remitting MS cohort (mean age 36.0 [range 24.1-55.6] years; 28 female, 11 male; median disease duration 1.6 [range 0.5-3] years; median EDSS 1.0 [range 0-3]) and 26 healthy volunteers (mean age 35.8 [range 23.2-52.7] years; 15 female, 11 male) were included in the study. The EDSS (Kurtzke, 1983) and MSFC (Cutter *et al.*, 1999) were recorded in each patient. Informed consent was obtained from all subjects and the study had approval of the Joint Medical Ethics Committee of the Institute of Neurology and National Hospital for Neurology and Neurosurgery, Queen Square, London.

MRI protocol

Scans were performed on a GE Signa 1.5 T scanner (General Electric Medical Systems, Milwaukee, USA). All subjects had a volume acquired inversion prepared FSPGR of the spinal cord (TR 15.6 ms; TE 4.2 ms; TI 450 ms; matrix 256x256; FOV 250x250) forming 60x1mm sagittal slices covering the whole of the cervical cord. From this, five contiguous 3mm pseudoaxial slices were reformatted using the centre of the C2/C3 intravertebral disc as a caudal landmark, with the slices perpendicular to the spinal cord (see Figure 2.4). In the same scanning session, after the FSPGR sequence was acquired, triple dose gadolinium (0.3 mmol/kg) was injected and approximately 15 minutes later a conventional spin-echo T_1-weighted sequence of the cord was acquired (TR 500 ms; TE 20 ms; matrix 512x512; FOV 480x240) forming 13x3mm sagittal slices of the cord. A 3D FSPGR sequence (TR 13.3ms; TE 4.2 ms; TI 450 ms; matrix 256x144; FOV 240x180 mm (zero filled to give an image pixel size of 1.2x1.2 mm)) providing 124x1.5 mm slices covering the whole cranium was also obtained at a separate scanning session (median 7 days from the cord imaging).

Image Analysis

These images were transferred to a Sun workstation (Sun Microsystems Inc, Mountain View, CA, USA). Using an automated program the images are uniformity corrected in comparison to a phantom and the mean area of the slices calculated from the 5 pseudoaxial cervical cord images with a technique described by Losseff *et al* (Losseff *et al.*, 1996a) with the observer (WR) blinded to clinical status. Gadolinium-enhancing lesions of the cord were identified from the post-contrast images of the

cord by an experienced observer (DHM) and outlined on the images using the Dispimage display software package (Plummer, Department of Physics, University College Hospitals NHS Trust, London, UK) and volumes calculated. The TICV was calculated from the 3D FSPGR cranial images using statistical parametric mapping (SPM99, Wellcome Department of Cognitive Neurology, Institute of Neurology, London, UK) as previously described (Chard *et al.*, 2002b).

In nine subjects (5 patients, 4 controls) the UCCA measurements were repeated twice on the same images 30 days apart in a blinded fashion to assess the reproducibility of the observer's measures. The coefficient of variation was calculated from this.

Statistical Analysis

Statistical analysis was performed using SPSS 11.0 (SPSS Inc., Chicago, IL, USA). Univariate association between TICV and UCCA was investigated using Pearson correlation analysis. Unpaired t-tests were used for univariate tests of UCCA difference between genders and between patients and controls. Multiple linear regression models were used to determine the potential effect of age, gender, TICV, disease duration (in patients only) and subject weight on UCCA allowing calculation for the potential disease effect (MS or control) on the UCCA controlling for the above variables. Linear regression with these covariates was also used to determine any association between MSFC and UCCA. Two-tailed Spearman rank correlation coefficients were used to assess any relationship between UCCA and the EDSS. A p value of < 0.05 was considered significant.

5.4.3 Results

Table 5.4 shows UCCA and TICV of controls and patients. When adjusting for TICV and gender, there was no significant UCCA loss in the MS subject group in comparison to controls (p=0.685; mean difference controls – patients 0.76mm^2; 95% CI: -2.98 to 4.5). Similarly, without adjusting for these covariates no difference between patients and controls was observed (p=0.671; mean difference controls – patients 0.94mm^2; 95% CI: -3.94 to 5.31). The UCCA in both patient and control cohorts had similar spread (SD patients 9.02; SD controls 8.04), and no patients were identified with UCCA more than two SD below the mean normal control UCCA. No significant association was noted in patients between UCCA and the MSFC, and no correlation was seen between the EDSS and UCCA (p=0.171).

In all subjects combined, univariate tests showed a strong positive association between TICV and UCCA (r=0.558; p=<0.001; see Figure 5.5), whilst there was a borderline significant lowering of UCCA in females (p=0.062; mean difference male - female = 4.2 mm^2 [95% CI -0.21 to 8.6]). Similar correlations were observed for controls only: TICV and UCCA (r=0.461; p=0.023) and gender and UCCA (p=0.064), nor was there any evidence of a difference in these associations between patients and controls. There was strong evidence that females have a lower TICV than males (p=<0.001; mean difference male - female = 181.83 mls [95% CI 112.88 to 250.77]). When adjusting for the TICV gender difference, the trend for gender to effect cord area was lost (p=0.260; mean difference male – female -2.61 mm^2 [95% CI -7.2 to 1.97]). No other significant covariates were found.

Table 5.4: *Upper cervical cord area and total intracranial volume of each cohort. (mean values [standard deviation] unless stated).*

	MS Subjects (n=39)	Controls (n=26)
Cord area (mm^2)	78.62 [9.02]	79.56 [8.04]
- Males	80.60 [5.63]	82.96 [8.94]
- Females	77.85 [10.03]	77.07 [6.53]
Total intracranial volume (mls)	1339.70 [160.26]	1334.97 [141.90]
- Males	1475.19 [156.44]	1446.90 [137.23]
- Females	1291.31 [133.45]	1255.03 [77.91]

Figure 5.5: *Scatter graph showing the correlation between upper cervical cord area (UCCA) and total intracranial volume (TICV) for all subjects with fitted regression line.*

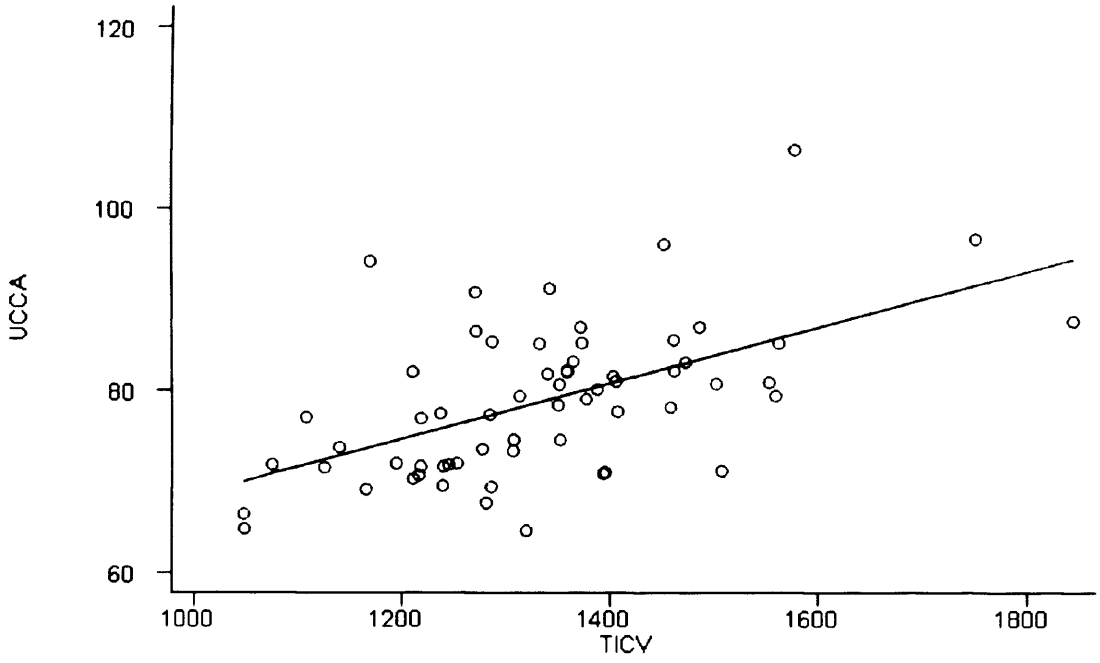

Four subjects had cervical cord gadolinium-enhancing lesions in the area corresponding to the section used to calculate UCCA. No significant difference was seen between these four subjects (mean UCCA= 78.96 [SD=8.79]) and the remainder of the patient or the control groups (mean UCCA 78.59 [SD 9.17]). Single operator same image scan reproducibility from 9 subjects' data was 1.06%.

5.4.4 Discussion

The results suggest that the main influences on UCCA in early relapsing-remitting MS are the TICV and gender, rather than any potential disease effect. The effect of gender appears to be mediated by the TICV, with no independent association with the spinal cord itself (illustrated by the non-significant adjusted gender effect).

The present analysis found that in early relapsing-remitting MS, no significant atrophy was seen in MS subjects. Given the correlation shown in many studies between UCCA to EDSS (Losseff *et al.*, 1996a; Filippi *et al.*, 1996a; Filippi *et al.*, 1997; Lycklama à Nijeholt *et al.*, 1998; Stevenson *et al.*, 1998; Rovaris *et al.*, 2001; Lin *et al.*, 2003a; Vaithianathar *et al.*, 2003) and the possible association between disease duration and cord atrophy in other studies (Edwards *et al.*, 1999; Rovaris *et al.*, 2001), the lack of significant atrophy in the present cohort of relapsing-remitting MS is consistent with the patient's short disease duration and mild clinical impairment.

A number of previous studies investigating UCCA or cord volumes in MS have suggested an association between the calculated cord values and TICV (Edwards *et*

al., 1999; Vaithianathar *et al.*, 2003; Lin *et al.*, 2003a; Lin *et al.*, 2003b) and have attempted to correct for this influence in the analysis, but have not explored the possible relationship between gender and TICV. Given the strong association between gender status and TICV, and the consequent relationship shown in this study between TICV, gender status and UCCA, the present results illustrate the importance of adjusting for both TICV and gender (particularly if TICV is unavailable) in any UCCA or cord volume analysis in MS. Previously subject height has been noted to have a possible relationship with UCCA (Kameyama *et al.*, 1994; Losseff *et al.*, 1996a), however this cohort information was not available for this analysis. Hence, we are unable to exclude the possibility that height differences between male and female subjects may be partially mediating gender UCCA differences. In contrast to a previous study (Losseff *et al.*, 1996a), the subject weight was not found to be a significant influence on UCCA. Also, in keeping with all other studies assessing cord area or volume, subject age was not found to be a significant covariate.

Previous studies investigating CIS and relapsing-remitting MS cord size have produced differing results. Most cross-sectional studies have shown no significant cord atrophy in relapsing-remitting MS cohorts (all with greater median disease durations greater than this cohort) compared with controls (Losseff *et al.*, 1996a; Stevenson *et al.*, 1998; Lin *et al.*, 2003a; Lin *et al.*, 2003b; Vaithianathar *et al.*, 2003). Conversely, a study investigating UCCA in CIS showed significant baseline atrophy in patients with T_2-visible white matter lesions on their MRI scans, in comparison to controls (Brex *et al.*, 2001). Further, a study measuring cord volume showed a significant decrease in relapsing-remitting MS in comparison to controls (Edwards *et al.*, 1999). However both these investigations had no gender correction between the

cohorts, whilst the CIS analysis (Brex *et al.*, 2001) also did not adjust for TICV. This study provides further evidence, using robust methodology, that significant UCCA atrophy is not apparent at the clinically earliest stages of relapsing-remitting MS.

Progressive MS patients have consistently showed cord atrophy in comparison to normal controls with correlation between atrophy and clinical disability (EDSS) (Losseff *et al.* 1996a; Filippi *et al.*, 1996a; Lycklama à Nijeholt *et al.*, 1998; Stevenson *et al.*, 1998; Rovaris *et al.*, 2001; Lin *et al.*, 2003a; Vaithianathar *et al.*, 2003). Hence, evidence exists in these clinical phenotypes of MS for the potential use of cord atrophy as a surrogate marker of disease severity, prognosis and also in disease modifying treatment trials. Although we have not found significant UCCA atrophy in a cohort of clinically early relapsing-remitting MS, the study does, however, emphasise that when evaluating disease related changes in UCCA, TICV and gender – in particular the former – should be considered as potentially confounding covariates. This should be taken into account when studying UCCA in any pathological process known to affect the cervical cord.

5.5 Cord cross-sectional area in early relapsing-remitting multiple sclerosis: longitudinal analysis

5.5.1 Introduction

Although most cross-sectional analyses have observed no significant UCCA tissue loss in relapsing-remitting MS, two studies in cohorts with well established disease have reported an increased rate of atrophy longitudinally over one year (Stevenson *et al.*, 1998) and four years (Lin *et al.*, 2003a) respectively. It is not clear from these studies, however, how early in the disease course this becomes evident.

In developing objective quantitative MRI measures of disease progression for studies of prognosis and disease modifying treatment, it is relevant to delineate the first stages of evolution of a detectable abnormality. If significant longitudinal UCCA atrophy were to occur in early relapsing-remitting MS patients it may also be possible that as the magnitude of tissue loss increases, related clinical dysfunction may become apparent as has been noted in studies of progressive MS patients (Losseff *et al.*, 1996a; Filippi *et al.*, 1996a; Stevenson *et al.*, 1998; Lin *et al.*, 2003a).

This study reports a three year serial investigation of UCCA measures in patients from the clinically early relapsing-remitting MS cohort and healthy volunteers to determine: (i) the comparative changes in UCCA within the two groups and whether there is a significant difference between them and (ii) whether change in UCCA at this early stage is related to clinical and other MR measures of the disease.

5.5.2 Methods

Subjects

Patients from the early relapsing-remitting cohort were scanned up to four times at approximately yearly intervals over three years; all those included had a minimum of two scans within the three year study period. At baseline there were 27 patients (mean age 37.3 [range 26.9-55.6] years; 19 female, 8 male; median disease duration 1.7 [range 0.5-3] years; median EDSS 1.0 [range 0-3]) and 20 healthy volunteers (mean age 35.3 [range 23.3-52.7] years; 10 female, 10 male). After one year, 25 patients and 20 controls were imaged. After two years, 25 patients and 17 controls scanned, and at three years 24 patients and 12 controls were studied. Median length of time from study start to completion was 1089 days in patients and 1088 days in controls.

No patients were on BIFN at recruitment; during the study follow up period, 12 of the 27 original MS patients received this treatment. The EDSS (Kurtzke, 1983) and MSFC (Cutter *et al.*, 1999) were assessed in each patient at all time-points. Informed consent was obtained from all subjects and the study had approval of the Joint Medical Ethics Committee of the Institute of Neurology and National Hospital for Neurology and Neurosurgery, Queen Square, London.

MRI protocol

At all time-points, scans were performed on a GE Signa 1.5 T scanner (General Electric Medical Systems, Milwaukee, USA). All subjects had a volume acquired

inversion prepared FSPGR sequence of the spinal cord with reconstruction to five contiguous 3mm pseudoaxial slices as detailed in the cross-sectional analysis (section 5.4). In the same session, PD-weighted (28 x 5mm axial slices; TE 95 ms; TR 2000 ms; matrix 256x256; FOV 240x180) and T_1-weighted (28 x 5mm axial slices; TE 20 ms; TR 540 ms; matrix 256x256; FOV 240x240) spin-echo images were acquired of the brain. In addition, post-contrast (triple dose gadolinium [0.3 mmol/kg]) T_1-weighted images of the brain (using the same acquisition method as described above) and cord spin-echo T_1-weighted images (13 x 3mm sagittal slices; TR 500 ms; TE 20 ms; matrix 512x512; FOV 480x240) were acquired at baseline and after six months in all patients and also at 1, 2 and 3 months post baseline – with 25 out of 27 patients undertaking at least two of these monthly scans – to provide an indication of the extent of early inflammatory lesions in the brain and cord. The contrast enhanced scans were acquired in the same scanning session as the cord FSPGR images with the gadolinium administered after the FSPGR sequence.

A cranial 3D FSPGR sequence was acquired yearly during a separate scanning session (median 5 days [baseline]; 7 days [one year]; 8 days [two years] and 7 days [three years] from the cord imaging) with parameters as described in the cross-sectional analysis (section 5.4). From these images, TICV and brain volumes were measured: (i) because of the reported association between TICV and UCCA (thus the former could be used as a covariate in analysing UCCA change) and (ii) in order to compare the early progressive brain volume loss that occurs in MS (Chard *et al.*, 2004; Tiberio *et al.*, 2005) with changes in UCCA.

Image Analysis

The UCCA was determined as in the cross-sectional study (Losseff *et al.*, 1996; see section 5.4) with the observer (WR) blinded to clinical status and time-point of the scan. Gadolinium-enhancing lesions of the brain and cord were identified from the post-contrast images of the cord by an experienced observer (DHM). T_1 (hypointense and gadolinium-enhancing) and T_2-weighted lesions (the latter measured from the PD-weighted images) were outlined on the images using the Dispimage display software package (Plummer, Department of Physics, University College Hospitals NHS Trust, London, UK) (Plummer, 1992) and segmented using a semiautomated contouring technique (Filippi *et al.* 1998a).

The TICV of each subject was calculated as described in the cross-sectional analysis (section 5.4). A recent study investigating brain volume in 21 of the patients taking part in this study showed progressive grey matter tissue loss over two years in comparison to controls (Tiberio *et al.*, 2005). This data was used along with the segmented brain tissue volumes from the remaining six patients in this study not included in the original brain volume cohort - calculated using identical methodology (Chard *et al.*, 2002a) – to investigate longitudinal associations between segmented brain tissue volumes (WBV, BPF, GMF and WMF) and UCCA tissue loss.

Statistical Analysis

For the comparison between patients and controls, values of UCCA over the four time points were modelled using random intercepts regression (Goldstein, 1995) with

random subject-specific intercepts and common linear slope on time from study baseline; MS indicator and MS x time interaction terms were used to estimate patient versus control differences. Potential confounding by age, gender, weight and TICV was examined by adding those terms singly as covariates, but the first three variables were not significant at $p=<0.1$, nor materially affect the coefficients of interest, and only TICV was kept in the final model. The longitudinal model was also used to estimate baseline and 3-year cross-sectional patient versus control differences. In patients only, a similar random intercepts model was used with BIFN treatment indicator and interaction with time to compare effect of treatment in patients, with disease duration as an additional covariate to be examined: again, only TICV contributed in this patient-only model. These analyses were implemented in Stata 8.2 (Stata Corporation, College Station, Texas, USA).

Multiple linear regression models of change in UCCA over the study period on corresponding change in: (i) MSFC; (ii) lesion volumes (pre-contrast T_1 and T_2) and (iii) brain tissue volume were used to examine associations between these covariates and UCCA atrophy in patients only. Two-tailed Spearman rank correlations were used to assess correlations between change in UCCA and (i) the mean number of gadolinium-enhancing lesions per patient in the first six months of the study (to evaluate whether early inflammation is related to the subsequent evolution of UCCA change over three years); (ii) change in the EDSS and (iii) the functional scores contained within the EDSS that may be more specific to cord pathology (pyramidal, brainstem, bowel or bladder symptoms and sensory) over the study period. Paired t-tests were used to compare changes within a single parametric variable over the study course, whilst Wilcoxon sign rank test was used for non-parametric variables. These

analyses were implemented in SPSS 11.0 (SPSS Inc., Chicago, IL, USA). A p value of < 0.05 was considered significant.

5.5.3 Results

Table 5.5 shows the demographic details, lesion volumes, UCCA and TICV of controls and patients at all time-points. The only potential covariate found to be significantly associated with UCCA was the TICV (p=0.002). The gender, weight, age and disease duration of subjects was not found to significantly confound UCCA values. In the patient cohort over the whole study course, a significant increase in EDSS (p=0.008), brainstem (p=0.008), pyramidal (p=0.016) and bowel and bladder (p=0.013) symptom functional scores were observed, however clinically no patient appeared to have entered the secondary progressive stage of MS. In the patient cohort (n=22), both the WBV (mean at baseline=1103.04 mls; mean at 24 months=1089.20 mls; p=0.001) and BPF (mean at baseline=0.812; mean at 24 months=0.802; p=0.011) significantly decreased over the study course, with the loss of tissue being predominantly seen in the grey matter (GMF mean at baseline=0.542; mean at 24 months=0.533; p=0.007) rather than white matter (WMF mean at baseline=0.270; mean at 24 months=0.269; p=0.589). The MSFC was not noted to change significantly during the study. Both the T_2-weighted (p=0.001) and T_1-weighted lesion volumes (p=<0.001) had significantly increased by the end of the study.

Assessment of UCCA

Figure 5.6 illustrates UCCA values at each time-point in patients and controls.

Cross-sectional UCCA comparisons: patients versus controls

At baseline, in models adjusting for TICV, no significant difference was found in UCCA between patients and controls (p=0.748). At three years, cross-sectional comparison of patients versus controls showed borderline evidence that patients have smaller UCCAs (mean difference patients – controls: -4.239 mm^2; p=0.074; 95% CI: -8.887, 0.408), after adjusting for TICV. At two years, no significant difference was seen between patient and control UCCAs; however, the size of the mean difference between the two cohorts is consistent with the three year analysis (i.e. approximately two-thirds of the mean difference at three years) (mean difference patients – controls: -2.902 mm^2; p=0.211; 95% CI: -7.452, 1.647) after adjusting for TICV.

Longitudinal UCCA analysis

Over the whole three year study period, there was a significant difference in the rates of decrease in UCCA between patients and controls (mean patient-control difference per year: -1.161 mm^2; p=0.001; 95% confidence interval [CI]: -1.843, -0.478) with significant UCCA atrophy noted in patients only (mean annual rate: -0.812 mm^2; p=<0.001; 95% CI: -1.215, -0.409) but not in controls (p=0.215) (see Figure 5.7).

Table 5.5: *Demographic, clinical and MRI parameters in patients (MS) and controls (NC) over the study course. Mean values unless stated, N/A= not applicable.*

	Baseline		**Year one**		**Year two**		**Year three**		**P-value for change over study**	
	MS N=27	***NC N=20***	***MS N=25***	***NC N=20***	***MS N=25***	***NC N=17***	***MS N=24***	***NC N=12***	***MS***	***NC***
Age (years)	37.26	35.31	38.60	36.32	39.25	38.17	39.97	40.75	N/A	
male: female	8:19	10:10	7:18	10:10	7:18	10:7	7:17	10:2	N/A	
Median EDSS	1.0	N/A	1.5	N/A	2.0	N/A	2.0	N/A	**0.008**	N/A
PD lesion vol (mls)	7.71	0	8.90	0	9.18	0	11.15	0	**0.001**	N/A
T_1 lesion vol (mls)	1.72	0	1.76	0	1.89	0	2.59	0	**<0.001**	N/A
Gd lesion vol (mls)	0.64	0	0.56	0	0.26	0	0.32	0	0.179	N/A
Cord area (mm^2)	78.91	80.50	77.90	81.37	77.12	81.07	76.25	83.88	**<0.001**	0.215
TICV (mls)	1348	1358	1346	1369	1355	1365	1333	1341	0.791	0.817

Figure 5.6: *Graphs showing measured upper cervical cord area values over time (days from baseline: days_b) for control (a) and patient (b) cohorts.*

(a) All controls

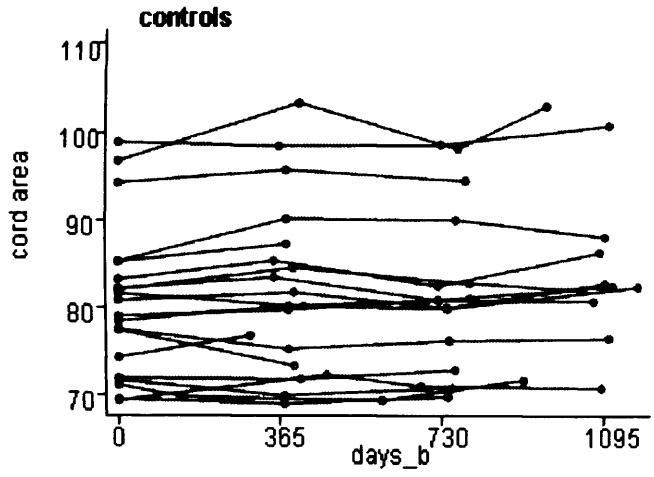

(b) All patients

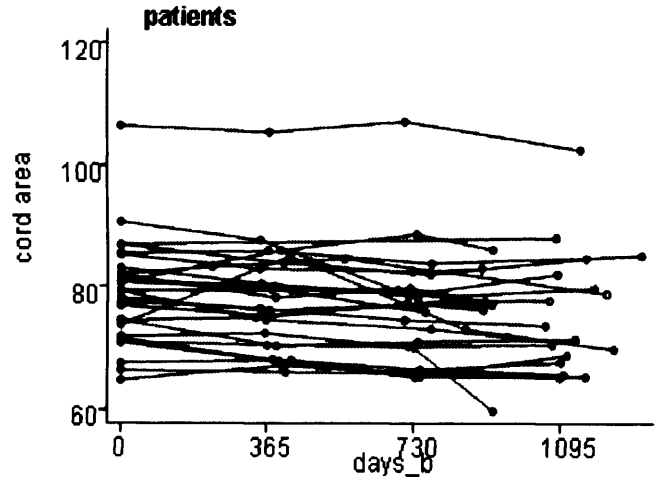

Figure 5.7: *Graph showing total cross-sectional mean of patient (solid line) and control (dashed line) cohorts at each time-point with contracted[a] confidence intervals.*

[a] The confidence intervals are contracted, so that bars overlap only if the difference is not statistically significant at the 5% level, by multiplying the factor:

$$t_N \sqrt{(S_1^2+S_1^2)}/(t_1S_1+t_2S_2)$$

where t_N, t_1 and t_2 are the appropriate t values for the whole sample, controls and patients respectively, and S_1 and S_2 are the standard errors in controls and patients.

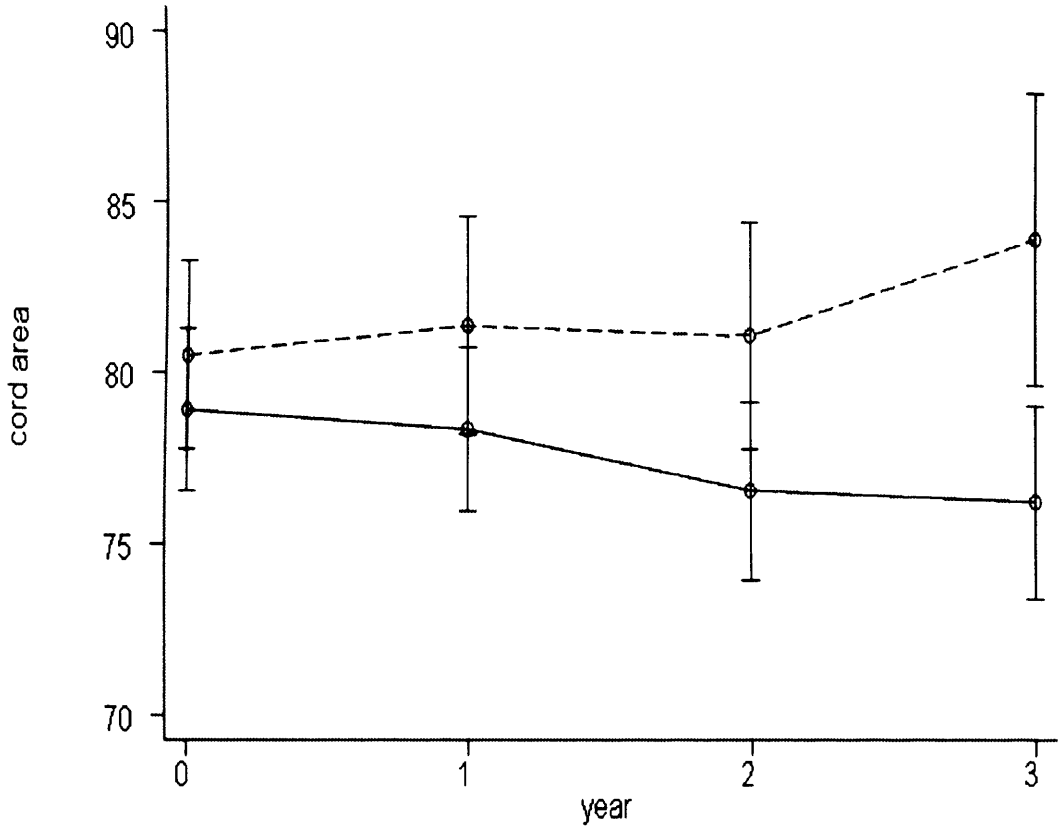

Because of differences in the control cohort size, gender and TICV distribution between the two and three year time-points, longitudinal analysis between baseline and two years was also performed to confirm results. At this time-point – again adjusting for TICV - there was a significant difference in the rates of decrease in UCCA between patients and controls (mean patient-control difference per year: -1.069 mm^2; p=0.026; 95% CI: -2.008, -0.130) with significant UCCA atrophy noted in patients only (mean annual rate: -0.890 mm^2; p=0.003; 95% CI: -1.497, -0.303) but not in controls (p=0.647).

Clinical and MRI correlations with UCCA

Evidence of a correlation was seen between the T_1-weighted brain lesion volume and change in UCCA over three years with increased T_1 hypointense lesion volume noted in patients with relatively less UCCA atrophy (p=0.020; r=0.515). No correlation was seen between mean gadolinium enhancement in the first six months (defined as the mean number of gadolinium-enhancing lesions from all post-contrast T_1-weighted scans in the first six months) and UCCA change over two or three years and no association was seen between changes in T_2-weighted lesion volume and UCCA over three years. No correlation was seen between changes in brain tissue volume and UCCA at two years. No significant relationships were noted between changes in UCCA and clinical measures (EDSS and MSFC) over the study duration.

No difference was seen when comparing the rate of UCCA loss in those 12 subjects who had started BIFN during the study and those who did not (p=0.135).

5.5.4 Discussion

The results showed decreasing UCCA in a cohort of patients with early relapsing-remitting MS; the rate of loss of UCCA did not relate to changes in disability.

No previous study has longitudinally investigated relapsing-remitting MS patients as early and for as long a period of time and in comparison with healthy controls. A previous longitudinal study investigating UCCA did demonstrate atrophy in a combined cohort of both secondary progressive and well established relapsing-remitting MS subjects (mean disease duration 5.5 years) over four years but the control population was imaged at baseline only (Lin *et al.*, 2003a). A further 12-month study showed UCCA atrophy in relapsing-remitting MS in comparison to controls, but the cohort had a longer disease duration (mean=5.6 years) and only six such patients were studied (Stevenson *et al.*, 1998).

From both the two and three year longitudinal analyses in this study, it is evident that cervical cord tissue loss does occur at this early stage of relapsing-remitting MS, even though there was no significant cross-sectional difference in comparison to controls. The negative latter finding likely reflects the large normal inter-individual variation in UCCA, which makes it difficult to detect a subtle degree of atrophy in a single time-point study. Although a gender imbalance did exist between the patient and control cohorts particularly at the final time-point, the relative similarities between the results at two and three years suggests that our longitudinal observations are consistent along the different time-points. Furthermore, several potential covariates – including gender

– were included in the statistical modelling for the analysis and the one found to influence UCCA (TICV) was accounted for in the final analysis.

The apparent absence of correlation between the cervical cord atrophy and disability in early relapsing-remitting MS may be due to a number of factors. Firstly, the pathological processes of inflammation, oedema and neuroaxonal degeneration which are likely to be causing clinical dysfunction at this stage of the condition may have competing effects on UCCA possibly masking a relationship between disability and atrophy. Secondly, given the minimal levels of clinical dysfunction in this cohort, an increase in EDSS partly reflects an increase in detection of clinical signs only, rather than significant dysfunction. Thirdly, disability in early relapsing-remitting MS results mainly from incomplete recovery from relapses that result from individual demyelinating lesions, some of which will not be located in nor affect the size of the upper cervical cord. Finally, the loss of cord tissue is relatively small – about 1% per annum - and *per se* would not seem likely to affect disability (particularly if most of the long tract fibres are still intact). The correlations of UCCA with disability noted in some previous studies were mainly seen in patients with progressive MS, greater disability and more severe atrophy (Losseff *et al.*, 1996a; Filippi *et al.*, 1996a; Lycklama à Nijeholt, 1998; Stevenson *et al.*, 1998; Edwards *et al.*, 1999; Rovaris *et al.*, 2001; Vaithianathar *et al.*, 2003; Lin *et al.*, 2003a; Lin *et al.*, 2003b). No patients in this cohort had clinically entered the secondary progressive phase by the study end and all still had relatively low levels of disability.

The absence of a correlation of UCCA change in the MS cohort with T_2-weighted brain lesion volume, the extent of early gadolinium enhancement and also progressive

brain tissue atrophy suggests that UCCA may be complementary to these existing MR measures as a marker of the evolution of MS. The dissociation between cord and brain atrophy noted in this study is supported by observations from previous studies in primary progressive (Ingle *et al.*, 2003) and benign and disabling MS (Brass *et al.*, 2004). It also suggests that monitoring of cord atrophy provides information which complements the measurement of brain atrophy. The association between preservation of UCCA and increasing T_1-weighted brain lesion volume is unexpected – and not readily explained - since T_1-hypointense lesions have been associated with greater axonal loss (van Walderveen *et al.*, 1998). The association is only moderate and we do not exclude the possibility that this is a chance finding.

Probably the mechanisms of upper cervical cord atrophy are complex and likely to be related to factors other than global measures of brain lesion load. Lesion location may be relevant and in particular the severity of axonal loss and Wallerian degeneration arising from lesions that occur in the spinal cord or in white matter tracts that traverse the upper cord is likely to relevant (Ganter *et* al., 1999; Lycklama à Nijeholt *et al.*, 2001; DeLuca *et al.*, 2004; Bot JC *et al.*, 2004b). Previous studies, investigating patients with longer disease durations, have suggested that the effects of demyelination, axonal loss (particularly small fibre loss in the cord) and Wallerian degeneration all contribute to cord atrophy (Ganter *et al.*, 1999; DeLuca *et* al., 2004; Minagar *et* al., 2004). In the early relapsing-remitting MS patients we studied, inflammation and oedema may be present in the cord - previous studies of patients with CIS and relapsing-remitting MS cohorts of early disease duration have reported 42-87.5% to have areas of abnormal cord MRI signal (Brex *et al.*, 1999; Lycklama à Nijeholt *et al.*, 2000; Bot JC *et al.*, 2004a) - and might have masked subtle tissue loss.

The relative extent of these processes may be important in determining cross-sectional cord area size. Further longitudinal follow-up of this cohort, particularly as some patients start to enter the progressive stage of the disease, will clarify the long-term evolution of cord atrophy and its relationship to prognosis.

The study did not observe a significant difference between the rate of UCCA loss in patients on or off BIFN therapy. However, it would be imprudent to draw conclusions from small subgroups studied in a post-hoc, non-randomised and retrospective manner.

Because the degree of UCCA atrophy in patients with progressive forms of MS is substantial and is also correlated with the extent of disability (Losseff *et al.*, 1996a; Filippi *et al.*, 1996a; Lycklama à Nijeholt, 1998; Stevenson *et al.*, 1998; Edwards *et al.*, 1999; Rovaris *et al.*, 2001; Vaithianathar *et al.*, 2003; Lin *et al.*, 2003a) the present finding that cord area loss is already emerging in a cohort of patients with early relapsing-remitting disease and minimal clinical dysfunction raises the question whether early cord atrophy may predict the later development of disability due to myelopathy. More prolonged follow up studies should investigate this possibility. Cord atrophy may be a useful outcome measure in controlled trials of new disease modifying treatments in relapsing-remitting MS.

CHAPTER 6

Summary and Conclusions

6.1 Rationale of investigating the clinical-pathological evolution in multiple sclerosis using MRI

Although much has been learned regarding the clinical and pathological genesis and evolution of MS, important questions remain. Previous studies have demonstrated the presence of inflammation and neurodegeneration in the condition (Trapp *et al.*, 1998; Lucchinetti *et al.*, 2000; Evangelou *et al.*, 2000; Kuhlmann *et al.*, 2002; Miller *et al.*, 2002), but it remains unclear precisely how these pathological processes interact in both the development of MS and the clinical evolution of the disease. In addition, it is possible that the relative importance of the inflammation and neurodegeneration may change over the course of MS and this may be important in both a patient's symptomatology and prognosis. A greater insight into this could identify pathological steps which could be amenable to drug therapy and also an improved understanding of factors which may determine future clinico-pathogenic development.

MR techniques provide a tool – albeit imperfect – for monitoring evolving pathological processes in MS *in vivo* and for gaining insights into potential pathogenic mechanisms. Standard MR imaging often provides visible evidence of inflammation in the white matter (hyperintense T_2-weighted lesion volume and identification of gadolinium-enhancing lesions), however T_2-weighted lesions are not specific for inflammation (Miller *et al.*, 1998; Barkhof *et al.*, 2003), whilst gadolinium-enhancing lesions are transient in appearance (Filippi, 2000b). Additional

information regarding the extent of axonal loss can be determined by the volume of persistent hypointense T_1-weighted lesions (Van Waesberghe *et al.*, 1999). However, the identification of such lesions is subjective and correlation to disability only moderate (Truyen *et al.*, 1996); furthermore many acute T_1 hypointense lesions resolve over six months or more of follow up, indicating that reversible pathological features such as oedema and demyelination contribute to T_1 hypointensity.

An explanation for the absence of a consistent correlation between standard MR lesion measures and concurrent disability and the difficulty in providing accurate prognostication to patients may be two-fold. Firstly, lesion measures only provide an index of pathology in discrete areas of the white matter and not in the NAWM or grey matter. Secondly, the majority of previous studies investigating correlations between MR sequences and disability have tended to include MS cohorts with a wide disease duration. Further, the suggestion that perfusion abnormalities may be involved or reflect disease pathogenesis (see section 1.4.9) has, prior to the study detailed in chapter three, only been investigated in small numbers of MS subjects with either relapsing-remitting or secondary progressive disease phenotypes.

At present, because a consistent and robust correlation between standard MRI lesion measures and clinical disability has not emerged, phase III therapeutic trials in MS rightly continue to rely on clinical relapses and changes in disability as primary outcome measures. Relapses can be relatively infrequent and the disability scales are potentially weighted to particular functional systems and may be poorly sensitive to change (Filippi *et al.*, 1998e). Therefore, delineating the *in-vivo* clinical and pathological course of MS, by concurrent clinical and MRI evaluation respectively,

may provide new insights into the mechanisms of disease progression and may also identify sequences that can be incorporated into drug trials to provide an objective, sensitive and clinically meaningful outcome measure.

6.2 Perfusion measurement in multiple sclerosis

The study detailed in chapter three demonstrates, for the first time, that it is possible to quantitatively measure cerebral perfusion in a wide range of MS subjects, of all clinical phenotypes, in comparison to controls using a non-invasive MR technique. The technique described is made more robust in that it also models for the semi-permeability of the BBB using the two-compartment theory (Parkes and Tofts, 2002), thus improving the quantification of perfusion *per se*. The increased perfusion observed in white matter in relapse onset MS may reflect the presence of inflammation and the decreased perfusion seen in grey matter in progressive forms of MS may indicate neuroaxonal loss or dysfunction. The results suggest that perfusion measurement has potential to be a quantitative marker for both inflammation and neurodegeneration because of the metabolic changes associated with these disease processes.

Although the results suggest that white matter perfusion may be partially modulated in relapsing-remitting subjects on BIFN therapy, the study was not designed to specifically investigate this. Further randomised studies - with greater power – are required to investigate the question of treatment effect and its potential to monitor with perfusion MRI. There may also be potential for investigating the possible relationship between cerebral perfusion and symptoms that may be associated with

decreased metabolic activity such as fatigue and cognition (Peyser *et al.*, 1980; Rao *et al.*, 1991). In previous metabolic studies, cognitive symptoms have shown regional correlations with decreased cerebral glucose uptake (Paulesu *et al.*, 1996; Blinkenberg *et al.*, 2000). The presented CASL technique – particularly with implementation of the methodological improvements illustrated in section 3.1.4 – has shown it may be possible to provide accurate non-invasive cerebral perfusion measurements in MS. Further investigation of longitudinal changes in perfusion and correlations with cognitive dysfunction may be worthwhile in the future and may provide further insights into regional perfusion change and its possible pathogenic relation to symptoms that commonly affect MS patients.

6.3 MR studies in clinically early relapsing-remitting multiple sclerosis

As detailed in section 4.1, factors early in the clinical course of relapsing-remitting MS - such as inflammatory axonal loss in acute lesions and T_2 visible lesion development in the first one to five years of first symptom onset (Brex *et al.*, 2002; Kuhlmann *et al.*, 2002) - have the potential to contribute to later clinical disability. Hence, determining the sensitivity to detect change and the longitudinal clinical relevance of a quantitative MR parameter studied in patients in the clinically earliest stages of relapsing-remitting MS - as has been undertaken in the studies presented in chapters four and five – may yield important information on prognosis and pathogenesis. Importantly, the investigated MS cohort were prospectively recruited such that they had a distinctly early and homogenous disease duration range; therefore, patients were likely to be at similar stages of disease evolution when the investigations commenced.

Intensive MR investigation of such a cohort may be uniquely revealing, for instance in determining why do some patients - with seemingly little difference between their hypointense T_1-weighted and T_2-visible lesion loads at disease onset – subsequently develop significantly different levels of clinical disability? Longitudinal quantitative MR investigations which serially follow-up this cohort may provide valuable additive information to this question.

6.3.1 Gadolinium-lesion enhancement

The studies detailed in chapter four were developed to optimise the detection of acute inflammatory lesions by using triple dose gadolinium contrast, an initial period of monthly scanning, and examination of both brain and spinal cord. The study illustrates that MR is a sensitive indicator of areas of acute CNS inflammation in MS (seen as regions of gadolinium enhancement in the brain or spinal cord) and that such active lesions are abundant in early relapsing-remitting MS. The studies presented also show that these lesions are relevant to clinical relapse events, although most occur without noticeable clinical symptoms.

However, over the intermediate term (up to two years) the level of gadolinium-enhancing lesions does not consistently correlate with clinical measures of impairment or disability. This suggests that measurement of such lesions may not be helpful in determining long term patient prognosis, and that inflammatory lesions are not the only or main pathogenic factor in determining clinical disability. However, the follow up was only two years, and continued follow-up may be relevant particularly as a previous MR study in CIS patients showed a correlation between T_2-visible

lesion development in the first five years and disability at 14 years (Brex *et al.*, 2002), and that the development of such T_2 lesions is partly related to the extent of gadolinium lesion enhancement (Molyneux *et al.*, 1998). Such a study is ongoing at the NMR Unit, Institute of Neurology. At present, on the basis of the studies presented in chapter four, gadolinium lesion enhancement is a common event in early relapsing-remitting MS but this measure is of limited relevance for disability or impairment prediction in the medium term, although it is related to relapse frequency.

6.3.2 Diffusion tensor imaging

The DTI studies presented in chapter five showed that subtle but measurable abnormalities are present in the NABT in early relapsing-remitting MS cohort. An increased FA peak height was observed at presentation and – in the follow up study – an increased MD was observed at the two year time-point. Additionally, these changes were not correlated with T_2 lesion load, suggesting a process in NABT early in the course of MS that may be evolving independently of visible lesions.

Few previous longitudinal DTI studies have been attempted in MS (see section 2.5.3) and this may in part be due to the difficulties associated with EPI sequences, particularly distortions and lower spatial resolution that can impact on the accuracy of tissue segmentation. The presented studies incorporate an automated segmentation technique not previously used in DTI studies in MS, to investigate if this may provide an analytical improvement. However, in the longitudinal study, although there was a suggestion that abnormalities were increasing over time, no clear longitudinal pattern could be determined. This suggests either that DTI is not a sensitive measure of

NABT pathology in early relapsing-remitting MS or that further improvement is necessary both in terms of image resolution and also analytical methods to enable more effective DTI monitoring of the evolution of MS abnormalities in NABT. The sequence used in the studies presented has since been improved (Jones *et al.*, 2002; Wheeler-Kingshott *et* al., 2002) hence, evaluation of MS cohorts using such developments may be informative.

6.3.3 Measurement of upper cervical cord area

The absence of significant cross-sectional upper cervical cord atrophy in comparison to controls in the clinically early relapsing-remitting MS cohort (Chapter 5) is in keeping with the minimal disability exhibited by the patients. The importance of accurate methodology and interpretation of UCCA is emphasised by the strong association between UCCA and TICV and also the possible role of gender; these factors should be accounted for in any statistical modelling using this MR parameter.

The longitudinal finding (Chapter 5) of a significantly increased rate of cord tissue loss in the early relapsing-remitting MS cohort studied in comparison to controls – and that this did not correlate with brain T_2 lesion volume or BPF change - illustrates the potential of UCCA measurement to provide complementary information on disease progression. Previous studies have shown in progressive MS phenotypes that significant cord atrophy occurs in comparison to controls and that this is related to disability (see section 2.5.4). Hence, the finding of measurable increasing but early cord area loss in patients with minimal levels of clinical disability (median EDSS 2.0) - which may be evolving from at least partially separate mechanisms to those causing

brain atrophy and lesion accumulation – indicates the potential of UCCA measurement to be an early marker of later prognosis and to provide a complementary tool for monitoring the disease in treatment trials.

The longitudinal study presented has a follow-up of three years, continued longitudinal follow-up of the cohort as the subjects develop higher levels of disability is important, particularly to see if those who have increasing clinical impairment also had evidence of greater cord area loss early in the course of the study, and whether the rate of UCCA atrophy is correlated to their level of clinical dysfunction. Longitudinal UCCA measurements of this cohort are therefore continuing.

6.4 Summary

MS as a disease still offers fundamental challenges to scientific understanding in terms of aetiology and pathogenesis, and is still in need of major progress to develop more effective disease modifying treatments. MRI offers a unique *in-vivo* investigative tool and has already provided some insight into the pathological processes and pathogenic mechanisms associated with MS, and has proved valuable in therapeutic monitoring.

The studies presented in this thesis have shown that measurable abnormalities exist in different MS phenotypes and that several different types of abnormality evolve from the earliest stages of the disease. It is important to note that early abnormalities have been shown beyond visible brain lesions (abnormalities in NABT and increasing spinal cord atrophy) and the potential of such abnormalities to help understand

pathogenic mechanisms or to assist with prognosis deserves further consideration. Systematic application of MR techniques – including but not confined to those described in this thesis - is required to elucidate the relationship of the quantitative measures derived with the evolution of the disease. The thesis indicates the potential importance of measuring cerebral perfusion in MS and the relative merits of several other MR parameters in their suitability for monitoring the early pathological evolution of a complex disease process.

It might be hoped that future systematic, prospective longitudinal studies – including the one described in this thesis – will ultimately define a combination of MR parameters which better describe the future prognosis of MS and which also provide reliable markers for the underlying pathogenic mechanisms. If achieved, such a comprehensive delineation of pathogenesis and prognosis would give a guide as to which patients are most likely to benefit from therapeutic intervention and would also identify the therapeutic strategies that need to be targeted particularly to mitigate against disease progression at an early stage.

CHAPTER 7

Reference List

Aarts E, Kurst J. In: *Simulated annealing and Boltzmann Machines.* New York: Wiley; 1989.

Adams CWM. Histology and cellular features of multiple sclerosis. In: *A colour atlas of multiple sclerosis and other myelin disorders.* London: Wolfe Medical Publication 1989; 130-184.

Allen IV, McKeown SR. A histological, histochemical and biochemical study of the macroscopically normal white matter in multiple sclerosis. *J of Neurol Sci* 1979; **41:** 81-91.

Allen IV, Glover G, Anderson R. Abnormalities in the macroscopically normal white matter in cases of mild or spinal multiple sclerosis. *Acta Neuropathol (Berl)* 1981; **suppl IV:** 176-178.

Alsop DC, Detre JA. Reduced transit-time sensitivity in non-invasive magnetic resonance imaging of human cerebral blood flow. *J Cereb Blood Flow Metab* 1996; **16:** 1236-1249.

Alsop DC, Detre JA. Multisection cerebral blood flow MR imaging with continuous arterial spin labelling. *Radiology* 1998; **208:** 410-416.

Antel J, Owens T. Multiple sclerosis and immune regulatory cells. *Brain* 2004; **127:** 1915-1916.

Arnold DL, Matthews PM. MRI in the diagnosis and management of multiple sclerosis. *Neurology* 2002; **58:** S23-S31.

Ashburner J, Friston K. Multimodal image coregistration and partitioning – a unified framework. *Neuroimage* 1997; **6:** 209-217.

Ashburner J, Friston KJ. Voxel-based morphometry – the methods. *Neuroimage* 2000; **11:** 805-821.

Bagnato F, Tancredi A, Richert N, Gasperini C, Bastianello S, Bash C, McFarland H, Pozzilli C, Frank JA. Contrast-enhanced magnetic resonance activity in relapsing-remitting multiple sclerosis patients: a short term natural history study. *Mult Scler* 2000; **6:** 43-49.

Bakshi R, Miletich RS, Kinkel PR, Emmet ML, Kinkel WR. High-resolution fluordeoxyglucose positron emission tomography shows both global and regional cerebral hypometabolism in multiple sclerosis. *J Neuroimaging* 1998; **8:** 228-234.

Bammer R, Augustin M, Strasser-Fuchs, Seifert T, Kapeller P, Stollberger R, Ebner F, Hartung HP, Fazekas F. Magnetic resonance diffusion tensor imaging for characterizing diffuse and focal white matter abnormalities in multiple sclerosis. *Magn Reson Med* 2000; **44:** 583-591.

Banati RB, Newcombe J, Gunn RN, Cagnin A, Turkheimer F, Heppner F, Price G, Wegner F, Giovannoni G, Miller DH, Perkin GD, Smith T, Hewson AK, Bydder G, Kreutzberg GW, Jones T, Cuzner ML, Myers R. The peripheral benzodiazepine binding site in the brain in multiple sclerosis: quantitative in vivo imaging of microglia as a measure of disease activity. *Brain* 2000; **123:** 2321-2337.

Barkhof F, Scheltens P, Frequin STFM, Nauta JJ, Tas MW, Valk J, et al. Relapsing-remitting multiple sclerosis: sequential enhanced MR imaging vs clinical findings in determining disease activity. *AJR* 1992; **159**: 1041-1047.

Barkhof F, Filippi M, Miller DH, Scheltens P, Campi A, Polman CH, Comi G, Ader HJ, Losseff N, Valk J. Comparison of MR imaging criteria at first presentation to predict conversion to clinically definite multiple sclerosis. *Brain* 1997; **120:** 2059-2069.

Barkhof F, Brück W, De Groot CJA, Bergers E, Hulshof S, Geurts J, Polman CH, van der Valk P. Remyelinated lesions in multiple sclerosis. Magnetic resonance image appearance. *Arch Neurol* 2003; **60:** 1073-1081.

Barnes D, Munro PM, Youl BD, Prineas JW, McDonald WI. The longstanding MS lesion. A quantitative MRI and electron microscopic study. *Brain* 1991; **114:** 1271-1280.

Barnes D, Hughes RA, Morris RW, Wade-Jones O, Brown P, Britton T, Francis DA, Perkin GD, Rudge P, Swash M, Katifi H. Randomised trial of oral and intravenous methylprednisolone in acute relapses of multiple sclerosis. *Lancet* 1997; **349:** 902-906.

Barnett MH, Prineas JW. Relapsing and remitting multiple sclerosis: pathology of the newly forming lesion. *Ann Neurol* 2004; **55:** 458-468.

Basser PJ, Mattiello J, Le Bihan D. Estimation of the effective self-diffusion tensor from NMR spin-echo. *J Magn Reson B* 1994; **103:** 247-254.

Basser PJ, Pierpaoli C. Microstructural and physiological features of tissues elucidated by quantitative-diffusion-tensor MRI. *J Magn Reson B* 1996; **111:** 209-219.

Bastianello S, Pozzilli C, Bernardi S, Bozzao L, Fantozzi LM, Buttinelli C, Fieschi C. Serial study of gadolinium-DTPA MRI enhancement in multiple sclerosis. *Neurology* 1990; **40:** 591-595.

Beck RW, Cleary PA, Anderson MM Jr, Keltner JL, Shults WT, Kaufman DI, Buckley EG, Corbett JJ, Kupersmith MJ, Miller NR. A randomised, controlled trial of corticosteroids in the treatment of acute optic neuritis. The Optic Neuritis Study Group. *N Engl J Med* 1992; **326:** 581-588.

Bensaid AM, Hall LO, Bezdek JC, Clarke LP. Fuzzy cluster validity in MR images. In: *Proceedings of SPIE* 1994; **2167:** 454-464.

Bergers E, Bot JC, De Groot CJ, Polman CH, Lycklama a Nijeholt GJ, Castelijns JA, van der Valk P, Barkhof F. Axonal damage in the spinal cord of MS patients occurs largely independent of T2 MRI lesions. *Neurology* 2002; **59:** 1766-1771.

Bitsch A, Schuchardt J, Bunkowski S, Kuhlmann T, Brück W. Acute axonal injury in multiple sclerosis. Correlation with demyelination and inflammation. *Brain* 2000; **123:** 1174-1183.

Bjartmar C, Kidd G, Mörk S, Rudick R, Trapp BD. Neurological disability correlates with spinal cord axonal loss and reduced N-acetyl aspartate in chronic multiple sclerosis patients. *Ann Neurol* 2000; **48:** 893-901.

Bjartmar C, Wujek JR, Trapp BD. Axonal loss in the pathology of MS: consequences for understanding the progressive phase of the disease. *J Neurol Sci* 2003; **206:** 165-171.

Blatter DD, Bigler ED, Gale SD, Gale SD, Johnson SC, Anderson CV, Burnett BM, Parker N, Kurth S, Hom SD. Quantitative volumetric analysis of brain MR: Normative database spanning 5 decades of life. *AJNR Am J Neuroradiol* 1995; **16:** 241-251.

Blinkenberg M, Rune K, Jensen CV, Ravnborg M, Kyllingsbæk S, Holm S, Paulson OB, Sørensen PS. Cortical cerebral metabolism correlates with MRI lesion load and cognitive dysfunction in MS. *Neurology* 2000; **54:** 558-564.

Bloch F. Nuclear induction. *Phys Rev* 1946; **70:** 460-474.

Bobowick AR, Kurtzke JF, Brody JA, Hrubec Z, Gillespie M. Twin study of multiple sclerosis: an epidemiologic inquiry. *Neurology* 1978: **28:** 978-987.

Bookstein FL. "Voxel-based morphometry" should not be used with imperfectly registered images. *Neuroimage* 2001; **14:** 1454-1462.

Bot JC, Barkhof F, Polman CH, Lycklama a Nijeholt GJ, de Groot V, Bergers E, Ader HJ, Castelijns JA. Spinal cord abnormalities in recently diagnosed MS patients: Added value of spinal MRI examination. *Neurology* 2004a; **62:** 226-233.

Bot JC, Blezer EL, Kamphorst W, Lycklama A Nijeholt GJ, Ader HJ, Castelijns JA, Ig KN, Bergers E, Ravid R, Polman C, Barkhof F. The spinal cord in multiple sclerosis: relationship of high-spatial-resolution quantitative MR imaging findings to histopathologic results. *Radiology* 2004b; **233:** 531-540.

Bozzali M, Cercignani M, Sormani MP, Comi G, Filippi M. Quantification of brain grey matter damage in different MS phenotypes by use of diffusion tensor MR imaging. *AJNR Am J Neuroradiol* 2002; **23:** 985-988.

Bradl M, Hohlfeld R. Molecular pathogenesis of neuroinflammation. *J Neurol Neurosurg Psychiatry* 2003; **74:** 1364-1370.

Brass SD, Narayanan S, Antel JP, Lapierre Y, Collins L, Arnold DL. Axonal damage in multiple sclerosis patients with high versus low expanded disability status scale score. *Can J Neurol Sci* 2004; **31:** 225-228.

Brex PA, O'Riordan JI, Miszkel KA, Moseley IF, Thompson AJ, Plant GT, Miller DH. Multisequence MRI in clinically isolated syndromes and the early development of MS. *Neurology* 1999; **53:** 1184-1190.

Brex PA, Leary SM, O'Riordan JI, Miszkiel KA, Plant GT, Thompson AJ, Miller DH. Measurement of spinal cord area in clinically isolated syndromes suggestive of multiple sclerosis. *J Neurol Neurosurg Psychiatry* 2001; **70:** 544-547.

Brex PA, Ciccarelli O, O'Riordan JI, Sailer M, Thompson AJ, Miller DH. A longitudinal study of abnormalities on MRI and disability from multiple sclerosis. *N Engl J Med* 2002; **346:** 156-164.

Brønnum-Hansen H, Koch-Henriksen N, Stenager E. Trends in survival and cause of death in Danish patients with multiple sclerosis. *Brain* 2004; **127:** 844-850.

Brooks DJ, Leenders KL, Head G, Marshall J, Legg NJ, Jones T. Studies on regional cerebral oxygen utilisation and cognitive function in multiple sclerosis. *J Neurol Neurosurg Psychiatry* 1984; **47:** 1182-1191.

Brück W, Bitsch A, Kolenda H, Brück Y, Stiefel M, Lassmann H. Inflammatory central nervous system demyelination: Correlation of Magnetic Resonance Imaging findings with lesion pathology. *Ann Neurol* 1997; **42**: 783-793.

Brück W, Kuhlmann T, Stadelmann C. Remyelination in multiple sclerosis. *J Neurol Sci* 2003; **206:** 181-185.

Caramia F, Pantano P, Di Legge S, Piatella MC, Lenzi D, Paolillo A, Nucciarelli W, Lenzi GL, Bozzao L, Pozzilli C. A longitudinal study of MR diffusion changes in normal appearing white matter of patients with early multiple sclerosis. *Magn Reson Imaging* 2002; **20:** 383-388.

Carswell R. *Pathological Anatomy: Illustrations of the Elementary Forms of Disease.* London: Orme, Brown, Green and Longman; 1838.

Cassol E, Ranjeva JP, Ibarrola D, Mékies C, Manelfe C, Clanet M, Berry I. Diffusion tensor imaging in multiple sclerosis: a tool for monitoring changes in normal-appearing white matter. *Mult Scler* 2004; **10:** 188-196.

Castriota Scanderbeg A, Tomaiuolo F, Sabatini U, Nocentini U, Grasso MG, Caltagirone C. Demyelinating plaques in relapsing-remitting and secondary-progressive multiple sclerosis: assessment with diffusion MR imaging. *AJNR Am J Neuroradiol* 2000; **21:** 862-868.

Cercignani M, Iannucci G, Rocca MA, Comi G, Horsfield MA, Filippi M. Pathological damage in MS assessed by diffusion-weighted and magnetization transfer MRI. *Neurology* 2000; **54:** 1139-1144.

Cercignani M, Inglese M, Pagani E, Comi G, Filippi M. Mean diffusivity and fractional anisotropy histograms in patients with multiple sclerosis. *AJNR Am J Neuroradiol* 2001a; **22:** 952-958.

Cercignani M, Bozzali M, Iannucci G, Comi G, Filippi M. Magnetisation transfer ratio and mean diffusivity of normal appearing white and grey matter from patients with multiple sclerosis. *J Neurol Neurosurg Psychiatry* 2001b; **70:** 311-317.

Charcot JM. Sclerose du cordons lateraux del la moelle epiniere chez une femme hysterique atteinte de contracture permaneste des quatres members. *L'Union Medicale* 1865; **25 :** 451-457, 467-472.

Charcot JM. Histologie de la sclerose en plaque. *Gazette Hopital (Paris)* 1868; **41:** 554-566.

Chard DT, Parker GJ, Griffin CM, Thompson AJ, Miller DH. The reproducibility and sensitivity of brain tissue volume measurements derived from an SPM-based segmentation methodology. *J Magn Reson Imaging* 2002a; **15:** 259-267.

Chard DT, Griffin CM, Parker GJM, Kapoor R, Thompson AJ, Miller DH. Brain atrophy in clinically early relapsing-remitting multiple sclerosis. *Brain* 2002b; **125:** 327-337.

Chard DT, Griffin CM, McLean MA, Kapeller P, Kapoor R, Thompson AJ, Miller DH. Brain metabolite changes in cortical grey and normal-appearing white matter in clinically early relapsing-remitting multiple sclerosis. *Brain* 2002c; **125:** 2342-2352.

Chard DT, Griffin CM, Rashid W, Davies GR, Altmann DR, Kapoor R, Barker GJ, Thompson AJ, Miller DH. Progressive grey matter atrophy in clinically early relapsing-remitting multiple sclerosis. *Mult Scler* 2004; **10:** 387-391.

Chilcott J, McCabe C, Tappenden P, O'Hagan A, Cooper NJ, Abrams K, Claxton K, Miller DH. Modelling the cost effectiveness of interferon beta and glatiramer acetate in the management of multiple sclerosis. Commentary: Evaluating disease modifying treatments in multiple sclerosis. *BMJ* 2003; **326:** 522.

Christiansen P, Gideon P, Thomsen C, Stubgaard M, Henriksen O, Larsson HB. Increased water self-diffusion in chronic plaques and in apparently normal white matter in patients with multiple sclerosis. *Acta Neurol Scand* 1993; **87:** 195-199.

Ciccarelli O, Werring DJ, Wheeler-Kingshott CAM, Barker GJ, Parker GJM, Thompson AJ, Miller DH. Investigation of MS normal-appearing brain using diffusion tensor MRI with clinical correlations. *Neurology* 2001; **56:** 926-933.

Ciccarelli O, Toosy AT, Parker GJ, Wheeler-Kingshott CA, Barker GJ, Miller DH, Thompson AJ. Diffusion tractography based group mapping of major white-matter pathways in the human brain. *Neurology* 2003; **19:** 1545-1555.

Cifelli A, Arridge M, Jezzard P, Esiri MM, Palace J, Matthews PM. Thalamic neurodegeneration in multiple sclerosis. *Ann Neurol* 2002; **52:** 650-653.

Cohen JA, Cutter GR, Fischer JS, Goodman AD, Heidenreich FR, Jak AJ, Kniker JE, Kooijmans MF, Lull JM, Sandrock AW, Simon JH, Simonian NA, Whitaker JN. Use of the multiple sclerosis functional composite as an outcome measure in a phase 3 clinical trial. *Arch Neurol* 2001; **58:** 961-967.

Coles AJ, Wing MG, Molyneux P, Paolillo A, Davie CM, Hale G, Miller D, Waldmann H, Compston A. Monoclonal antibody treatment exposes three mechanisms underlying the clinical course of multiple sclerosis. *Ann Neurol* 1999; **46:** 296-304.

Compston A. Genetic susceptibility to multiple sclerosis. In: Compston A, Ebers G, Lassmann H, McDonald WI, Matthews B, Wekerle H, eds. *McAlpine's multiple sclerosis, 3rd ed.* London: Churchill Livingstone; 1998: 101-144.

Compston A. The genetic epidemiology of multiple sclerosis. *Philos Trans R Soc Lond B Biol Sci* 1999; **354:** 1623-1634.

Compston A, Coles A. Multiple sclerosis. *Lancet* 2002 ; **359:** 1221-1231.

Compston A. The pathogenesis and basis for treatment in multiple sclerosis. *Clinical Neurology and Neurosurgery* 2004; **106:** 246-248.

Confavreux C, Vukusic S, Adeleine P. Early clinical predictors and progression of irreversible disability in multiple sclerosis: an amnesic process. *Brain* 2003; **126:** 770-782.

Cottrell DA, Kremenchutzky M, Rice GP, Hader W, Baskerville J, Ebers GC. The natural history of multiple sclerosis: a geographically based study. 5. The clinical features and natural history of primary progressive multiple sclerosis. *Brain* 1999; **122:** 625-639.

Coulon O, Hickman SJ, Parker GJ, Miller DH, Arridge SR. Quantification of spinal cord atrophy from magnetic resonance images via a B-spline active surface model. *Mag Reson Med* 2002; **47:** 1176-1185.

Cruveilhier J. *Anatomie pathologique du corps humain; descriptions avec figures lithographiees et coloriees; des diverses alterations morbides dont le corps humain est susceptible.* Paris : JB Baillière, 40 livraisons ; c1841.

Cutter GR, Baier ML, Rudick RA, Cookfair DL, Fischer JS, Petkau J, Syndulko K, Weinshenker BG, Antel JP, Confavreux C, Ellison GW, Lublin F, Miller AE, Rao SM, Reingold S, Thompson A, Willoughby E. Development of a multiple sclerosis functional composite as a clinical trial outcome measure. *Brain* 1999; **122:** 871-882.

Dalton CM, Brex PA, Miszkel KA, Hickman SJ, MacManus DG, Plant GT, Thompson AJ, Miller DH. Application of the new McDonald criteria to patients with clinically isolated syndromes suggestive of multiple sclerosis. *Ann Neurol* 2002a; **52:** 47-53.

Dalton CM, Brex PA, Jenkins R, Fox NC, Miszkiel KM, Crum WR, O'Riordan JI, Plant GT, Thompson AJ, Miller DH. Progressive ventricular enlargement in patients with clinically isolated syndromes is associated with the early development of multiple sclerosis. *J Neurol Neurosurg Psychiatry* 2002b; **73:** 141-147.

Davie CA, Barker GJ, Webb S, Tofts PS, Thompson AJ, Harding AE, McDonald WI, Miller DH. Persistent functional deficit in multiple sclerosis and autosomal dominant cerebellar ataxia is associated with axonal loss. *Brain* 1995; **188:** 1583-1592.

Davie CA, Barker GJ, Thompson AJ, Tofts PS, McDonald WI, Miller DH. 1H magnetic resonance spectroscopy of chronic cerebral white matter lesions and normal appearing white matter in multiple sclerosis. *J Neurol Neurosurg Psychiatry* 1997; **63:** 736-742.

Davies GR, Ramio-Torrenta L, Hadjiprocopis A, Chard DT, Griffin CM, Rashid W, Barker GJ, Kapoor R, Thompson AJ, Miller DH. Evidence for grey matter MTR abnormality in minimally disabled patients with early relapsing-remitting multiple sclerosis. *J Neurol Neurosurg Psychiatry* 2004; **75:** 998-1002.

Davies GR, Altmann DR, Hadjiprocopis A, Rashid W, Chard DT, Griffin CM, Tofts PS, Barker G, Kapoor R, Thompson AJ, Miller DH. Increasing normal-appearing grey and white matter MTR abnormality in early relapsing-remitting MS. *J Neurol* 2005; in press.

Dean G. Annual incidence, prevalence and mortality of MS in white South African-born and in white immigrants to South Africa. *BMJ* 1967; **2:** 724-730.

Dean G, Grimaldi G, Kelly R, Karheusen L. Multiple sclerosis on southern Europe. I. Prevalence in Sicily in 1975. *J Epidemiol Comm Health* 1979; **33:** 107-110.

Debruyne JC, Versijpt J, Van Laere KJ, De Vos F, Keppens J, Strijckmans K, Achten E, Slegers G, Dierckx RA, Korf J, De Reuck JL. PET visualization of microglia in multiple sclerosis patients using [11C]PK11195. *Eur J Neurol* 2003; **10:** 257-264.

DeLuca GC, Ebers GC, Esiri MM. Axonal loss in multiple sclerosis: a pathological survey of the corticospinal and sensory tracts. *Brain* 2004; **127:** 1009-1018.

De Stefano N, Matthews PM, Fu L, Narayanan S, Stanley J, Francis GS, Antel JP, Arnold DL. Axonal damage correlates with disability in patients with relapsing-remitting multiple sclerosis. Results of a longitudinal magnetic resonance spectroscopy study. *Brain* 1998; **121:** 1469-1477.

De Stefano N, Matthews PM, Filippi M, Agosta F, De Luca M, Bartolozzi ML, Guidi L, Ghezzi A, Montanari E, Cifelli A, Federico A, Smith SM. Evidence of early cortical atrophy in MS: relevance to white matter changes and disability. *Neurology* 2003; **60:** 1157-1162.

Detre JA, Leigh DS, Williams DS, Koretsky AP. Perfusion imaging. *Magn Reson Med* 1992; **23:** 37-45.

Dousset V, Grossman RI, Ramer KN, Schnall MD, Young LH, Gonzalez-Scarano F, Lavi E, Cohen JA. Experimental allergic encephalomyelitis and multiple sclerosis: lesion characterization with magnetization transfer imaging. *Radiology* 1992; **182:** 483-491.

Droogan AG, Clark CA, Werring DJ, Barker GJ, McDonald WI, Miller DH. Comparison of multiple sclerosis clinical subgroups using navigated spin echo diffusion-weighted imaging. *Magn Reson Imaging* 1999; **17:** 653-661.

Duda RO, Hart PE. *Pattern Classification and Scene Analysis*. London: John Wiley and Sons; 1973.

Ebers GC, Sadovnick AD. Epidemiology. In: Paty DW, Ebers GC, eds. *Multiple sclerosis*. Philadelphia: FA Davis; 1997: 5-28.

Edan G, Miller D, Clanet M, Confavreux C, Lyon-Caen O, Lubetzki C, Brochet B, Berry I, Rolland Y, Froment JC, Cabanis E, Iba-Zizen MT, Gandon JM, Lai HM, Moseley I, Sabouraud O. Therapeutic effect of mitoxantrone combined with methylprednisolone in multiple sclerosis: a randomised multicentre study of active disease using MRI and clinical criteria. *J Neurol Neurosurg Psychiatry* 1997; **62:** 112-118.

Edelman RR, Stewart B, Darby DG, Thangaraj BS, Nobre AC, Mesulam MM, Warach S. Qualitative mapping of cerebral blood flow and functional localization with echo-planar imaging and signal targeting with alternating radio frequency. *Radiology* 1994; **192:** 513-520.

Edwards SGM, Gong QY, Lui C, Zvartau ME, Jaspan T, Roberts N, Blumhardt LD. Infratentorial atrophy on magnetic resonance imaging and disability in multiple sclerosis. *Brain* 1999; **122:** 291-301.

Enzinger C, Ropele S, Smith S, Strasser-Fuchs S, Poltrum B, Schmidt H, Matthews PM. Fazekas F. Accelerated evolution of brain atrophy and "black holes" in MS patients with *APOE-*ϵ4. *Ann Neurol* 2004; **55:** 563-569.

Eriksson M, Andersen O, Runmarker B. Long term follow up of patients with clinically isolated syndromes, relapsing-remitting and secondary progressive multiple sclerosis. *Mult Scler* 2003; **9:** 260-274.

European Study Group on Interferon β-1b in secondary progressive MS. Placebo-controlled multicentre randomised trial of interferon β-1b in treatment of secondary progressive multiple sclerosis. *Lancet* 1998; **352:** 1491-1497.

Evangelou N, Esiri MM, Smith S, Palace J, Matthews PM. Quantitative pathological evidence for axonal loss in normal appearing white matter in multiple sclerosis. *Ann Neurol* 2000; **47:** 391-395.

Ferguson B, Matyszak MK, Esiri MM, Perry VH. Axonal damage in acute multiple sclerosis lesions. *Brain* 1997; **120:** 393-399.

Fieschi C, Gasperini C, Ristori G, Bastianello S, Girmenia F, Leuzzi V, Buttinelli C, Rasura M. Patients with clinically definite multiple sclerosis, white matter abnormalities on MRI and normal CSF: if not multiple sclerosis, what is it? *J Neurol Neurosurg Psychiatry* 1995; **58:** 255-256.

Filippi M, Paty DW, Kappos L, Barkhof F, Compston DA, Thompson AJ, Zhao GJ, Wiles CM, McDonald WI, Miller DH. Correlations between changes in disability and T2-weighted brain MRI activity in multiple sclerosis: a follow-up study. *Neurology* 1995; **45:** 255-260.

Filippi M, Campi A, Colombo B, Pereira C, Martinelli V, Baratti C, Comi G. A spinal cord MRI study of benign and secondary progressive multiple sclerosis. *J Neurol* 1996a; **243:** 502-505.

Filippi M, Yousry T, Campi A, Kandziora C, Colombo B, Voltz R, Martinelli V, Spuler S, Bressi S, Scotti G, Comi G. Comparison of triple dose versus standard dose gadolinium-DTPA for detection of MRI enhancing lesions in patients with MS. *Neurology* 1996b; **46:** 379-384.

Filippi M, Colombo B, Rovaris M, Pereira C, Martinelli V, Comi G. A longitudinal magnetic resonance imaging study of the cervical cord in multiple sclerosis. *J Neuroimaging* 1997; **7:** 78-80.

Filippi M, Gawne-Cain ML, Gasperini C, vanWaesberghe JH, Grimaud J, Barkhof F, Sormani MP, Miller DH. Effect of training and different measurement strategies on the reproducibility of brain MRI lesion load measurements in multiple sclerosis. *Neurology* 1998a; **50:** 238-244.

Filippi M, Mastronardo G, Bastianello S, Rocca MA, Rovaris M, Gasperini C, Pozilli C, Comi G. A longitudinal brain MRI study comparing the sensitivities of the conventional and a newer approach for detecting active lesions in multiple sclerosis. *J Neurol Sci* 1998b; **159:** 94-101.

Filippi M, Rocca MA, Rizzo G, Horsfield MA, Rovaris M, Minicucci L, Colombo B, Comi G. Magnetization transfer ratios in multiple sclerosis lesions enhancing after different doses of gadolinium. *Neurology* 1998c; **50:** 1289-1293.

Filippi M, Rovaris M, Capra R, Gasperini C, Yousry TA, Sormani MP, Prandini F, Horsfield MA, Martinelli V, Bastianello S, Kuhne I, Pozzilli C, Comi G. A multi-centre longitudinal study comparing the sensitivity of monthly MRI after standard and triple dose gadolinium-DTPA for monitoring disease activity in multiple sclerosis. Implications for phase II clinical trials. *Brain* 1998d; **121:** 2011-2020.

Filippi M, Horsfield MA, Ader HJ, Barkhof F, Bruzzi P, Evans A, Frank JA, Grossman RI, McFarland HF, Molyneux P, Paty DW, Simon J, Tofts PS, Wolinsky JS, Miller DH. Guidelines for using quantitative measures of brain magnetic resonance imaging abnormalities in monitoring the treatment of multiple sclerosis. *Ann Neurol* 1998e; **43:** 499-506.

Filippi M, Iannucci G, Tortorella C, Minicucci L, Horsfield MA, Colombo B, Sormani MP, Comi G. Comparison of MS clinical phenotypes using conventional and magnetization transfer MRI. *Neurology* 1999; **52:** 588-594.

Filippi M, Iannucci G, Cercignani M, Rocca MA, Pratesi A, Comi G. A quantitative study of water diffusion in multiple sclerosis lesions and normal-appearing white matter using echo-planar imaging. *Arch Neurol* 2000a; **57:** 1017-1021.

Filippi M. Enhanced magnetic resonance imaging in multiple sclerosis. *Mult Scler* 2000b; **6:** 320-326.

Filippi M, Inglese M, Rovaris M, Sormani MP, Horsfield P, Iannucci PG, Colombo B, Comi G. Magnetization transfer imaging to monitor the evolution of MS: a 1-year follow-up study. *Neurology* 2000c; **55:** 940-946.

Filippi M, Tortorella C, Rovaris M, Bozzali M, Possa F, Sormani MP, Iannucci G, Comi G. Changes in the normal appearing brain tissue and cognitive impairment in multiple sclerosis. *J Neurol Neurosurg Psychiatry* 2000d; **68:** 157-161.

Filippi M. *In-vivo* tissue characterization of multiple sclerosis and other white matter diseases using magnetic resonance based techniques. *J Neurol* 2001a; **248:** 1019-1029.

Filippi M, Cercignani M, Inglese M, Horsfield MA, Comi G. Diffusion tensor magnetic resonance imaging in multiple sclerosis. *Neurology* 2001b; **56:** 304-311.

Filippi M, Rovaris M, Inglese M, Barkhof, De Stefano N, Smith S, Comi G, for the ETOMS Study Group. Interferon beta-1a for brain tissue loss in patients at presentation with syndromes suggestive of multiple sclerosis: a randomised, double-blind, placebo-controlled trial. *Lancet* 2004; **364:** 1489-1496.

Firbank MJ, Coulthard A, Harrison RM, Williams ED. Partial volume effects in MRI studies of multiple sclerosis. *Magn Reson Imaging* 1999; **17:** 593-601.

Fisher E, Rudick RA, Simon JH, Cutter G, Baier M, Lee JC, Miller D, Weinstock-Guttman B, Mass MK, Dougherty DS, Simonian NA. Eight year follow-up study of brain atrophy in patients with MS. *Neurology* 2002; **59:** 1412-1420.

Folkman J. Angiogenesis in cancer, vascular, rheumatoid and other disease. *Nat Med* 1995; **1:** 27-31.

Fox NC, Jenkins R, Leary SM, Stevenson VL, Losseff NA, Crum WR, Harvey RJ, Rossor MN, Miller DH, Thompson AJ. Progressive cerebral atrophy in MS: a serial study usjng registered, volumetric MRI. *Neurology* 2000; **54:** 807-812.

Franklin RJM. Why does remyelination fail in multiple sclerosis? *Nature* 2002; **3:** 705-714.

Freeman JA, Langdon DW, Hobart JC, Thompson AJ. The impact of in-patient rehabilitation on progressive multiple sclerosis. *Ann Neurol* 1997; **42:** 236-244.

Freeman JA, Langdon DW, Hobart JC, Thompson AJ. Inpatient rehabilitation in multiple sclerosis: do the benefits carry over into the community? *Neurology* 1999; **52:** 50-56.

Friston KJ, Holmes AP, Worsley KJ, Poline JB, Frith CD, Frackowiak RSJ. Statistical parametric maps in functional imaging: A general linear approach. *Hum Brain Mapp* 1995; **2:** 189-210.

Fu L, Matthews PM, De Stefano N, Worsley KJ, Narayanan S, Francis GS, Antel JP, Wolfson C, Arnold DL. Imaging axonal damage of normal-appearing white matter in multiple sclerosis. *Brain* 1998; **121:** 103-113.

Ganter P, Prince C, Esiri MM. Spinal cord axonal loss in multiple sclerosis: a *post-mortem* study. *Neuropathology and Applied Neurobiology* 1999; **25:** 459-467.

Gasperini C, Paolillo A, Giugni E, Galgani S, Bagnato F, Mainero C, Onesti E, Bastianello S, Pozzilli C. MRI brain volume changes in relapsing remitting multiple sclerosis patients treated with interferon β-1a. *Mult Scler* 2002; **8:** 119-123.

Gass A, Barker GJ, Kidd D, Thorpe JW, MacManus D, Brennan A, Tofts PS, Thompson AJ, McDonald WI, Miller DH. Correlation of magnetization transfer ratio with clinical disability in multiple sclerosis. *Ann Neurol* 1994; **36:** 62-67.

Ge Y, Grossman RI, Udupa JK, Wei L, Mannon LJ, Polansky M, Kolson DL. Brain atrophy in relapsing-remitting multiple sclerosis and secondary progressive multiple sclerosis: longitudinal quantitative analysis. *Radiology* 2000; **214:** 665-670.

Ge Y, Grossman RI, Udupa JK, Babb JS, Kolson DL, McGowan JC. Magnetization transfer ratio histogram analysis of gray matter in relapsing-remitting multiple sclerosis. *AJNR Am J Neuroradiol* 2001; **22:** 470-475.

Giovannoni G, Miller DH, Losseff NA, Sailer M, Lewellyn-Smith N, Thompson AJ, Thompson EJ. Serum inflammatory markers and clinical/MRI markers of disease progression in multiple sclerosis. *J Neurol* 2001; **248:** 487-495.

Goodin DS, Ebers GC, Johnson KP, Rodriguez M, Sibley WA, Wolinsky JS. The relationship of MS to physical trauma and psychological stress. *Neurology* 1999; **52:** 1737-1745.

Goldstein H. *Multilevel statistical models*. London: Arnold; 1995.

Granieri E, Casetta I, Tola MR. Multiple sclerosis: does epidemiology contribute to providing etiological clues? *J Neurol Sci* 1993; **115 (suppl):** 16-23.

Griffin CM, Chard DT, Ciccarelli O, Kapoor B, Barker GJ, Thompson AJ, Miller DH. Diffusion tensor imaging in early relapsing-remitting multiple sclerosis. *Mult Scler* 2001; **7:** 290-297.

Grossmann RI, Gonzalez-Scarano F, Atlas SW, Galetta S, Silberberg DH. Multiple Sclerosis: Gadolinium enhancement in MR imaging. *Radiology* 1986; **161**: 721-725.

Guo AC, Jewells VL, Provenzale JM. Analysis of normal-appearing white matter in multiple sclerosis: comparison of diffusion tensor MR imaging and magnetization transfer imaging. *AJNR Am J Neuroradiol* 2001; **22:** 1893-1900.

Hadjiprocopis A, Rashid W, Tofts PS. Segmentation of T2-weighted MRI using an ensemble of neural network and clustering experts. *Proc Intl Soc Mag Reson Med* 2003; **11:** 3504.

Hammond SR, McLeod JG, Millingen KS, Stewart-Wynne EG, English D, Holland JT, McCall MG. The epidemiology of multiple sclerosis in three Australian cities: Perth, Newcastle and Hobart. *Brain* 1988a; **111:** 1-25.

Hammond SR, English D, de Wytt C, Maxwell IC, Millingen KS, Stewart-Wynne EG, McLeod JG, McCall MG. The clinical profile of MS in Australia: a comparison between medium- and high-frequency prevalence zones. *Neurology* 1988b; **38:** 980-6.

Hartung H-P, Gonsette R, Konig N, Kwiecinski H, Guseo A, Morrissey SP, Krapf H, Zwingers T; Mitoxantrone in Multiple Sclerosis Study Group (MIMS). Mitoxantrone in progressive multiple sclerosis: a placebo-controlled, double-blind, randomised, multicentre trial. *Lancet* 2002; **360:** 2018-2025.

Haselhorst R, Kappos L, Bilecen D, Scheffler K, Möri D, Radü EW, Seelig J. Dynamic susceptibility contrast MR imaging of plaque development in multiple sclerosis: Application of an extended blood-brain barrier leakage correction. *J. Magn. Reson. Imaging* 2000; **11:** 495-505.

Hashemi RH, Bradley WG jr. *MRI: the basics.* Philadelphia: Lippincott Williams and Wilkins; 1997.

Hayes CE, Cantorna MT, DeLuca HF. Vitamin D and multiple sclerosis. *Proc Soc Exp Biol Med.* 1997; **216:** 21-7.

Heltberg A, Holm NV. Concordance in twins and recurrence in sibships in multiple sclerosis. *Lancet* 1982; **1:** 1068. Letter.

Hickman SJ, Coulon O, Parker GJ, Stevenson VL, Chard DT, Arridge SR, Thompson AJ, Miller DH. Application of a B-spline active surface technique to the measurement of cervical cord volume in multiple sclerosis from three-dimensional MR images. *J Magn Reson Imaging* 2003; **18:** 368-371.

Hillert J, Masterman T. The genetics of multiple sclerosis. In: Cook SD, ed. *Handbook of multiple sclerosis, 3rd ed.* New York: Marcel Dekker; 2001: 33-65.

Hohlfeld R, Kerschensteiner M, Stadelmann C, Lassmann H, Wekerle H. The neuroprotective effect of inflammation: implications for the therapy of multiple sclerosis. *J of Neuroimmunolgy* 2000; **107:** 161-166.

Hohol MJ, Guttmann CR, Orav J, Mackin GA, Kikinis R, Khoury SJ, Jolesz FA, Weiner HL. Serial neuropsychological assessment and magnetic resonance imaging analysis in multiple sclerosis. *Arch Neurol* 1997; **54:** 1018-25.

Homes J, Madgwick T, Bates D. The cost of multiple sclerosis. *Br J Med Econ* 1995; **18:** 181-193.

Horsfield MA, Lai M, Webb SL, Barker GJ, Tofts PS, Turner R, Rudge P, Miller DH. Apparent diffusion coefficients in benign and secondary progressive multiple sclerosis by nuclear magnetic resonance. *Magn Reson Med* 1996; **36:** 393-400.

IFNB Multiple Sclerosis Study Group. Interferon beta-1b is effective in relapsing-remitting multiple sclerosis. I. Clinical results of a multicenter, randomized, double-blind, placebo-controlled trial. *Neurology* 1993; **43:** 655-661.

IFNB Multiple Sclerosis Study Group, and the University of British Columbia MS/MRI Analysis Group. Interferon beta-1b in the treatment of multiple sclerosis: final outcome of the randomized controlled trial. *Neurology* 1995; **45:** 1277-1285.

Ingle GT, Stevenson VL, Miller DH, Thompson AJ. Primary progressive multiple sclerosis: a 5-year clinical and MR study. *Brain* 2003; **126:** 2528-2536.

Jackson JR, Seed MP, Kircher CH, Willoughby DA, Winkler JD. The codependence of angiogenesis and chronic inflammation. *FASEB J* 1997; **11:** 457-465.

Jacobs LD, Cookfair DL, Rudick RA, Herndon RM, Richert JR, Salazar AM, Fischer JS, Goodkin DE, Granger CV, Simon JH, Alam JJ, Bartoszak DM, Bourdette DN, Braiman J, Brownscheidle CM, Coats ME, Cohan SL, Dougherty DS, Kinkel KP, Mass MK, Munschauer FE 3rd, Priore RL, Pullicino PM, Scherokman BJ, Whitham RH. Intramuscular interferon beta-1a for disease progression in relapsing multiple sclerosis. The Multiple Sclerosis Collaborative Research Group (MSCRG). *Ann Neurol* 1996; **40:** 285-294.

Jensen CV, Rostrup E, Blinkenberg M, Larrson HBW, Henriksen O. Relative regional cerebral blood-volume in MS. *In Proc SMR* 1995; **2:**1297.

Johnson KP, Brooks BR, Cohen JA, Ford CC, Goldstein J, Lisak RP, Myers LW, Panitch HS, Rose JW, Schiffer RB. Copolymer 1 reduces relapse rate and improves disability in relapsing-remitting multiple sclerosis: results of a phase III multicenter, double-blind placebo-controlled trial. The Copolymer 1 Multiple Sclerosis Study Group. *Neurology* 1995; **45:** 1268-1276.

Jones CK, Riddehough A, Li DKB, Zhao GJ, Paty DW. MRI cerebral atrophy in relapsing-remitting MS: results of the PRISMS trial. *Neurology* 2001; **56 (suppl 3):** A379.

Jones DK, Williams SC, Gasston D, Horsfield MA, Simmons A, Howard R. Isotropic resolution diffusion tensor imaging with whole brain acquisition in a clinically acceptable time. *Hum Brain Mapp* 2002; **15:** 216-230.

Jones DK, Symms MR, Cercignani M, Howard RJ. The effects of the smoothing filter size on VBM analyses of DT-MRI data. *Neuroimage* 2005; in press.

Kalkers NF, Bergers E, Castelijns JA, van Walderveen MA, Bot JC, Ader HJ, Polman CH, Barkhof F. Optimizing the association between disability and biological markers in MS. *Neurology* 2001a; **57:** 1253-1257.

Kalkers NF, Hintzen RQ, van Waesberghe JH, Lazeron RH, van Schijndel RA, Ader HJ, Polman CH, Barkhof F. Magnetization transfer histogram parameters reflect all dimensions of MS pathology, including atrophy. *J Neurol Sci* 2001b; **184:** 155-162.

Kameyama T, Hashizume Y, Ando T, Takahashi A. Morphometry of the normal cadaveric spinal cord. *Spine* 1994; **19:** 2077-2081.

Kapoor R. Multiple sclerosis and related conditions. In: Fowler TJ, Scadding JW, eds. *Clinical Neurology, 3rd ed.* London: Arnold; 2003: 413-426.

Kappos L, Moeri D, Radue EW, Schoetzau A, Schweikert K, Barkhof F, Miller D, Guttmann CRG, Weiner HL, Gasperini C, Filippi M. Predictive value of gadolinium-enhanced magnetic resonance imaging for relapse rate and changes in disability or impairment in multiple sclerosis: a meta-analysis. *Lancet* 1999; **353:** 964-969.

Kappos L, Duda P. The janus face of CNS-directed autoimmune response: a therapeutic challenge. *Brain* 2002; **125:** 2379-2380.

Katz D, Taubenberger JK, Cannella B, McFarlin DE, Raine CS, McFarland HF. Correlation between Magnetic Resonance Imaging findings and lesion development in chronic, active multiple sclerosis. *Ann Neurol* 1993; **34**: 661-669.

Keir SL, Wardlaw JM. Systematic review of diffusion and perfusion imaging in acute ischaemic stroke. *Stroke* 2002; **31:** 2723-2731.

Khoury SJ, Guttmann CRG, Orav EJ, Hohol MJ, Ahn SS, Hsu L, Kikinis R, Mackin GA, Jolesz FA, Weiner HL. Longitudinal MRI in multiple sclerosis: Correlation between disability and lesion burden. *Neurology* 1994; **44:** 2120-2124.

Kidd D, Thorpe JW, Thompson AJ, Kendall BE, Moseley IF, MacManus DG, McDonald WI, Miller DH. Spinal cord MRI using multi-array coils and fast spin echo, II: findings in multiple sclerosis. *Neurology* 1993; **43:** 2632-2637.

Kidd D, Barkhof F, McConnell R, Algra PR, Allen IV, Revesz T. Cortical lesions in multiple sclerosis. *Brain* 1999; **122:** 17-26.

Kim SG. Quantification of relative blood flow change by flow-sensitive alternating inversion recovery (FAIR) technique: application to functional mapping. *Magn Reson Med* 1995; **34:** 293-301.

Kinnunen E, Juntunen J, Ketonen L, Koskimies S, Konttinen YT, Salmi T, Koskenvuo M, Kaprio J. Genetic susceptibility to multiple sclerosis: a co-twin study of a nationwide series. *Arch Neurol* 1988; **45:** 1108-1111.

Kirk SL, Karlik SJ. VEGF and vascular changes in chronic neuroinflammation. *J Autoimmun* 2003; **21:** 353-363.

Kirk S, Frank JA, Karlik S. Angiogenesis in multiple sclerosis: is it good, bad or an epiphenomenon? *J Neurol Sci* 2004; **217:** 125-130.

Kirkpatrick S, Gelatt Jr CD, Vecchi MP. Optimization by simulated annealing. *Science* 1983; **220:** 671-680.

Koudriavtseva T, Thompson AJ, Fiorelli M, Gasperini C, Bastianello S, Bozzao A, Paolillo A, Pisani A, Galgani S, Pozzilli C. Gadolinium enhanced MRI predicts clinical and MRI disease activity in relapsing-remitting multiple sclerosis. *J Neurol Neurosurg Psychiatry* 1997; **62:** 285-287.

Kremenchutzky M, Cottrell D, Rice G, Hader W, Baskerville J, Koopman W, Ebers GC. The natural history of multiple sclerosis: a geographically based study. 7. Progressive-relapsing and relapsing-progressive multiple sclerosis: a re-evaluation. *Brain* 1999; **122:** 1941-1950.

Kuhlmann T, Lingfeld G, Bitsch A, Schuchardt J, Brück W. Acute axonal damage in multiple sclerosis is most extensive in early disease stages and decreases over time. *Brain* 2002; **125:** 2202-2212.

Kuroiwa Y, Shibasaki H, Ikeda M. Prevalence of multiple sclerosis and its north-south gradient in Japan. *Neuroepidemiology* 1983; **2:** 62-69.

Kurtzke JF. A new scale for evaluating disability in multiple sclerosis. *Neurology* 1955; **5:** 580-583.

Kurtzke JF. A reassessment of the distribution of the distribution of multiple sclerosis: parts I and II. *Acta Neurol Scand* 1975; **51:** 110-157.

Kurtzke JF, Beebe GW, Norman JE. Epidemiology of multiple sclerosis in US veterans. I. Race, sex and geographic distribution. *Neurology* 1979; **29:** 1228-1235.

Kurtzke JF. Rating neurologic impairment in multiple sclerosis: An expanded disability status scale (EDSS). *Neurology* 1983; **33:** 1444-1452.

Kwon EE, Prineas JW. Blood-brain barrier abnormalities in longstanding multiple sclerosis lesions. An immunohistochemical study. *J Neuropathol Exp Neurol* 1994; **53:** 625-636.

Kwong KK, Belliveau JW, Chesler DA, Goldberg IE, Weisskoff RM, Poncelet BP, Kennedy DN, Hoppel BE, Cohen MS, Turner R, Cheng HM, Brady TJ, Rosen BR. Dynamic resonance imaging of human brain activity during primary sensory stimulation. *Proc Natl Acad Sci USA* 1992; **89:** 5675-5679.

Lai M, Hodgson T, Gawne-Cain M, Webb S, MacManus D, McDonald W, Thompson A, Miller D. A preliminary study into the sensitivity of disease activity detection by serial weekly magnetic resonance imaging in multiple sclerosis. *J Neurol Neurosurg Psychiatry* 1996; **60:** 339-341.

Larsson HBW, Thomsen C, Frederiksen J, Stubgaard M, Henriksen O. In vivo magnetic resonance diffusion measurement in the brain of patients with multiple sclerosis. *Magn Reson Imaging* 1992; **10:** 7-12.

Lassmann H. Neuropathology in multiple sclerosis: new concepts. *Mult Scler* 1998a; **4:** 93-98.

Lassman H. Pathology of multiple sclerosis. In: Compston A, Ebers G, Lassman H, McDonald WI, Matthews B, Wekerle H, eds. *McAlpine's multiple sclerosis, 3rd ed.* London: Churchill Livingstone; 1998b: 323-357.

Lassmann H. Hypoxia-like tissue injury as a component of multiple sclerosis lesions. *J Neurol Sci* 2003a; **206:** 187-191.

Lassmann H. Axonal injury in multiple sclerosis. *J Neurol Neurosurg Psychiatry* 2003b; **74:** 695-697.

Lassmann H. Recent neuropathological findings in MS- implications for diagnosis and therapy. *J Neurol* 2004; **251 (suppl 4):** IV/2-IV/5.

Lauer K. Diet and multiple sclerosis. *Neurology* 1997; **492 (suppl 2):** S55-61.

Law M, Saindane AM, Ge Y, Babb JS, Johnson G, Mannon LJ, Herbert J, Grossman RI. Microvascular abnormality in relapsing-remitting multiple sclerosis: perfusion MR imaging findings in normal-appearing white matter. *Radiology* 2004; **231:** 645-652.

Le Bihan, Breton E, Lallemand D, Grenier P, Cabanis E, Laval-Jeantet M. MR imaging of intravoxel incoherent motions: application to diffusion and perfusion in neurologic disorders. *Radiology* 1986; **161:** 401-407.

Le Bihan D, Breton E, Lallemand D, Aubin MI, Vignaud J, Laval-Jeantet M. Separation of diffusion and perfusion in intravoxel incoherent motion MR imaging. *Radiology* 1988; **168:** 497-505.

Leary SM, Davie CA, Parker GJ, Stevenson VL, Wang L, Barker GJ, Miller DH, Thompson AJ. 1H magnetic resonance spectroscopy of normal appearing white matter in primary progressive multiple sclerosis. *J Neurol* 1999; **246:** 1023-1026.

Leenders KL, Perani D, Lammertsma AA, Heather JD, Buckingham P, Healy MJ, Gibbs JM, Wise RJ, Hatazawa J, Herold S. Cerebral blood flow, blood volume and oxygen utilization. Normal values and effect of age. *Brain* 1990; **113:** 27-47.

Leist TP, Gobbini MI, Frank JA, McFarland HF. Enhancing magnetic resonance imaging lesions and cerebral atrophy in patients with relapsing multiple sclerosis. *Arch Neurol* 2001; **58:** 57-60.

Li DK, Paty DW. Magnetic resonance imaging results of the PRISMS trial: a randomised, double-blind, placebo-controlled study of interferon-beta 1a in relapsing-remitting multiple sclerosis. *Ann Neurol* 1999; **46:** 197-206.

Lin X, Tench CR, Turner B, Blumhardt LD, Constantinescu CS. Spinal cord atrophy and disability in multiple sclerosis over four years: application of a reproducible automated technique in monitoring disease progression in a cohort of the interferon β-1a (Rebif) treatment trial. *J Neurol Neurosurg Psychiatry* 2003a; **74:** 1090-1094.

Lin X, Blumhardt LD, Constantinescu CS. The relationship of brain and cervical cord volume to disability in clinical subtypes of multiple sclerosis: a three-dimensional MRI study. *Acta Neurol Scand* 2003b; **108:** 401-406.

Lin X, Tench CR, Evangelou N, Jaspan T, Constantinesu CS. Measurement of spinal cord atrophy in multiple sclerosis. *J Neuroimaging* 2004; **14:** 20S-26S.

Liu C, Edwards S, Gong Q, Roberts N, Blumhardt LD. Three dimensional MRI estimates of brain and spinal cord atrophy in multiple sclerosis. *J Neurol Neurosurg Psychiatry* 1999; **66:** 323-330.

Lojkowska W, Ryglewicz D, Jedrezejczak T, Sienkiewicz-Jarosz H, Minc S, Jakubowska T, Kozlowicz-Gudzinska I. SPECT as a diagnostic test in the investigation of dementia. *J Neurol Sci* 2002; **203-204:** 215-219.

Losseff NA, Webb SL, O'Riordan JI, Page R, Wang L, Barker GJ, Tofts PS, McDonald WI, Miller DH, Thompson AJ. Spinal cord atrophy and disability in multiple sclerosis: a new reproducible and sensitive MRI method with potential to monitor disease progression. *Brain* 1996a; **119:** 701-708.

Losseff NA, Wang L, Lai HM, Yoo DS, Gwawne-Cain ML, McDonald WI, Miller DH, Thompson AJ. Progressive cerebral atrophy in multiple sclerosis. A serial study. *Brain* 1996b; **119:** 2009-2019.

Losseff NA, Miller DH, Kidd D, Thompson AJ. The predictive value of gadolinium enhancement for long term disability in relapsing-remitting multiple sclerosis – preliminary results. *Mult Scler* 2001; **7:** 23-25.

Lovas G, Szilagyi N, Majtenyi K, Palkovits M, Komoly S. Axonal changes in chronic demyelinated cervical spinal cord plaques. *Brain* 2000; **123:** 308-317.

Lublin FD, Reingold SC. Defining the clinical course of multiple sclerosis: Results of an international survey. *Neurology* 1996; **46:** 907-911.

Lublin FD, Baier M, Cutter G. Effect of relapses on development of residual deficit in multiple sclerosis. *Neurology* 2003; **61:** 1528-1532.

Lucchinetti CF, Brück W, Rodriguez M, Lassmann H. Distinct patterns of multiple sclerosis indicates heterogeneity of pathogenesis. *Brain Pathol* 1996; **6:** 259-261.

Lucchinetti C, Brück W, Parisi J, Scheithauer B, Rodriguez M, Lassmann H. Heterogeneity of multiple sclerosis lesions: Implications for the pathogenesis of demyelination. *Ann Neurol* 2000; **47:** 707-717.

Lucchinetti CF. The MS Lesion Project: merging of minds and matter. *Mult Scler* 2003; **9 (Suppl 1):** 47.

Lucchinetti C, Brück W. The pathology of primary progressive multiple sclerosis. *Mult Scler* 2004; **10:** S23-S30.

Lycke J, Wikkelsö C, Bergh A, Jacobsson L, Andersen O. Regional cerebral blood flow in Multiple sclerosis measured by single photon emission tomography with technetium-99m hexamethyl-propyleneamine oxime. *Eur Neurol* 1993; **33:** 163-167.

Lycklama à Nijeholt GJ, Barkhof F, Scheltens P, Castelijns JA, Adèr H, van Waesberghe JH, Polman C, Jongen SJH, Valk J. MR of the spinal cord in multiple sclerosis: relation to clinical subtype and disability. *AJNR Am J Neuroradiol* 1997; **18:** 1041-1048.

Lycklama à Nijeholt GJ, van Walderveen MAA, Castelijns JA, van Waesberghe JHTM, Polman C, Scheltens P, Rosier PFWM, Jongen PJH, Barkhof F. Brain and spinal cord abnormalities in multiple sclerosis. Correlations between MRI parameters, clinical subtypes and symptoms. *Brain* 1998; **121:** 687-697.

Lycklama à Nijeholt GJ, Uitdehaag BM, Bergers E, Castelijns JA, Polman CH, Barkhof F. Spinal cord magnetic resonance imaging in suspected multiple sclerosis. *Eur Radiol* 2000; **10:** 368-376.

Lycklama à Nijeholt GJ, Bergers E, Kamphorst W, Bot J, Nicolay K, Castelijns JA, van Waesberghe JH, Ravid R, Polman CH, Barkhof F. Post-mortem high-resolution MRI of the spinal cord in multiple sclerosis. A correlative study with conventional MRI, histopathology and clinical phenotype. *Brain* 2001; **124:** 154-166.

Lycklama à Nijeholt G, Barkhof F. Differences between subgroups of MS: MRI findings and correlation with histopathology. *J Neurol Sci* 2003; **206:** 173-174.

Lycklama à Nijeholt G, Thompson A, Filippi M, Miller D, Polman C, Fazekas F, Barkhof F. Spinal-cord MRI in multiple sclerosis. *Lancet Neurol* 2003; **2:** 555-562.

Maggs FG, Palace J. The pathogenesis of multiple sclerosis: is it really a primary inflammatory process? *Mult Scler* 2004; **10:** 326-329.

Maldjian JA, Grossman RI. Future applications of DWI in MS. *J Neurol Sci* 2001; **186 (suppl):** 55-57.

Mansfield P, Pykett IL. Biological and medical imaging by NMR. *J Magn Reson* 1978; **29:** 355.

Martino G, Adorini L, Rieckmann P, Hillert J, Kallmann B, Comi G, Filippi M. Inflammation in multiple sclerosis: the good, the bad, and the complex. *Lancet Neurology* 2002; **1:** 499-509.

Martyn CN. Infection in childhood and neurological diseases in adult life. *Br Med Bull.* 1997; **53:** 24-39.

Masulli F, Schenone A. A fuzzy clustering based segmentation system as support to diagnosis in medical imaging. *Artificial Intelligence in Medicine* 1999; **16:** 129-147.

Matthew E, Anderson P, Casson RE, Herscovitch P, Pettigrew K, Cohen R, King C, Johanson CE, Paul SM. Reproducibility of resting cerebral blood flow measurements with $H_2{}^{15}O$ positron emission tomography in humans. *J Cereb Blood Flow Metab* 1993; **13:** 748-754.

Matthews PM, Pioro E, Narayanan S, De Stefano N, Fu L, Francis G, Antel J, Wolfson C, Arnold DL. Assessment of lesion pathology in multiple sclerosis using quantitative MRI morphometry and magnetic resonance spectroscopy. *Brain* 1996; **119;** 715-722.

Matthews PM. Primary progressive multiple sclerosis takes centre stage. *J Neurol Neurosurg Psychiatry* 2004; **75:** 1232-1233.

McAlpine D, Compston ND, Lumsden CE. *Multiple sclerosis, 1st ed.* Edinburgh : Livingstone; 1955.

McDonald WI, Compston A, Edan G, Goodkin D, Hartung HP, Lublin FD, McFarland HF, Paty DW, Polman CH, Reingold SC, Sandberg-Wollheim M, Sibley W, Thompson A, van den Noort S, Weinshenker BY, Wolinsky JS. Recommended diagnostic criteria for multiple sclerosis: guidelines from the International Panel on the diagnosis of multiple sclerosis. *Ann Neurol* 2001; **50:** 121-127.

McFarland HF, Frank JA, Albert PS, Smith ME, Martin R, Harris JO, et al. Using gadolinium-enhanced magnetic resonance imaging lesions to monitor disease activity in multiple sclerosis. *Ann Neurol* 1992; **32**: 758-766.

McLeod JG, Hammond SR, Hallpike JF. Epidemiology of multiple sclerosis in Australia. With NSW and SA results. *Med J Aust* 1994; **1603:** 117-122.

Millefiorini E, Gasperini C, Pozzilli C, D'Andrea F, Bastianello S, Trojano M, Morino S, Morra VB, Bozzao A, Calo A, Bernini ML, Gambi D, Prencipe M. Randomized placebo-controlled trial of mitoxantrone in relapsing-remitting multiple sclerosis: 24-month clinical and MRI outcome. *J Neurol* 1997; **244:** 153-159.

Miller AE. Clinical features. In: Cook SD, ed. *Handbook of multiple sclerosis, 3rd ed.* New York: Marcel Dekker; 2001: 231-232.

Miller DH, Rudge P, Johnson G, Kendall BE, MacManus DG, Moseley IF, et al. Serial gadolinium enhanced magnetic resonance imaging in multiple sclerosis. *Brain* 1988; **111**: 927-939.

Miller DH, Johnson G, Tofts PS, MacManus D, McDonald WI. Precise relaxation time measurements of normal-appearing white matter in inflammatory central nervous system disease. *Magn Reson Med* 1989; **11:** 331-336.

Miller DH, Barkhof F, Berry I., Kappos L, Scotti G, Thompson AJ. Magnetic resonance imaging in monitoring the treatment of multiple sclerosis: concerted action guidelines. *J Neurol Neurosurg Psychiatry* 1991; **54**: 683-688.

Miller DH, Grossman RI, Reingold SC, McFarland HF. The role of magnetic resonance techniques in understanding and managing multiple sclerosis. *Brain* 1998; **121:** 3-24.

Miller DH, Barkof F, Frank JA, Parker GJ, Thompson AJ. Measurement of atrophy in multiple sclerosis: pathological basis, methodological aspects and clinical relevance. *Brain* 2002; **125:** 1676-1695.

Miller DH, Khan OA, Sheremata WA, Blumhardt LD, Rice GP, Willmer-Hulme AJ, Dalton CM, Miszkiel KA, O'Connor PW; International Natalizumab Multiple Sclerosis Trial Group. *N Engl J Med* 2003; **348:** 15-23.

Miller DH, Filippi M, Fazekas F, Frederiksen JL, Matthews PM, Montalban X, Polman CH. Role of magnetic resonance imaging within diagnostic criteria for multiple sclerosis. *Ann Neurol* 2004a; **56:** 273-278.

Miller DH. Biomarkers and surrogate outcomes in neurodegenerative disease: lessons from multiple sclerosis. *NeuroRx* 2004b; **1:** 284-294.

Milligan NM, Newcombe R, Compston DA. A double-blind controlled trial of high dose methylprednisolone in patients with multiple sclerosis: 1. Clinical effects. *J Neurol Neurosurg Psychiatry* 1987; **50:** 511-516.

Minagar A, Alexander JS. Blood brain barrier disruption in multiple sclerosis. *Mult Scler* 2003; **9:** 540-549.

Minagar A, Toledo EG, Alexander JS, Kelley RE. Pathogenesis of brain and spinal cord atrophy in multiple sclerosis. *J Neuroimaging* 2004;**14(Suppl):**5S-10S.

Molyneux PD, Filippi M, Barkhof F, Gasperini C, Yousry TA, Truyen L, Lai HM, Rocca MA, Moseley IF, Miller DH. Correlations between monthly enhanced MRI lesion rate and changes in T2 lesion volume in multiple sclerosis. *Ann Neurol* 1998; **43:** 332-339.

Molyneux PD, Kappos L, Polman C, Pozzilli C, Barkhof F, Filippi M, Yousry T, Hahn D, Wagner K, Ghazi M, Beckmann K, Dahlke F, Losseff N, Barker GJ, Thompson AJ, Miller DH. The effect of interferon beta-1b treatment on MRI measures of cerebral atrophy in secondary progressive multiple sclerosis. European Study Group on Interferon beta-1b in secondary progressive multiple sclerosis. *Brain.* 2000; **123:** 2256-63.

Morgen K, Jeffries NO, Stone R, Martin R, Richert ND, Frank JA, McFarland. Ring-enhancement in multiple sclerosis: marker of disease severity. *Mult Scler* 2001; **7:** 167-171.

Mumford CJ, Wood NW, Kellar-Wood H, Thorpe JW, Miller DH, Compston DAS. The British Isles survey of multiple sclerosis in twins. *Neurology* 1994; **44:** 11-15.

Noseworthy JH, Lucchinetti C, Rodriguez M, Weinshenker BG. Multiple sclerosis. *N Engl J Med* 2000; **343:** 938-952.

Nusbaum AO, Tang CY, Wei TC, Buchsbaum MS, Atlas SW. Whole brain diffusion MR histograms differ between MS subtypes. *Neurology* 2000a; **54:** 1421-1426.

Nusbaum AO, Lu D, Tang CY, Atlas SW. Quantitative diffusion measurements in focal multiple sclerosis lesions: correlations with appearance on T1-weighted MR images. *AJR Am J Roentgenol* 2000b; **175:** 821-825.

O'Connor P. Key issues in the diagnosis and treatment of multiple sclerosis. *Neurology* 2002; **59:** S1-S33.

O'Riordan JI, Gomez-Anson B, Moseley IF, Miller DH. Long term MRI follow-up of patients with post infectious encephalomyelitis: evidence for a monophasic disease. *J Neurol Sci* 1999; **167:** 132-6.

Oppenheimer DR. The cervical cord in multiple sclerosis. *Neuropathol Appl Neurobiol* 1978; **4:** 151-162.

Ormerod IE, Miller DH, McDonald WI, du Boulay EP, Rudge P, Kendall BE, Moseley IF, Johnson G, Tofts PS, Halliday AM. The role of NMR imaging in the assessment of multiple sclerosis and isolated neurological lesions. A quantitative study. *Brain* 1987; **110:** 1579-1616.

Paolillo A, Coles AJ, Molyneux PD, Gwane-Cain ML, MacManus DG, Barker GJ, Compston DA, Miller DH. Quantitative MRI in patients with secondary progressive MS treated with monoclonal antibody campath 1H. *Neurology* 1999; **53:** 751-757.

Paolillo A, Piattella MC, Pantano P, Di Legge S, Caramia F, Russo P, Lenzi GL, Pozzilli C. The Relationship between inflammation and atrophy in clinically isolated syndromes suggestive of multiple sclerosis. A monthly MRI study after triple-dose gadolinium-DTPA. *J Neurol* 2004; **251:** 432-439.

Papadakis NG, Xing D, Houston GC, Smith JM, Smith MI, James MF, Parsons AA, Huang CL, Hall LD, Carpenter TA. A study of rotationally invariant and symmetric indices of diffusion anisotropy. *Magn Reson Imaging* 1999; **17:** 881-892.

Parkes LM, Tofts PS. Improved accuracy of human cerebral perfusion measurements using arterial spin labelling; accounting for capillary water permeability. *Magn Reson Med* 2002; **48:** 27-41.

Parkes LM, Rashid W, Chard DT, Tofts PS. Normal cerebral perfusion measurements using arterial spin labelling: reproducibility, stability, and age and gender effects. *Magn Reson Med* 2004; **51:** 736-743.

Pasquier J, Michel BF, Brenot-Rossi I, Hassan-Sebbag N, Sauvan R, Gastaut JL. Value of (99m) Tc-ECD SPET for diagnosis of dementia with Lewy bodies. *Eur J Nucl Med Mol Imaging* 2002; **29:** 1342-1348.

Paty DW, Noseworthy JH, Ebers GC. Diagnosis of multiple sclerosis. In: Paty DW, Ebers GC, eds. *Multiple sclerosis*. Philadelphia: FA Davis; 1997: 48-134.

Paty DW, Ebers GC. Clinical features. In: Paty DW, Ebers GC, eds. *Multiple sclerosis.* Philadelphia: FA Davis; 1997: 135-191.

Paulesu E, Perani D, Fazio F, Comi G, Pozzilli C, Martinelli V, Filippi M, Bettinardi V, Sirabian G, Passafiume D, Anzini A, Lenzi GL, Canal N, Fieschi C. Functional basis of memory impairment in multiple sclerosis: a [18F] FDG PET study. *Neuroimage* 1996; **4:** 87-96.

Pelletier D, Nelson SJ, Oh J, Antel JP, Kita M, Zamvil SS, Goodkin DE. MRI lesion volume heterogeneity in primary progressive MS in relation with axonal damage and brain atrophy. *J Neurol Neurosurg Psychiatry* 2003; **74:** 950-952.

Peterson JW, Bo L, Monk S, Chang A, Trapp BD. Transected neuritis, apoptotic neurons, and reduced inflammation in cortical multiple sclerosis lesions. *Ann Neurol* 2001; **50:** 389-400.

Petrella JR, Yang Y, Richert N, Lewis B, Duyn JH, McFarland H, Frank JA. Dynamic contrast MR measurements of relative cerebral blood volume in enhancing multiple sclerosis lesions: Comparison to nonenhancing lesions and normal appearing white matter. *In Proc Intl Soc of Magn. Reson. Med* 1997; **1:** 646.

Peyser JM, Edwards KR, Poser CM, Filskov SB. Cognitive function in patients with multiple sclerosis. *Arch Neurol* 1980; **37:** 577-9.

Phillips CJ. The cost of multiple sclerosis and the cost effectiveness of disease-modifying agents in its treatment. *CNS Drugs* 2004; **18:** 561-574.

Pierpaoli C, Jezzard P, Basser PJ, Barnett A, DiChiro G. Diffusion tensor MR imaging of the human brain. *Radiology* 1996; **201:** 637-648.

Pierpaoli C, Basser PJ. Toward a quantitative assessment of diffusion anisotropy. *Magn Reson Med* 1996; **36:** 893-906.

Piras MR, Magnano I, Canu EDG, Paulus KS, Satta WM, Soddu A, Conti M, Achene A, Solinas G, Aiello I. Longitudinal study of cognitive dysfunction in multiple sclerosis: neuropsychological, neuroradiological, and neurophysiological findings. *J Neurol Neurosurg Psychiatry* 2003; **74:** 878-885.

Plummer DL. Dispimage: a display and analysis tool for medical images. *Riv Neuroradiol* 1992; **5:** 489-495.

Podreka I, Baumgartner C, Suess E, Müller C, Brücke T, Lang W, Holzner F, Steiner M, Deecke L. Quantification of regional cerebral blood flow with IMP-SPECT. *Stroke* 1989; **20:** 183-191.

Poser CM, Paty DW, Scheinberg L, McDonald WI, Davis FA, Ebers GC, Johnson KP, Sibley WA, Silberberg DH, Tourtellotte WW. New diagnostic criteria for multiple sclerosis: guidelines for research protocols. *Ann Neurol* 1983; **13:** 227-231.

Poser CM, Brinar VV. The nature of multiple sclerosis. *Clinical Neurology and Neurosurgery* 2004; **106:** 159-171.

Pozzilli C, Passafiume D, Bernardi S, Pantano P, Incoccia C, Bastianello S, Bozzao L, Lenzi GL, Fieschi C. SPECT, MRI and cognitive functions in multiple sclerosis. *J Neurol Neurosurg Psychiatry* 1991; **54:** 110-115.

Prentice RL. Surrogate markers in clinical trials: definition and operational criteria. *Stat Med* 1989; **8:** 431-440.

PRISMS Study Group. Randomised double-blind placebo-controlled study of interferon β-1a in relapsing/remitting multiple sclerosis. *Lancet* 1998; **352:** 1498-1504.

Proescholdt MA, Jacobson S, Tresser N, Oldfield EH, Merrill MJ. Vascular endothelial growth factor is expressed in multiple sclerosis plaques and can induce inflammatory lesions in experimental allergic encephalomyelitis rats. *J Neuropathol Exp Neurol* 2002; **61:** 914-925.

Pryse-Phillips W. The incidence and prevalence of multiple sclerosis in Newfoundland and Labrador, 1960-1984. *Ann Neurol* 1986; **20:** 323-328.

Rao SM, Leo GJ, Bernardin L, Unverzagt F. Cognitive dysfunction in multiple sclerosis. I. Frequency, patterns, and prediction. *Neurology* 1991; **41:** 685-91

Revesz T, Kidd D, Thompson AJ, Barnard RO, McDonald WI. A comparison of the pathology of primary and secondary progressive multiple sclerosis. *Brain* 1994; **117:** 759-765.

Rindfleisch E. Pathological Histology : An introduction to the study of Pathological Anatomy. Translated from the German by WC Kloman and FT Miles. London: Trubner & Co.; 1872: 652-658.

Roelcke U, Kappos L, Lechner-Scott J, Brunnschweiler H, Hubner S, Ammann W, Plohmann A, Dellas S, Maguire RP, Missimer J, Radü EW, Steck A, Leenders KL. Reduced glucose metabolism in the frontal cortex and basal ganglia of multiple sclerosis patients with fatigue: A ^{18}F-fluorodeoxyglucose positron emission tomography study. *Neurology* 1997; **48:** 1566-1571.

Roemer PB, Edelstein WA, Hayes CE, Souza SP, Mueller OM. The NMR phased array. *Magn Reson Med* 1990; **16:** 192-225.

Rosen BR, Belliveau JW, Chien D. Perfusion imaging by nuclear magnetic resonance. *Magn Reson Q* 1989; **5:** 263-281.

Rosen BR, Belliveau JW, Vevea JM, Brady TJ. Perfusion imaging with NMR contrast agents. *Magn Reson Med* 1990; **14:** 249-265.

Rovaris M, Mastronardo G, Gasperini C, Prandini F, Yousry TA, Filippi M. MRI gadolinium of new MS lesions enhancing after different doses of gadolinium. *Acta Neurol Scand* 1998; **98:** 90-93.

Rovaris M, Mastronardo G, Prandini F, Bastianello S, Comi G, Filippi M. Short-term evaluation of new multiple sclerosis lesions enhancing on standard dose and triple dose gadolinium-enhanced MRI scans. *J Neurol Sci* 1999; **164:** 148-152.

Rovaris M, Filippi M, Minicucci L, Iannucci G, Santuccio G, Possa F, Comi G. Cortical/subcortical disease burden and cognitive impairment in patients with multiple sclerosis. *AJNR Am J Neuroradiol* 2000; **21:** 402-408.

Rovaris M, Bozzali M, Santuccio G, Ghezzi A, Caputo D, Montanari E, Bertolotto A, Bergamaschi R, Capra R, Mancardi G. *In vivo* assessment of the brain and cervical cord pathology with primary progressive multiple sclerosis. *Brain* 2001; **124:** 2540-2549.

Rovaris M, Iannucci G, Falantano M, Possa F, Martinelli V, Comi G, Filippi M. Cognitive dysfunction in patients with mildly disablingnrelapsing-remitting multiple sclerosis: an exploratory study with diffusion tensor MR imaging. *J Neurol Sci* 2002a; **195:** 103-109.

Rovaris M, Bozzali M, Iannucci G, Ghezzi A, Caputo D, Montanari E, Bertolotto A, Bergamaschi R, Capra R, Mancardi GL. Assessment of normal-appearing white and grey matter in patients with primary progressive MS: a diffusion-tensor magnetic resonance imaging study. *Arch Neurol* 2002b; **59:** 1406-1412.

Rovaris M, Gallo A, Valsasina P, Benedetti B, Caputo D, Ghezzi A, Montanari E, Sormani MP, Bertolotto A, Mancardi G, Bergamaschi R, Martinelli V, Comi G, Filippi M. Short-term accrual of gray matter pathology in patients with progressive multiple sclerosis: an in vivo study using diffusion tensor MRI. *Neuroimage* 2005; **24:** 1139-1146.

Roxburgh RH, Seaman SR, Masterman T, Hensiek AE, Sawcer SJ, Vukusic S, Achiti I, Confavreux C, Coustans M, le Page E, Edan G, McDonnell GV, Hawkins S, Trojano M, Liguori M, Cocco E, Marrosu MG, Tesser F, Leone MA, Weber A, Zipp F, Miterski B, Epplen JT, Oturai A, Sorensen PS, Celius EG, Lara NT, Montalban X, Villoslada P, Silva AM, Marta M, Leite I, Dubois B, Rubio J, Butzkueven H, Kilpatrick T, Mycko MP, Selmaj KW, Rio ME, Sa M, Salemi G, Savettieri G, Hillert J, Compston DA. Multiple Sclerosis Severity Score: using disability and disease duration to rate disease severity. *Neurology* 2005; **64:** 1144-51.

Roychowdhury S, Maldijan JA, Grossman RI. Multiple sclerosis: comparison of trace apparent diffusion coefficients with MR enhancement pattern of lesions. *AJNR Am J Neuroradiol* 2000; **21:** 869-874.

Rudick RA, Schiffer RB, Schwetz KM, Herndon RM. Multiple sclerosis: the problem of incorrect diagnosis. *Arch Neurol* 1986; **43:** 578-583.

Rudick RA, Goodman A, Herndon RM, Panitch RM. Selecting relapsing-remitting multiple sclerosis patients for treatment: the case for early treatment. *J Neuroimmunol* 1999a; **98:** 22-28.

Rudick RA, Fischer E, Lee J-C, Simon J, Jacobs L. Use of brain parenchymal fraction to measure whole brain atrophy in relapsing-remitting MS. *Neurology* 1999b; **53:** 1698-1704.

Runmarker B, Andersen O. Prognostic factors in a multiple sclerosis incidence cohort with twenty-five years of follow-up. *Brain* 1993; **116:** 117-134.

Rutschmann OT, McCrory DC, Matchar DB, Immunization Panel of the Multiple Sclerosis Council for Clinical Practice Guidelines. Immunization and MS. A summary of published evidence and recommendations. *Neurology* 2002; **59:** 1837-1843.

Sadovnick AD, Baird PA. The familial nature of multiple sclerosis: age-corrected empiric recurrence risks of children and siblings of parents. *Neurology* 1988; **38:** 990-991.

Sadovnick AD, Baird PA, Ward RH. Multiple sclerosis: update risks for relatives. *Am J Med Genet* 1988; **29:** 533-541.

Sadovnick AD, Armstrong H, Rice GP, Bulman D, Hashimoto L, Paty DW, Hashimoto SA, Warren S, Hader W, Murray TJ. A population-based twin study of multiple sclerosis: update. *Ann Neurol* 1993; **33:** 282-285.

Sadovnick AD, Ebers GC, Dyment, Risch NJ. Canadian Collaborative Study Group. Evidence for the genetic basis of multiple sclerosis. *Lancet* 1996; **347:** 1728-1730.

Saindane AM, Ge Y, Udupa JK, Babb JS, Mannon LJ, Grossman RI. The effect of gadolinium-enhancing lesions on whole brain atrophy in relapsing-remitting MS. *Neurology* 2000; **55:** 61-65.

Sarchielli P, Presciutti O, Pelliccioli GP, Tarducci R, Gobbi G, Chiarini P, Alberti A, Vicinanza F, Gallai V. Absolute quantification of brain metabolites by proton magnetic resonance spectroscopy in normal-appearing white matter of multiple sclerosis patients. *Brain* 1999; **122:** 513-522.

Schmierer K, Scaravilli F, Altmann DR, Barker GJ, Miller DH. Magnetisation transfer ratio and myelin in postmortem multiple sclerosis brain. *Ann Neurol* 2004a; **56:** 407-415.

Schmierer K, Altmann DR, Kassim N, Kitzler H, Kerskens CM, Doege CA, Aktas O, Lünemann JD, Miller DH, Zipp F. Progressive changes in primary progressive multiple sclerosis normal-appearing white matter: a serial diffusion magnetic resonance imaging study. *Mult Scler* 2004b; **10:** 182-187.

Schmierer K, Scaravilli F, Boulby P, Wheeler-Kingshott CAM, Miller DH. Pathological correlates of diffusion tensor imaging (DTI) in post-mortem MS brain. *Mult Scler* 2004c; **10 (suppl 2):** S229.

Schumacher GA, Beebe G, Kibler RF, Kurland LT, Kurtzke JF, McDowell F, Nagler B, Sibley WA, Tourtellote WW, Willmon TL. Problems of experimental trials of therapy in multiple sclerosis: report by the panel on the evaluation of experimental trials of therapy in multiple sclerosis. *Ann NY Acad Sci* 1965; **122:** 552-568.

Secondary Progressive Efficacy Trial of Recombinant Interferon-beta-1a in MS (SPECTRIMS) Study Group. Randomized controlled trial of interferon-beta-1a in secondary progressive MS. *Neurology* 2001; **56:** 1496-1504.

Silver NC, Good CD, Barker GJ, MacManus DG, Thompson AJ, Moseley IF, McDonald WI, Miller DH. Sensitivity of contrast enhanced MRI in multiple sclerosis. Effects of gadolinium dose, magnetization transfer contrast and delayed imaging. *Brain* 1997; **120:** 1149-1161.

Silver NC, Good CD, Sormani MP, MacManus DG, Thompson AJ, Filippi M, Miller DH. A modified protocol to improve the detection of enhancing brain and spinal cord lesions in multiple sclerosis. *J Neurol* 2001a; **248:** 215-224.

Silver NC, Tofts PS, Symms MR, Barker GJ, Thompson AJ, Miller DH. Quantitative contrast-enhanced magnetic resonance imaging to evaluate blood-brain barrier integrity in multiple sclerosis: a preliminary study. *Mult Scler* 2001b; **7:** 75-82.

Simon JH, Jacobs LD, Campion MK, Rudick RA, Cookfair DL, Herndon RM, Richert JR, Salazar AM, Fischer JS, Goodkin DE, Simonian N, Lajaunie M, Miller DE, Wende K, Martens-Davidson A, Kinkel RP, Munschauer FE 3rd, Brownscheidle CM. A longitudinal study of brain atrophy in relapsing multiple sclerosis. *Neurology* 1999; **53:** 139-148.

Skegg DC, Corwin PA, Craven RS, Malloch JA, Pollock M. Occurrence of multiple sclerosis in the north and south of New Zealand. *J Neurol Neurosurg Psychiatry* 1987; **50:** 134-139.

Smith KJ, McDonald WI. Spontaneous and mechanically evoked activity due to central demyelinating lesion. *Nature* 1980; **286:** 154-155.

Smith ME, Stone LA, Albert PS, Frank JA, Martin R, Armstrong M, et al. Clinical worsening in multiple sclerosis is associated with increased frequency and area of Gadopentetate Dimeglumine-enhancing imaging lesions. *Ann Neurol* 1993; **33**: 480-489.

Smith SM, De Stefano N, Jenkinson M, Matthews PM. Normalized accurate measurement of longitudinal brain change. *J Comput Assist Tomogr* 2001; **25:** 466-475.

Solari A, Radice D, Manneschi L, Motti L, Montanari E. The multiple sclerosis functional composite: different practice effects in the three test components. *J Neurol Sci* 2005; **228:** 71-74.

Steen RG, Gronemeyer SA, Kingsley PB, Reddick WE, Langston JS, Taylor JS. Precise and accurate measurement of proton T1 in human brain *in vivo*: validation and preliminary clinical application. *J Magn Reson Imaging* 1994; **4:** 681-691.

Stevenson VL, Leary SM, Losseff NA, Parker GJ, Barker GJ, Husmani Y, Miller DH, Thompson AJ. Spinal cord atrophy and disability in MS: A longitudinal study. *Neurology* 1998; **51:** 234-238.

Stevenson VL, Miller DH, Rovaris M, Barkhof F, Brochet B, Dousset V, Filippi M, Montalban X, Polman CH, Rovira A, de Sa J, Thompson AJ. Primary and transitional progressive MS: a clinical and MRI cross-sectional study. *Neurology* 1999; **52:** 839-845.

Stevenson VL, Miller DH, Leary SM, Rovaris M, Barkhof F, Brochet B, Dousset V, Filippi M, Hintzen R, Montalban X, Polman CH, Rovira A, de Sa J, Thompson AJ. One year follow up study of primary and transitional progressive multiple sclerosis. *J Neurol Neurosurg Psychiatry* 2000; **68:** 713-718.

Stone LA, Smith ME, Albert PS, Bash CN, Maloni H, Frank JA, McFarland HF. Blood-brain barrier disruption on contrast-enhanced MRI in patients with mild relapsing-remitting multiple sclerosis: Relationship to course, gender and age. *Neurology* 1995; **45:** 1122-1126.

Stromblad S, Cheresh DA. Integrins, angiogenesis and vascular survival. *Chem Biol* 1996; **3:** 881-885.

Studholme C, Hill DLG, Hawkes DJ. An overlap invariant entropy measure of 3D medical image alignment. *Pattern Recognit* 1999; **32:** 71-86.

Stys PK. Axonal degeneration in multiple sclerosis: Is it time for neuroprotective strategies? *Ann Neurol* 2004; **55:** 601-603.

Sundstrom P, Juto P, Wadell G, Hallmans G, Svenningsson A, Nystrom L, Dillner J, Forsgren L. An altered immune response to Epstein-Barr virus in multiple sclerosis: a prospective study. *Neurology* 2004; **62:** 2277-2282.

Symms MR, Barker GJ, Holmes P, Wang L, Yoo DS, Lemieux L, Tofts PS. A rapid automated system for detection of serial changes in transient ishaemic attack using registration and subtraction of three-dimensional images. In: *Proc Intl Soc Magn Reson Med* 1995; **5:** 584.

Tartaglino LM, Friedman DP, Flanders AE, Lublin FD, Knobler RL, Liem M. Multiple sclerosis in the spinal cord: MR appearance and correlation with clinical parameters. *Radiology* 1995; **195:** 725-732.

Taxt T, Lundervold A, Fuglaas B, Lien H, Abele V. Multispectral analysis of uterine corpus tumours in magnetic resonance imaging. *Magn Reson Med* 1992; **23:** 55-76.

Thielen KR, Miller GM. Multiple sclerosis of the spinal cord: magnetic resonance appearance. *J Comput Assist Tomogr* 1996; **20:** 434-438.

Thompson AJ, Kermode AG, Wicks D, MacManus DG, Kendall BE, Kingsley DPE, McDonald WI. Major differences in the dynamics of primary and secondary progressive multiple sclerosis. *Ann Neurol* 1991; **29:** 53-62.

Thompson AJ, Miller DH, Youl B, MacManus D, Moore S, Kingsley D, et al. Serial gadolinium-enhanced MRI in relapsing-remitting multiple sclerosis of varying disease duration. *Neurology* 1992; **42**: 60-63.

Thompson AJ, Montalban X, Barkhof F, Brochet B, Filippi M, Miller DH, Polman CH, Stevenson VL, McDonald WI. Diagnostic criteria for primary progressive multiple sclerosis: A position paper. *Ann Neurol* 2000; 47: 831-835.

Thorpe JW, Kidd D, Moseley IF, Kendall BE, Thompson AJ, MacManus DG, McDonald WI, Miller DH. Serial gadolinium-enhanced MRI of the brain and spinal cord in early relapsing-remitting multiple sclerosis. *Neurology* 1996; **46:** 373-378.

Tiberio M, Chard DT, Altmann DR, Davies GR, Griffin CM, Rashid W, Sastre-Garriga J, Thompson AJ, Miller DH. Grey and white matter volume changes in early RRMS: a two-year longitudinal study. *Neurology* 2005; **65:** 1001-1007.

Tintoré M, Rovira A, Martínez M, Rio J, Diaz-Villoslada P, Briera L, Borras C, Grive E, Capellades J, Montalban X. Isolated demyeinating syndromes: comparison of different MR imaging criteria to predict conversion to clinically definite multiple sclerosis. *Am J Neuroradiol* 2000; **21:** 702-706.

Tintoré M, Rovira A, Rio J, Nos C, Grive E, Sastre-Garriga J, Pericot I, Sanchez E, Comabella M, Montalban X. New diagnostic criteria for multiple sclerosis: application in first demyelinating episode. *Neurology* 2003; **60:** 27-30.

Tofts PS, Kermode AG. Blood-brain barrier permeability in multiple sclerosis using labelled DTPA with PET, CT and MRI. *J Neurol Neurosurg Psychiatry* 1989; **52:** 1019-1020.

Tofts PS, Davies GR, Dehmeshki J. Histograms: Measuring subtle diffuse disease. In: Tofts P, ed. *Quantitative MRI of the brain. Measuring changes caused by disease, 1st ed.* London: Wiley; 2003a: 581-610.

Tofts PS, Waldman AD. Spectroscopy: ^{1}H Metabolite Concentrations. In: Tofts P, ed. *Quantitative MRI of the brain. Measuring changes caused by disease, 1st ed.* London: Wiley; 2003b: 299-340.

Tortorella C, Codella M, Rocca MA, Gasperini C, Capra R, Bastianello S, Filippi M. Disease activity in multiple sclerosis studied by weekly triple-dose magnetic resonance imaging. *J Neurol* 1999; **246:** 689-692.

Tortorella C, Viti B, Bozzali M, Sormani MP, Rizzo G, Gilardi MF, Comi G, Filippi M. A magnetization transfer histogram study of normal-appearing brain tissue in MS. *Neurology* 2000; **54:** 186-193.

Tourbah A, Stievenart JL, Abanou A, Fontaine B, Cabanis EA, Lyon-Caen O. Correlating multiple MRI parameters with clinical features: an attempt to define a new strategy in multiple sclerosis. *Neuroradiology* 2001; **43:** 712-20.

Trapp BD, Peterson J, Ransohoff RM, Rudick R, Mork S, Bo L. Axonal transection in the lesions of multiple sclerosis. *N Engl J Med* 1998; **338:** 278-285.

Trapp BD, Ransohoff R, Rudick R. Axonal pathology in multiple sclerosis: relationship to neurologic disability. *Curr Opin Neurol* 1999; **12:** 295-302.

Trapp BD. Pathogenesis of multiple sclerosis: the eyes only see what the mind is prepared to comprehend. *Ann Neurol* 2004; **55:** 455-457.

Truyen L, van Waesberghe JH, van Waldervenn MA, van Oostem BW, Polman CH, Hommes OR, Ader HJ, Barkhof F. Accumilation of hypointense lesions ("black holes") on T1 spin-echo MRI correlates with disease progression in multiple sclerosis. *Neurology* 1996; **47:** 1469-1476.

Tuohy VK, Yu M, Yin L, Kawczak JA, Johnsen JM, Mathiesen PM, Weinstock-Guttman B, Kinkel RP. The epitope spreading cascade during progression of experimental autoimmune encephalomyelitis and multiple sclerosis. *Immunol Rev* 1998; **164:** 93-100.

Turner R, Le Bihan D, Maier J, Vavrek R, Hedges LK, Pekar J. Echo-planar imaging of intravoxel incoherent motion. *Radiology* 1990; **177:** 407-414.

Uhlenbrock D, Sehlen S. The value of T1-weighted images in the differentiation between MS, white matter lesions, and subcortical arteriosclerotic encephalopathy (SAE). *Neuroradiology* 1989; **31:** 203-212.

Vaithianathar L, Tench CR, Morgan PS, Constantinescu CS. Magnetic resonance imaging of the cervical spinal cord in multiple sclerosis. A quantitative T_1 relaxation time mapping approach. *J Neurol* 2003; **250:** 307-315.

Van Meir EG. Cytokines and tumors of the central nervous system. *Glia* 1995; **15:** 264-288.

Vannier MW, Butterfield RL, Jordan D, Murphy WA, Levitt RG, Gado M. Multispectral analysis of magnetic resonance images. *Radiology* 1985; **154:** 221-224.

Van Waesberghe JH, Castelijns JA, Roser W, et al. Single-dose gadolinium with magnetization transfer versus triple-dose gadolinium in the MR detection of multiple sclerosis lesions. *AJNR Am J Neuroradiol* 1997; **18:** 1279-1285.

Van Waesberghe JHTM, van Walderveen MAA, Castelijns JA, Scheltens P, Lycklama à Nijeholt GJ, Polman CH, Barkhof F. Patterns of lesion development in multiple sclerosis: longitudinal observations with T1-weighted spin-echo and magnetization transfer MR. *AJNR Am J Neuroradiol* 1998; **19:** 675-683.

Van Waesberghe JH, Kamphorst W, De Groot CJ, van Walderveen MA, Castelijns JA, Ravid R, Lycklama à Nijeholt GJ, van der Valk P, Polman CH, Thompson AJ, Barkhof F. Axonal loss in multiple sclerosis lesions: magnetic resonance imaging insights into substrates of disability. *Ann Neurol* 1999; **46:** 747-754.

van Walderveen MA, Kamphorst W, Scheltens P, van Waesberghe JH, Ravid R, Valk J, Polman CH, Barkhof F. Histopathologic correlate of hypointense lesions on T1-weighted spin-echo MRI in multiple sclerosis. *Neurology* 1998; **50:** 1282-1288.

Varrone A, Pappata S, Caraco C, Soricelli A, Milan G, Quarantelli M, Alfano B, Postiglione A, Salvatore M. Voxel-based comparison of rCBF SPET images in frontotemporal dementia and Alzheimer's disease highlights the involvement of different cortical networks. *Eur J Nucl Med Mol Imaging* 2002; **29:** 1447-1454.

Vassallo L, Elian M, Dean G. Multiple sclerosis in southern Europe. II. Prevalence in Malta in 1978. *J Epidemiol Comm Health* 1979; **33:** 111-113.

Vukusic S, Confareux C. The natural history of multiple sclerosis. In: Cook SD, ed. *Handbook on multiple sclerosis, 3rd ed.* New York: Marcel Dekker; 2001: 433-447.

Vulpian A. Note sur la sclerose en plaques de la moelle epiniere. *L'Union Medicale* 1866; **30 :** 459-465, 475-482, 507-512, 541-548.

Vymazal J, Righini A, Brooks RA, Canesi M, Mariani C, Leonardi M, Pezzoli G. T1 and T2 in the brain of healthy subjects, patients with Parkinson disease, and patients with multiple system atrophy: relation to iron content. *Radiology* 1999; **211:** 489-495.

Weatherby SJ, Mann CL, Davies MB, Carthy D, Fryer AA, Boggild MD, Young C, Strange RC, Ollier W, Hawkins CP. Polymorphisms of apolipoprotein E; outcome and susceptibility in multiple sclerosis. *Mult Scler* 2000; **6:** 32-6.

Weiner HL, Guttmann CR, Khoury SJ, Orav EJ, Hohol MJ, Kikinis R, Jolesz FA. Serial magnetic resonance imaging in multiple sclerosis: correlation with attacks, disability and disease stage. *J Neuroimmunol* 2000; **104:** 164-173.

Weinshenker BG, Ebers GC. The natural history of multiple sclerosis. *Can J Neurol Sci* 1987; **14:** 255-261.

Weinshenker BG, Bass B, Rice GP, Noseworthy J, Carriere W, Baskerville J, Ebers GC. The natural history of multiple sclerosis: a geographically based study. I. Clinical course and disability. *Brain* 1989a; **112:** 133-146.

Weinshenker BG, Bass B, Rice GP, Noseworthy J, Carriere W, Baskerville J, Ebers GC. The natural history of multiple sclerosis: a geography based study. II. Predictive value of the early clinical course. *Brain* 1989b; **112:** 1419-1428.

Werring DJ, Clark CA, Barker GJ, Thompson AJ, Miller DH. Diffusion tensor imaging of lesions and normal-appearing white matter in multiple sclerosis. *Neurology* 1999; **52:** 1626-1632.

Werring DJ, Brassat D, Droogan AG, Clark CA, Symms MR, Barker GJ, MacManus DG, Thompson AJ, Miller DH. The pathogenesis of lesions and normal-appearing white matter changes in multiple sclerosis: a serial diffusion MRI study. *Brain* 2000a; **123:** 1667-1676.

Werring DJ, Bullmore ET, Toosy AT, Miller DH, Barker GJ, MacManus DG, Brammer MJ, Giampietro VP, Brusa A, Brex PA, Moseley IF, Plant GT, McDonald WI, Thompson AJ. Recovery from optic neuritis is associated with a change in the distribution of cerebral response to visual stimulation: a functional magnetic resonance imaging study. *J Neurol Neurosurg Psychiatry* 2000b; **68:** 441-449.

Westin CF, Maier SE, Mamata H, Nabavi A, Jolesz FA, Kikinis R. Processing and visualisation for diffusion tensor MRI. *Med Image Anal* 2002; **6:** 93-108.

Wheeler-Kingshott CAM, Boulby P, Symms MR, Barker GJ. Optimised cardiac gating for high-resolution whole brain DTI on a standard scanner. *Proc Intl Soc Magn Reson Med* 2002; **10:** 1118.

Wheeler-Kingshott CAM, Barker GJ, Steens SCA, van Buchem MA. *D*: the Diffusion of Water. In: Tofts P, ed. *Quantitative MRI of the brain. Measuring changes caused by disease, 1st ed.* London: Wiley; 2003:203-256.

Wiebe S, Lee DH, Karlik SJ, Hopkins M, Vandervoort MK, Wong CJ, Hewitt L, Rice GP, Ebers GC, Noseworthy JH. Serial cranial and spinal cord magnetic resonance imaging in multiple sclerosis. *Ann Neurol* 1992; **32:** 643-650.

Williams DS, Detre JA, Leigh JS, Koretsky AP. Magnetic Resonance imaging of perfusion using spin inversion of arterial water. *Proc Natl Acad Sci USA* 1992; **89:** 212-216.

Woods RP, Grafton ST, Holmes CJ, Cherry SR, Mazziotta JC. Automated image registration: I. General methods and intrasubject, intramodality validation. *J Comput Assist Tomogr.* 1998; **22:** 139-152.

Worsley KJ, Marrett S, Neelin P, Vandal AC, Friston KJ, Evans AC. A unified statistical approach for determining images of cerebral activation. *Hum Brain Mapp* 1996; **4:** 58-73.

Wuerfel J, Bellmann-Strobl J, Brunecker P, Aktas O, McFarland H, Villringer A, Zipp F. Changes in cerebral perfusion precede plaque formation in multiple sclerosis: a longitudinal perfusion MRI study. *Brain* 2004; **127:** 111-119.

Wujek JR, Bjartmar C, Richer E, Ransohoff RM, Yu M, Tuohy VK, Trapp BD. Axon loss in the spinal cord determines permanent neurological disability in an animal model of multiple sclerosis. *J Neuropathol Exp Neurol* 2002; **61:** 23-32.

Wynn DR, Kurland LT, O'Fallon WM, Rodriguez M. A reappraisal of the epidemiology of multiple sclerosis in Olmstead County, Minnesota. *Neurology* 1990; **40:** 780-786.

Young IR, Hall AS, Pallis CA, Legg NJ, Bydder GM, Steiner RE. Nuclear magnetic resonance imaging of the brain in multiple sclerosis. *Lancet* 1981; **2:** 1063-1066.

Yu YL, Woo E, Hawkins BR, Ho HC, Huang CY. Multiple sclerosis amongst Chinese in Hong Kong. *Brain* 1989; 112: 1445-1467.

Zajicek J, Fox P, Sanders H, Wright D, Vickery J, Nunn A, Thompson A; UK MS Research Group. Cannabinoids for treatment of spasticity and other symptoms related to multiple sclerosis (CAMS study): multicentre randomised placebo-controlled trial. *Lancet* 2003; **362:** 1517-1526.

Zeman AZ, Kidd D, McLean BN, Kelly MA, Francis DA, Miller DH, Kendall BE, Rudge P, Thompson EJ, McDonald WI. A study of oligoclonal band negative multiple sclerosis. *J Neurol Neurosurg Psychiatry* 1996; **60:** 27-30.

Ziche M, Morbidelli L. Nitric oxide and angiogenesis. *J Neurooncol* 2000; **50:** 139-148.

Zivadinov R, Zorzon M. Is gadolinium enhancement predictive of the development of brain atrophy in multiple sclerosis? A review of the literature. *J Neuroimaging* 2002; **12:** 302-309.